Jukka Hietaniemi & Esko Mikkola

Design Fires for Fire Safety Engineering

Author(s)
Jukka Hietaniemi & Esko Mikkola

Title
Design Fires for Fire Safety Engineering

Abstract

For construction design fire safety is one of the key requirements. Fire loads, which define the possible fires that can occur, need to be known both in magnitude and quality. This report describes design fires appropriate for use in Fire Safety Engineering (FSE) design in general and thus applicable also for building with wood, of which some specifics are described. In the approach used the initial fires are quantified using heat release rates which are dependent on the usage of the building. Assessment of fire growth and spread is based on the capability of the FDS fire simulator to make conservative estimations how rapidly and to how large a fire may grow within a given space.

Preface

This report describes design fires appropriate for use in Fire Safety Engineering (FSE) design in general and thus applicable also for building with wood, of which some specifics are described. In the approach used the initial fires are quantified using heat release rates which are dependent on the usage of the building. Assessment of fire growth and spread is based on the capability of the FDS fire simulator to make *conservative estimations* how rapidly and to how large a fire may grow within a given space.

At the end of the report key issues concerning timber structures and design fires are described with the idea to provide visions for future development.

This report has been written within the European research project FireInTimber (Fire Resistance of Innovative Timber structures). The project has been sponsored by national funding organisations within the WoodWisdom-Net framework and by industry through the European network BWW (Building With Wood).

Espoo 2010

Contents

1. Introduction

For construction design fire safety is one of the key requirements. Fire loads, which define the possible fires that can occur, need to be known both in magnitude and quality. This report describes a simplified approach to fire characterisation that is based on the concept of fire load entities. Entity means a fundamental 'unit' that is describing the initial fire (not only MJ/m^2, but also heat release versus time). This concept utilises the fact that our empirically-based knowledge on initial fires in premises typically designed by using Fire Safety Engineering (FSE) is sufficient for setting up simplified descriptions for the time evolution of the initial fire and, that advanced fire-simulation programs can to a certain extent extrapolate the fire spread from the initial fire to secondary igniting objects. This means that it is possible to make conservative assessment how a large fire – meaning a mega-watt-order fire or larger – may propagate within the given space.

The fire load entity approach is analogous to the approach used in normal temperature structural design in which it is assumed that the live loads in some building can be categorised according to the usage of the building, i.e., we have some live load for offices, another for warehouses, etc. We are so used to this approach of assessing the static live loads that we usually do not even think that actually in most cases the live load used in design will in most cases be inaccurate! With then expression "inaccurate" meaning that if we would go and measure the actual live load in some building, the result will most probably differ from the value used in design. Yet it does not matter in practise as the live load values are selected in a conservative manner, i.e., they are some high percentile fractile values of the statistical distribution that describes the variability of the live loads encountered real situations. More precisely, the design live load values used in normal-temperature structural design are 80 % fractile values which mean that probability of having an actual live load higher than the design value is 20 % or once out of five. Such high probability can not, of course, be accepted for structural failures and this is taken care of by using safety factors that require increasing the capacity to such extent that the structural failure probability becomes tolerably low.

1. Introduction

Similar approach is applied in the determination of the fire load entities, which quantify the magnitude of the thermal action exposing the structures. The fire load entities are a source of heat and the rate at which they release heat affect fire development. The key factor, the heat release rate (HRR) of the fire load entities, is selected so that the time evolution the fire load entity HRR includes all the experimental data within an envelope curve. This approach guarantees a safe-side assessment in full analogy the live-load design values.

In the following also the necessary background concerning acceptability of the methods used and the design process are dealt with before describing the methods for building up design fires and the applications.

2. Performance criteria and fulfilment of the criteria

National building regulations (such as the National Building Code of Finland, Part E1: Fire safety of buildings [1]) may define performance criteria to be applied in structural fire safety engineering (FSE) design, for example in the following way:

- a building of more than two storeys must not generally collapse during the fire or cooling phase

- a building of not more than two storeys must not collapse during the period of time required for securing evacuation, rescue operations and controlling the fire.

These are statements which immediately lead to need for interpretations when they are applied in a building design:

- What does the phrase "building of more than two storeys must not generally collapse" mean? It seems that there are some so unlikely fire scenarios in which the more-than-two-storey building may collapse; the probability of such fire scenarios just has to be so low that the resulting risk can be tolerated by the society and other stakeholders. And this 'rule' cannot be interpreted as "a building of more than two storeys never collapses during the fire or cooling phase".

- The performance criterion applied for 1–2 storey buildings is much clearer. Yet, in practice there are difficulties that arise from the quantitative determination of how long time it actually takes to evacuate, rescue and get the fire under control.

There are basically two ways to attest that a design solution fulfils the performance criteria:

1) Based on absolute values:

- determination of the risk of non-performance of the solution

- comparison of this risk with a limiting risk value that has been agreed to represent a tolerable risk.

2) Based on relative values:

- assessment of the risks related to the FSE design solution

- assessment of the risks that would result from application of the prescriptive rules of fire regulations (deemed-to-satisfy-solution)

- comparison of these risks.

Both these approaches have advantages and disadvantages. The approach based on absolute values has the advantage that the designer has to carry out only FSE design but the disadvantage is that there may be no well established tolerable risk level available to compare with. In the approach based on relative values the acceptance is basically simple as the requirement is that the FSE solution shall have equal or better safety than the design based on prescriptive rules but disadvantage is that the designer has to carry out two assessments: First the FSE design and then the analysis of prescriptive design.

2.1 Verification of safety through comparison with a tolerable risk level

The risks involved in a potential structural failure differ widely, depending on the damage that might be caused. For example, the collapse of a basically unmanned single-storey warehouse is completely different from the collapse of a multi-storey building having a large number of occupants. Fire safety design aims at providing solutions with risk levels that our society can tolerate. As the risk is composed of the probability p_f of the failure – or more generally, the unwanted event – and the associated consequence C, high-consequence events must have considerably lower probability of occurrence than low-consequence events. However, it is important to realise and acknowledge the fact that there is always some – though very small – probability that the unwanted and unexpected event will happen. Consequently, a tolerable risk level greater than zero exists.

Eurocodes are based on reliability theory, and Eurocode 1990 [2] actually gives quantitative, numerically expressed levels of the probability of structural failure deemed to be tolerably low. It distinguishes between three consequence classes (CC1, CC2 and CC3), and associates three reliability classes (RC1, RC2 and RC3) to them (see Table 1). The reliability in each reliability class is quantified by the reliability index β, which for *normally distributed variables* is related to the failure probability p_f as

$$\beta = \Phi^{-1}\left(1 - p_f\right)$$

$$p_f = 1 - \Phi\beta$$

(2-1)

where Φ is the cumulative distribution function of the standardised Normal distribution.

It should noted that these values depend on the risk-relevancy of the building, not on the potential cause – excessive snow or wind load, earthquake, fire or some other cause

– of the unwanted event. Hence they give a plausible starting point for the assessment of the tolerable risk in case of fire.

Table 1. Risk levels set up in Eurocode 1990.

Consequence class	Reliability class	Minimum values for β		Maximum values for p_f	
		1 year reference period	50 year reference period	1 year reference period	50 year reference period
CC3	RC3	5.2	4.3	9.96E-08	8.54E-06
CC2	RC2	4.7	3.8	1.30E-06	7.23E-05
CC1	RC1	4.2	3.3	1.33E-05	4.83E-04

2.2 Verification of safety through comparison with a deemed-to-satisfy solution

Verification of safety through comparison with a deemed-to-satisfy (DTS) solution is a straightforward method with the great benefit that the designer is not required to justify the safety of the solution. The drawback of this approach is that one has to carry out two analyses, one for the Fire Safety Engineering design and one for the design that complies with the classes and numerical requirements given in the fire regulations.

In brief, using fire safety assessment of structures as an example, the process is as follows:

1) Establish the design fires using the fire load entities.

2) Carry out the Fire Safety Engineering (FSE) analysis of the design that you plan to have accepted, including the assessment of structural adequacy.

3) Assess the likelihood of structural failure in the FSE design (against some failure criterion, e.g. a critical temperature approach in which the structural performance is deemed to be acceptable if the temperature of the structure does not exceed a defined critical temperature).

4) Carry out the Fire Safety Engineering (FSE) analysis, including assessment of structural adequacy for a similar building (or part of it) with design solutions taken from the fire regulations (the DTS design solution).

5) Assess the likelihood of structural failure in DTS design, using the same failure criterion as used for the FSE solution.

Compare the results and, if the FSE solution gives at least as low a failure likelihood as the DTS solution, the FSE solution is acceptable.

3. The Fire Safety Engineering design process

The Fire Safety Engineering (FSE) design process is schematically shown in Figure 1 and the basic factors of FSE analysis in Figure 2.

DESIGN PROCESS: ISO TC 92/SC 4/WG 10 N55Rev4

AGREEMENT ON THE BASIS OF THE WORK

BUILDING (OR PART OF IT)

FIRE SCENARIOS
- what burns, where & when
- operation/operation failures of safety systems
- how many people are threatened
- what is the percentage of children, elderly people, disabled

DESIGN FIRES
- fire growth rate
- max. fire size (HRR, MW)
- production of smoke & hazardous gases
- duration

ACCEPTANCE CRITERIA
- maintaining tolerable conditions for safe evacuation (heat & smoke)
- ensuring operable conditions for the fire department
- other, if needed

TREATMENT OF UNCERTAINTIES: SENSITIVITY ANALYSIS

FIRE SAFETY ENGINEERING ANALYSIS

ANALYSIS OF A FIRE SCENARIO
- heat, smoke (fire simulation) incl. influence of safety measures
- evacuation (evac. calculations)

ANOTHER SCENARIO

IS THE RESULT SAFE? INCLUDING SENSITIVITY ANALYSIS
- heat, smoke (fire simulation)
- evacuation (evac. calculations)

RE-ANALYSE

deterministic
- for example:
  $ASET > RSET + $ safety margin

probabilistic
- for example:
  $P[ASET < RSET] < p_{target}$

risk-based
- for example:
  acceptable F-N -curve

YES   **NO**   **CHANGE THE DESIGN**

ALL SCENARIOS AND ALTERNATIVES ANALYSED

CHECKING

SUMMARY, INTERPRETATION, FINAL REPORTING
- including statement of service and maintenance needs as well as statement when potential changes in the building or part of it necessitate partial or complete re-design

Figure 1. The FSE design process scheme.

14

SCENARIO

VENTILATION:
how much O_2 fire gets

DESIGN FIRE

FIRE SIMULATION

PASSIVE FIRE SAFETY MEASURES
- load-bearing (R)
- compartments (EI)
- reaction-to-fire
- safety distances

CHANGES IN CONDITIONS:
- heat
- smoke
- toxicity

ACTIVE FIRE SAFETY MEASURES
- first-aid extinguishing
- fire detection
- smoke control
- suppression systems
- fire department

ASSESSMENT CONSEQUENCES:
- evacuation
- hazards from heat and smoke (incl. fire dept.)
- heat transfer and structural response

SENSITIVITY ANALYSIS

• The load-bearing capacity of the construction can be assumed for a specific period of time;
• The generation and spread of fire and smoke within the works are limited;
• The spread of fire to neighbouring construction works is limited;
• Occupants are able to leave the building in case of fire or can be rescued by other means;
• The safety of rescue teams is taken into consideration.

Figure 2. Fire safety engineering analysis scheme.

In performance-based design, the assessed level of fire risk defines the acceptability of the design. It is therefore essential that all features affecting the total fire risk are included in the analysis. All factors must be quantified, such as ignition and fire development, performance of structural elements (including detailed solutions), performance of the building occupants, level and reliability of fire safety systems (incorporating both the active and passive measures), intervention of the fire department, and damage caused by fire.

15

In assessing whether the results are safe (the analysis part of the diagram of Figure 1) the following abbreviations have been used:

- ASET = available safe egress time

- RSET = required safe egress time

- F-N curves are frequency-number plots, showing the cumulative frequencies (F) of events causing N or more losses (fatalities, injuries, etc.).

4. Basics of the estimation of the design fires

For defining design fires, an approach in which the combustibles are described as fire load entities can be used. The procedure is described below. In this approach, the fire compartment analysed is filled with a suitable number of fire load entities with proper dimensions and placing. For simplicity of presentation, the fire load entities are rectangles with all faces except the one directed to floor releasing heat according to the specifications of the particular fire load entity.

The development of the fire is described as follows:

- One of the fire load entities is selected by the user as the initial fire.

  – Typically several initial fire positions must be used, even in a single analysis, in order to achieve a sufficiently comprehensive picture of the fire incident.

- All other fire load entities are secondary igniting objects that will ignite when their surface temperature reaches the ignition temperature specified by the user. After ignition, the ignited fire load entity starts to release heat following the same time evolution as the initial fire.

- It should be noted that ventilation has a significant influence on fire development, as combustion cannot continue unless there is a supply of fresh air and exhaust of smoke gases. Ventilation typically occurs via

  – voids and crack in the building envelope;
  – normal heating, ventilation and air conditioning systems
  – windows that break and fallout due to heat from the fire
  – smoke exhaust systems.

- The influence of fire suppression is partially incorporated into the fire load entity descriptions, and partially it must be assessed by the user:

  – The influence of a normal sprinkler system on the HRR development is incorporated in the fire load entity description (see section 4.6).

- The influence of the fire brigade is <u>not</u> directly incorporated in the fire load entity description. It must be taken into account through a post-processing procedure described in section 4.7.

- The influence of first-aid extinguishing is <u>not</u> incorporated in the fire load entity description.

The fire load entity approach is analogous to the procedure used in normal-temperature structural design, in which live loads are categorised depending on the use of the building, i.e. different live loads for offices, warehouses, etc.

4.1 Description of the initial fire

There are basically two ways to assess the heat release rate (HRR) in fires:

1. analysis and synthesis of experimental data
2. modelling and fire simulation.

Whenever reliable and relevant data is available, it should be used. However, the larger the initial fire is, the less relevant data exists. In this case, HRR can be estimated using modelling and fire simulation. These two approaches are described in more detail below.

4.1.1 HRR curves on the basis of analysis and experimental data

The basic constituent of the fire load entity approach is a rectangular object that releases heat according to a certain time dependent function which is determined from fire experiments. The procedure is described below for office fires:

1) First, data available in literature is compiled (an example of compilation of data relevant to office fires are shown in Figure 3 and Table 2) and given a simplified model representation (an example of this simplification is shown in Figure 4). In the model used, the growth phase of the fire is modelled by a $\sim t^p$ dependence where the power p is usually 2; after the growth phase at time t_1 the fire burns at a steady HRR until time t_2 when it starts to decay; in most cases the decay phase is best modelled by using an exponential model in which HRR decreases as $\sim \exp(-(t-t_2)/\tau)$, where τ is the parameter that characterises how fast the HRR decays.

2) Next, the compiled data is analysed to obtain parameters that allow generalisation of the results: For example, in the office workstation (WS) cases, the data are obtained from WS's of different sizes and a suitable generalisation parameter is the maximum HRR per unit area of the WS (HRR"$_{max}$). Similarly, with respect to the total heat released during the burning is the total energy released per unit area of the WS (q").

3) Next, all the characteristic fire parameters are tabulated (see Table 2) and analysed using statistical methods, see Figure 5.

4) Finally, suitably high or low fractiles[1] of the characteristic fire parameters are selected as the ones that are used to describe the fire load entities.
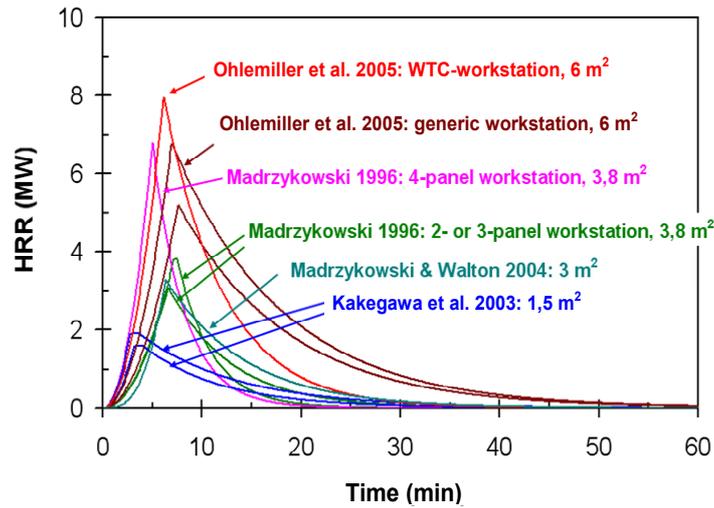
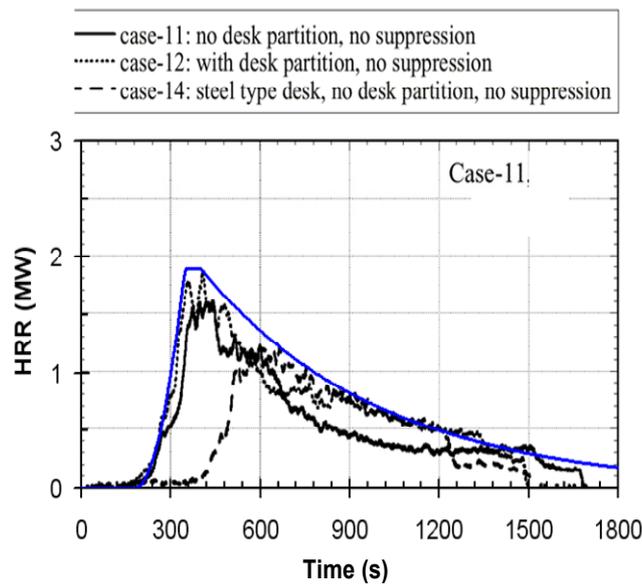Figure 3. Data from fire experiments with office workstations [3, 4, 5, 6].

Figure 4. Example of modelling of experimental HRR data by a simplified model.

---

[1] High fractiles are used for HRR''_{max}, q'' and τ and low fractile for t_g.

4. Basics of the estimation of the design fires

Table 2. Parameters describing office workstation fires.

	Madrzykowski 1996 [4] 2-panel workstation	Madrzykowski 1996 [4] 3-panel workstation	Madrzykowski 1996 [4] 4-panel workstation	Kakegawa et al. 2003 [6] case 11	Kakegawa et al. 2003 [6] case 12	Ohlemiller et al. 2005 [3] generic workstation, test 2	Ohlemiller et al. 2005 [3] generic workstation, test 3	Ohlemiller et al. 2005 [3] WTC-workstation, test 4	Madrzykowski & Walton 2004 [5] County Cook workstation	Average	Standard deviation
p	2	2	2	2	2	2	2	2	3		
t_g (s)	225	220	115	150	120	160	200	130	255	175	51
HRR_{max} (kW)	3 100	3 800	6 800	1 600	1 900	6 800	5 200	8 000	3 300		
t_1 (s)	396	429	300	190	165	417	456	368	380		
t_2 (s)	–	450	–	240	220	–	–	–	–		
τ (s)	380	210	190	480	600	660	660	360	480	447	177
Q_{tot} (MJ)	1 587	1 422	1 972	958	1 358	5 444	4 225	3 907	1 916		
D_{eff} (m)	2.19	2.19	2.19	1.38	1.38	2.75	2.75	2.75	1.97		
A_b (m)	3.78	3.78	3.78	1.50	1.50	5.95	5.95	5.95	3.04		
HRR''_{max} (kW/m^2)	820	1 005	1 799	1 067	1 267	1 142	873	1 344	1 086	1 156	294
q'' (MJ/m^2)	420	376	522	639	905	914	710	656	630	641	188
τ (s)	380	210	190	480	600	660	660	360	480	447	177
Q_{tot} (MJ)	1 587	1 422	1 972	958	1 358	5 444	4 225	3 907	1 916		
D_{eff} (m)	2.19	2.19	2.19	1.38	1.38	2.75	2.75	2.75	1.97		
A_b (m)	3.78	3.78	3.78	1.50	1.50	5.95	5.95	5.95	3.04		
HRR''_{max} (kW/m^2)	820	1 005	1 799	1 067	1 267	1 142	873	1 344	1 086	1 156	294
q'' (MJ/m^2)	420	376	522	639	905	914	710	656	630	641	188

Figure 5. Example of statistical analysis of office workstations: a) HRR/m^2, b) total heat release/m^2, c) HRR growth time factor t_g and d) HRR decay factor τ. (CDF = cumulative density function).

4.1.2 Estimating HRR curve by modelling and fire simulation

When relevant data is not available, it is possible to use modelling and fire simulation to assess the heat release rate. A novel methodology, enabled by the version 5 of the FDS fire simulation program [7], has been developed *for using the fire simulation program to predict the heat release rate*.

The methodology utilises basic combustion characteristics that are simply measurable, i.e.

- − the Heat Release Rate Per Unit Area (HRRPUA [kW/m^2]) that can be measured by the cone calorimeter and hence, due to the simplicity of the measurement, data is already available for most combustibles in our living environment

- − the Effective Heat of Combustion (EHC [MJ/kg]) that can be measured by the cone calorimeter or some other calorimetric technique such as the bomb calorimeter.

21

The other parameters that have to be specified are

- density ρ [kg/m^3]

- specific heat c [JK^{-1}kg^{-1}]

- thermal conductivity k [WK^{-1}m^{-1}]

- ignition temperature T_{ig} [°C]

- timing of the ignition and early HRR evolution: ignition time t_{ig} [s] and time-to-peak HRRPUA t_p [s]

- the amount of combustible material and its characteristic thickness [m]

- geometry: overall size (floor area and volume), voids and spatial extensions in the *xyz*-directions [m]

- the size of the initial fire (area and heat release rate) that describes the fire ignition, and its position.

The use of this methodology requires careful analysis and, naturally, the approach must be validated. The results show that – given the inherent uncertainties involved in our knowledge of the fire load of a particular building – the accuracy of HRR predictions obtained by using the methodology is sufficient for FSE usage.

The methodology and its validation are described in more detail in section 6, including examples and data used.

4.2 Selection of the number of fire load entities

To assess the number of fire load units in a space, one must have an estimate on the energy Q_{unit} [MJ] that a fire load unit can release in the fire and the fire load density q'' [MJ] that nowadays is expressed per floor area of the space considered.

The energy Q_{unit} that a fire load unit can release in the fire is a weight averaged product of the effective heat of combustion $\Delta H_{c,eff,k}$ and the mass M_k of the $k = 1, 2, ..., K$ combustibles in the fire load unit

$$Q_{unit} = \sum_{k=1}^{K} \varphi_k \cdot \Delta H_{c,eff,k} \cdot M_k \tag{4-1}$$

where the proportions sum up to unity $\sum_{k=1}^{K} \varphi_k = 1$. The effective heat of combustion $\Delta H_{c,eff,k}$ differs from the heat of combustion $\Delta H_{c,k}$ by a factor χ taking into account that in fires the combustion is rarely complete. Typical values suggested to the factor χ range around 80 %; a safe-side assumption is to set the factor $\chi = 1$. Heats of combustion of some typical fuels are listed in Table 3.

22

Table 3. Heat of combustion values of typical fuels [8].

Part 3 — Data — International Fire Engineering Guidelines

Solids	Calorific value (MJ/kg)
Anthracite	34
Asphalt	41
Bitumen	42
Cellulose	17
Charcoal	35
Clothes	19
Coal, coke	31
Cork	29
Cotton	18
Grain	17
Grease	41
Kitchen refuse	18
Leather	19
Linoleum	20
Paper, cardboard	17
Paraffin wax	47
Foam rubber	37
Rubber isoprene	45
Rubber tyre	32
Silk	19
Straw	16
Wood	18
Wool	23
Particle board	18

Conversion factor:
1MJ/kg ≈ 430 Btu/lb

Plastics	Calorific value (MJ/kg)
ABS	36
Acrylic	28
Celluloid	19
Epoxy	34
Melamine resin	18
Phenol formaldehyde	29
Polyester	31
Polyester fibre reinforced	21
Polyethylene	44
Polystyrene	40
Polyisocyanurate foam	24
Polycarbonate	29
Polypropylene	43
Polyurethane	23
Polyurethane foam	26
Polyvinyl chloride	17
Urea formaldehyde	15
Urea formaldehyde foam	14

Conversion factor:
1MJ/kg ≈ 430 Btu/lb

4.3 Propagation of fire to other igniting objects

Most commonly, a fire of a single unit can propagate to other igniting objects by

- heating due to direct heat radiation from the flames of the first ignited item
- heating due to the build-up of hot smoke layer in the space.

According to Babrauskas [9], some secondary items may ignite readily at 10 kW/m^2 heat exposure while others may sustain 40 kW/m^2, see Figure 6.

The most important issue in fire spread to other items is that the fire may grow very large. Therefore, the occurrence of such fire must be kept very unlikely by suitable fire safety measures. Here the high reliability and efficiency of automatic suppression systems are of utmost importance.
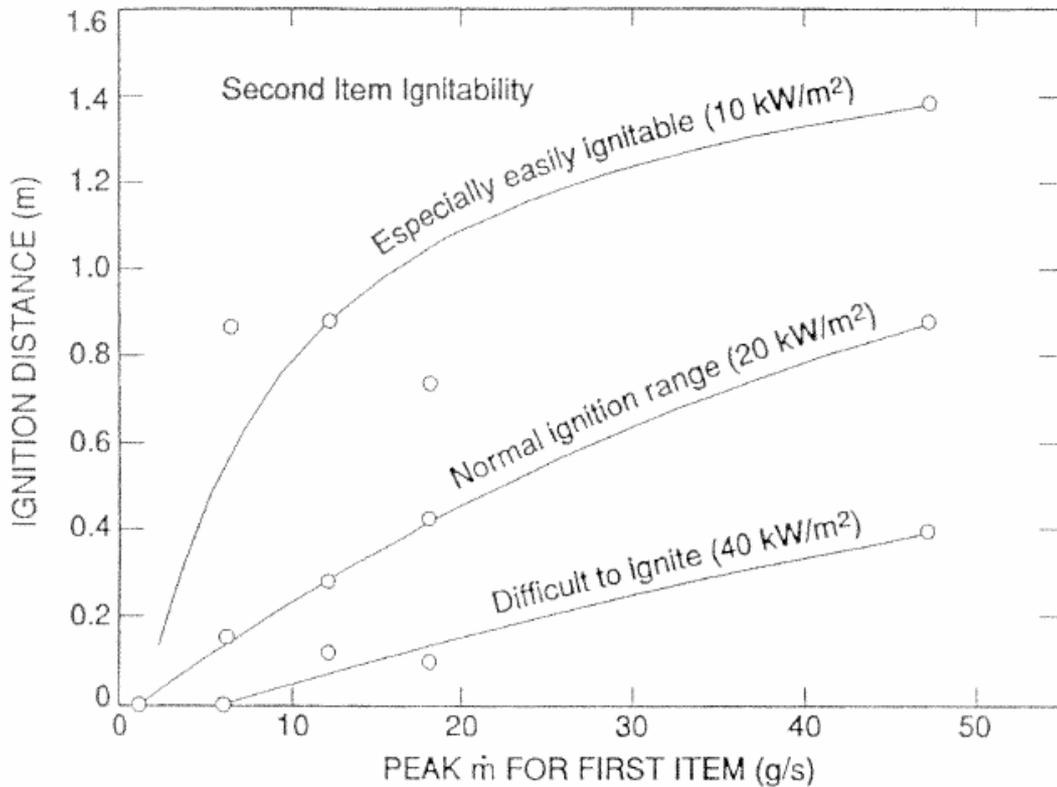
Figure 6. Relationship between peak mass loss rate and ignition distance for various ignitability levels (radiant flux) [8, 9].

4.4 Influence of first-aid extinguishers

In practice, first-aid extinguishers have a significant effect on the fire development as a notable fraction of fires is extinguished by first-aid extinguishers before they grow to an extent posing significant threats. Yet, as a safe-side assumption the influence of first-aid extinguishers is omitted in this report.

4.5 Influence of fire detection systems

The operation of fire detection systems can be modelled by using a model that describes heat exposure and the consequent heating of the sensor. It should be noted that this approach is applicable also to smoke detectors because in the initial phases of the fire there one-to-one correspondence between the smoke density and the temperature rise [8, 10].

Heating of the sensor can be described by the following equation:

$$\frac{dT_d}{dt} = \frac{1}{\tau}\left(T_g - T_d\right) \tag{4-2}$$

where T_d is the sensor temperature [°C], T_g is the temperature of the hot gases and flames from the fire [°C] and τ is a time constant [s]

$$\tau = \frac{RTI}{\sqrt{u}} \tag{4-3}$$

where RTI [$m^{1/2}s^{1/2}$] is response-time index of the sensor and u is the flow velocity of the hot gases. The simplest method to assess T_g and u is the use Alpert's [11] correlations

$$T_g - T_\infty = \frac{16{,}9 \cdot \dot{Q}^{2/3}}{H^{5/3}}, \text{ when } r < 0{,}18H, \tag{4-4}$$

$$T_g - T_\infty = \frac{5{,}38 \cdot \left(\dot{Q}/r\right)^{2/3}}{H}, \text{ when } r \geq 0{,}18H, \tag{4-5}$$

$$u = 0{,}96 \cdot \left(\frac{\dot{Q}}{H}\right)^{1/3}, \text{ when } r < 0{,}15H, \tag{4-6}$$

$$u = \frac{0{,}195 \cdot \dot{Q}^{1/3} \cdot H^{1/2}}{r^{5/6}}, \text{ when } r \geq 0{,}15H, \tag{4-7}$$

where T_∞ [°C] is ambient temperature (typically 20 °C), $\dot{Q}$ is the heat release rate (HRR) [kW], H [m] is the height from the fire origin to the ceiling and r [m] is the horizontal distance from the fire centre line. In practice, the sensor temperature development is easy to solve by the forward Euler integration method:

$$T_d(t_k + t_{k+1}) = T_d(t_k) + \frac{\sqrt{u(t_k)}}{RTI}\left(T_g(t_k) - T_d(t_k)\right)\left(t_{k+1} - t_k\right). \tag{4-8}$$

The sensor activates when its temperature reaches its activation temperature T_{act}. When RTI index, T_{act} and r are known, the sensor activation depends on the HRR growth time factor t_g and the distance between the fire origin and the ceiling H.

A smoke detector can be modelled as a fast low-temperature-activation heat sensing device. For heat detector, the following parameter values are typical:

- RTI = 50,…, 150 $m^{1/2}s^{1/2}$ [12]

- T_{act} = 57 °C or higher [13]

- $r = 0,\ldots, r_{\max,h}$, where $r_{\max,h} \approx \sqrt{A_h/2} \approx 4$ m is the maximum distance of the heat detector from the fire determined by the maximum protection area ($A_h = 30$ m^2) of a heat detector [13].

For heat detector, the following parameter values are typical:

- $RTI = 5,\ldots, 10$ m$^{1/2}$s$^{1/2}$ (uniform distribution) [8]

- $T_{act} = T_\infty + \Delta T_s$, where $\Delta T_s \approx 13,\ldots, 20$ °C (applicable distribution is the uniform distribution or the more elaborated one given in ref. [10])

- $r = 0, \ldots, r_{\max,s}$, where $r_{\max,s} \approx \sqrt{A_s/2} \approx 5,5$ m is the maximum distance of the heat detector from the fire determined by the maximum protection area ($A_s = 60$ m^2) of a heat detector [13].

4.6 Influence of automatic fire suppression systems

Properly designed, constructed and maintained automatic suppression systems [14] shall be able to detect the fire and activate accordingly. After activation, the system shall either suppress the fire or keep it under control so that the fire can be extinguished by other means. The relevant physical mechanisms are

- slowing down the fire growth

- reduction of the peak heat release rate

- cooling of the gases flowing in the fire plume and consequently reduction of the heat exposure from the hot smoke layer

- reduction of the direct heat exposure from the burning item to other items.

As a rule on thumb, one may assume that if there is an automatic suppression system that functions as designed, fire remains limited to the first igniting item.

An expert-judgement which is fairly frequently applied in FSE design may be also used. This very simplistic model is as follows:

1. Calculate the time t_{act}, e.g., using the formulae given in 4.5.

2. Look at what is HRR at the time t_{act}, $\dot{Q}(t_{act})$.

3. The design HRR, $\dot{Q}_d$, is obtained by doubling this value $\dot{Q}_d = 2 \times \dot{Q}(t_{act})$, and the fire is assumed to burn on the design HRR until the end of calculation.

4.7 Influence of fire brigade

The influence of the fire brigade depends on the time when it arrives at the fire scene, resources available and the time when being ready to start fire fighting. These issues are

thus dependent on the relative distance to the fire department and allocation of resources in community level.

There is another issue that may become important especially in fires where the performance of automatic suppression systems is inadequate. It is the ability of the fire brigade to extinguish the fire. This issue has been quantified in the NFPA Fire Protection Handbook [15] as curves on the ability of different kinds of fire fighting units to extinguish a fire of a given size. The units considered are

1. an average person with an extinguisher
2. a trained fire brigade
3. an average fire department
4. the strongest fire department.

The results can be summarised as follows:

- "an average person with an extinguisher" is likely to be able to extinguish a fire of size of $\sim 2 \text{ m}^2$

- "a trained fire brigade" is likely to be able to extinguish a fire of size of $\sim 5 \text{ m}^2$

- "an average fire department" is likely to be able to extinguish a fire of size of $\sim 50 \text{ m}^2$

- "the strongest fire department" is likely to be able to extinguish a fire of size of $\sim 100 \text{ m}^2$.

5. Design fires for different occupancies

5.1 Sports and multipurpose halls

Examples of typical fire load objects of sports and multipurpose halls are described below. In order to define a design fire for specific premises and fire scenarios, the total amount of fire load and the assumed development of fire must be determined.

5.1.1 Halls used for sports training

In halls used for sports training, the fire load and number of persons inside the building are typically low. Combustibles typical for sports training halls are listed in Table 4. However, the hall can also be used for other purposes, such as exhibitions. In this case, the amount fire load may increase considerably, and also the number of persons may rise to hundreds or even thousands. In this case, the hall is used as a multipurpose hall which is dealt with in Section 5.1.2.

Table 4. Some combustible items in sports training halls.

• Pole vault and high jump mattresses

• Miscellaneous wooden items that may be treated as
    – wooden cribs
    – wooden pallets.

• Vehicles used for service purposes

• Chairs that may be used to form small-scale audience stands
    – plastic chairs that may be piled and stacked in some corner when not in use, and placed next to each other when in use
    – wooden chairs (with configurations as plastics chairs).

• Gym bags
• Combustibles in changing rooms

5.1.2 Multi-purpose sports halls

Multi-purpose halls are typically used for sports training, competitions, exhibitions, concerts, etc. The sports training usage was treated in the previous section and the other usages are analysed separately below.

5.1.2.1 Fire loads and design fires relevant to sports competitions

All fire loads and design fires established in the previous section for sports training halls are relevant also to halls where sports competitions are held. Additional features of the sports-competition halls are, e.g.

- fixed audience stands that are typically inclined so that uppermost chairs may come rather close to the structures
- the audience stands are larger than in training halls
- There may be the media present with commentator booths, cablings and other equipment.

5.1.2.2 Fire loads and design fires relevant to concert usage

In concerts, there may be a large area covered with chairs for the audience. Another important fire load concentration is on the stage, which may be large both in horizontal and vertical direction and which may have combustible constructions, curtains and other fixed fire load. In addition to this, in many concerts, the amplifiers and other equipment of the performers may form a notable fire load.

5.1.2.3 Fire loads and design fires relevant to exhibition usage

In exhibitions, the fire load consists typically of

- exhibition booths that – if constructed so that they form an enclosure – may cause a severe, local flashover fire
- items that are displayed that may be, e.g., leisure-time vehicles such as motorbikes, buggies or caravans.

5.2 Dwellings

5.2.1 Fire load density

Holm and Oksanen [16] published in 1970 a research on fire loads of blocks of dwellings in Finland. In the study, fire load in 62 dwellings was calculated for buildings built in year 1966. Fire load density was reported using old units: dwelling's fire load was presented using the equivalent amount of dried wood that has the same energy content as the original furniture in the dwelling. Fire load per floor area was reported using the unit 'dried wood per floor area'. This fire load density can be converted to more common units by using wood's calorific value (16.7 MJ/kg).

Holm and Oksanen found that 1) different types of dwellings had roughly the same fire load density and 2) the ratio between the fire load entity of furniture and of immovable fittings differs in various parts of the dwelling so that 60 % of the whole dwelling's fire load comes from furnishing in average. However, this number is 85 % in the living room, 64 % in the bedroom and 13 % in the kitchen. The other way around, 87 % of the kitchen's fire load comes from immovable fittings.

This research analyses further the results obtained from the study by Holm and Oksanen. Analysis is done by fitting a Gumbel distribution to the fire load results. Same kind of statistical model is used also in Eurocode 1 [17]. Analysed results from fire load study by Holm and Oksanen are presented with the fire load density obtained from Eurocode 1, see Figure 7. Units used in the figure are 'dried wood per floor area'. In Figure 8, the same results are presented in more familiar units (MJ/m^2). Key figures like average value and 80 % fractile from fire load density distribution are presented in Table 5.

Figure 7, Figure 8 and Table 5 clearly point out that the fire load density in Eurocode 1 is about twice as high as presented in the study by Holm and Oksanen. Why is the difference so big? Perhaps the improved economical situation in Europe shows as increased fire load density in dwellings. However, the values presented in Eurocode 1 are based on 25–40 year old fire load density studies. Studies carried out in Sweden by Nilsson 1970 [18], Kersken-Bradley 1983 [19] about fire load in dwellings, and in Switzerland by Bryl 1975 [20], Kersken-Bradley 1983 about multi-storey buildings fire load, have had an influence to values presented in Eurocode 1.

In the studies on the background of Eurocode 1, the fire load densities were typically presented in MJ per unit area of the surfaces bounding the fire compartment (i.e. the combined area of the ceiling, walls and floor). For Eurocode 1, the fire load densities were converted to MJ per unit floor area by multiplying with a factor 5.2. This value is the ratio of bounding surfaces area and floor area in a room with a height of 2.9 m and a floor area of 3.2×4.3 m^2 (14 m^2). If the chosen room would have a height of 2.6 m and a floor area of 4×5 m^2 (20 m^2), the multiplying factor would be 4.3! The values presented in Eurocode 1 were possibly chosen to be definitely on the safe side.

a)

b)
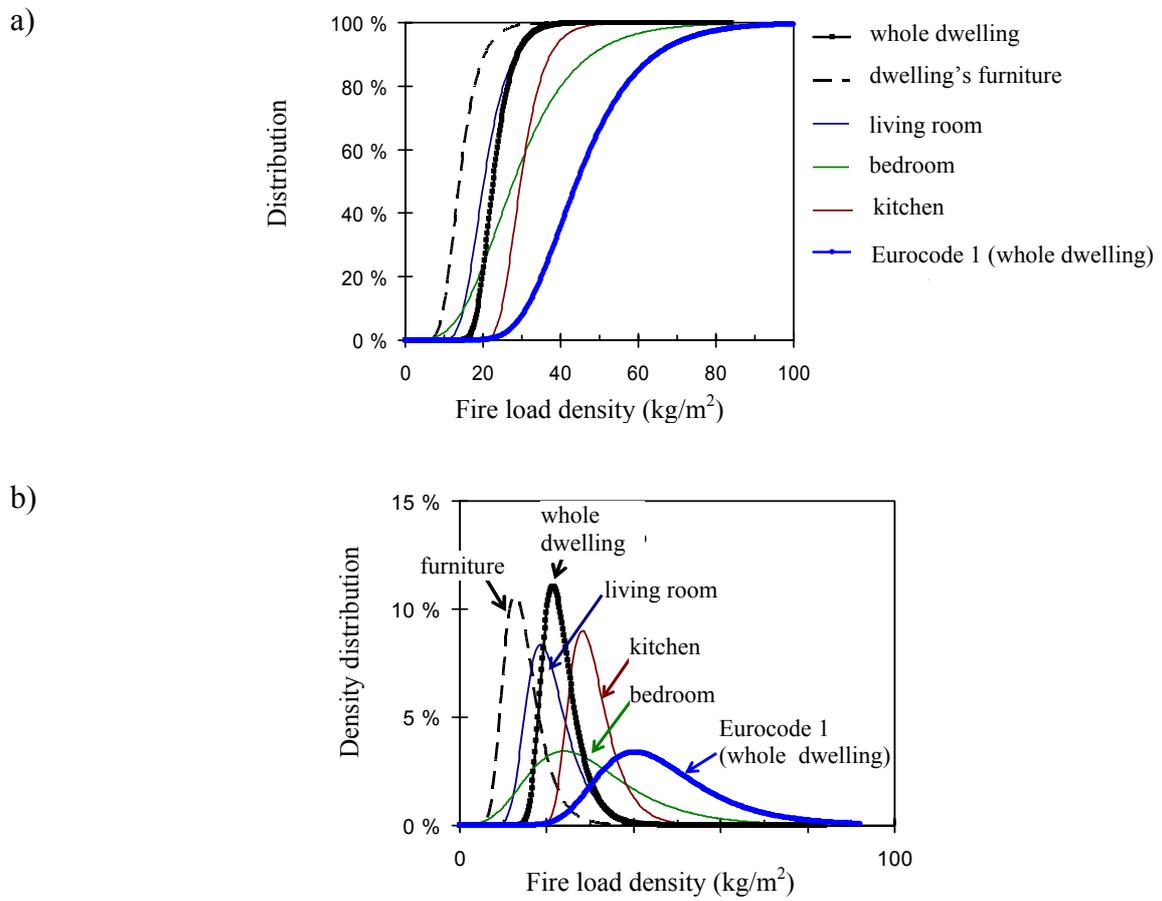
Figure 7. Comparison between results on block of dwellings fire load density distribution from Holm and Oksanen [16], a study published in 1970, and Eurocode 1 [17]. Units presented in a) cumulative distribution function and b) density function are kg dried wood per floor area (m^2).

5. Design fires for different occupancies

a)

b)
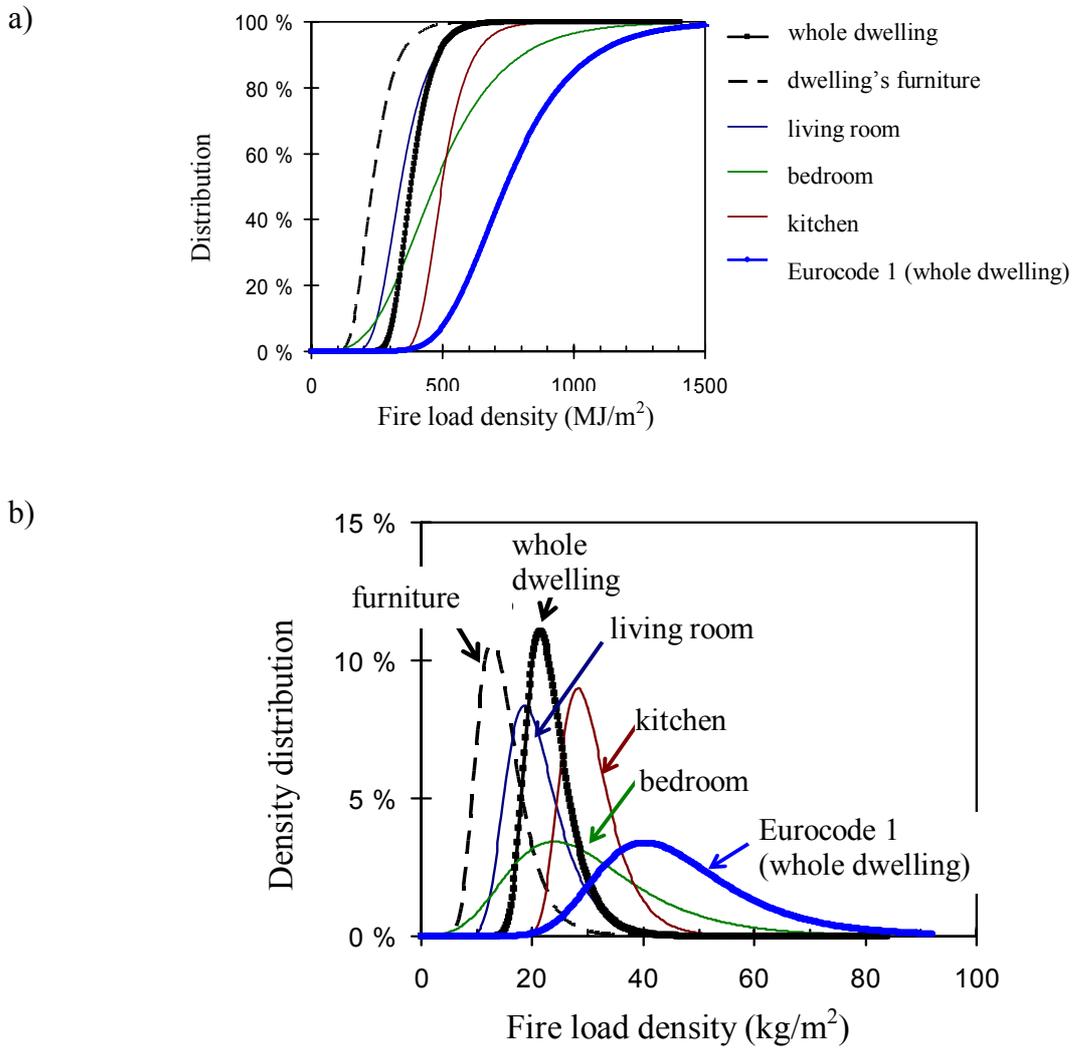
Figure 8. Holm and Oksanen [16] research results and values presented in Eurocode 1 (MJ/m^2).

Table 5. Key figures of fire load density distributions.

		Whole dwelling	Dwelling's furniture	Living room	Bedroom	Kitchen
Holm ja Oksanen [16]						
q'' (MJ/m^2)	Average value	391	247	354	505	511
	80 % fractile	443	300	422	670	574
Eurocode 1 [17]						
q'' (MJ/m^2)	Average value	780	-	-	-	-
	80 % fractile	948	-	-	-	-
USA, 1970's [21]						
q'' (MJ/m^2)	Average value	320	-	350	390	290
	80 % fractile	425	-	430	485	415
Canada 2004 [22]						
q'' (MJ/m^2)	Average value	445	-	-	-	-
	80 % fractile	565	-	-	-	-

The increase of prosperity may result in the increase of fire load in dwellings. There are no recent studies about the amount of fire load in Finland or in Europe, and the increase of fire load since 1970 is therefore unknown. However, there are two comparable studies performed in USA 1970 and Canada 2004: fire load in dwellings in USA by Cambell [21], and fire load in living rooms in Canada by Bwalya [22]. These two reports can give us the growth rate of fire load in North America. Figure 9 and Figure 10 show the results of these studies. The distribution parameters have increased about 30–40 % in 30 years.

In order to roughly estimate the fire load density in dwellings at present, the values presented by Holm and Oksanen are updated 30 % upwards. The distribution shown in Figure 11 and the parameters presented in Table 6 have been created based on the results in North America.

5. Design fires for different occupancies
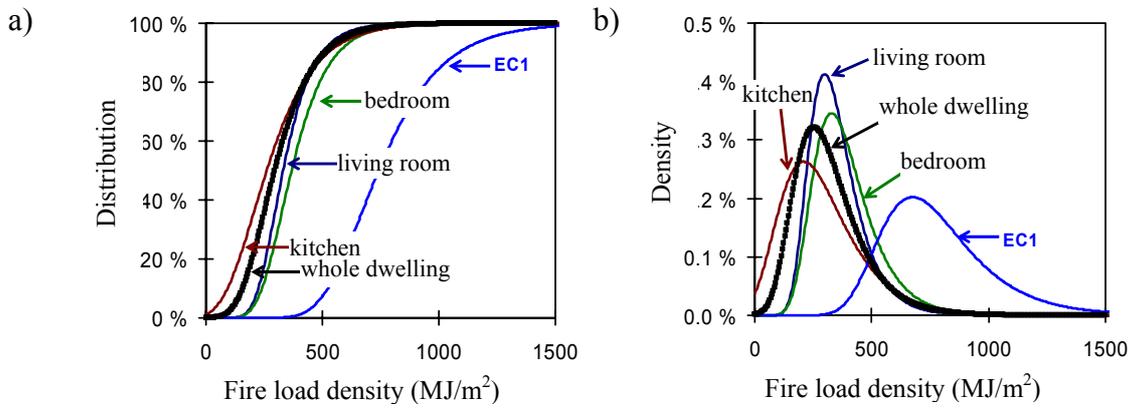
Figure 9. Fire load density of dwellings measured 1970 in USA and the values presented in Eurocode.
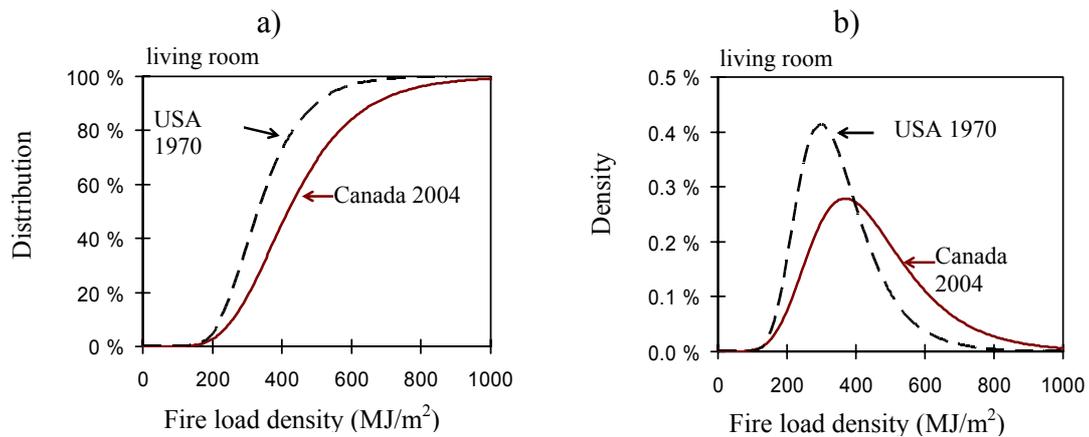
Figure 10. Fire load density in living rooms in Canada 2004 with comparison to a congruous study in USA 1970: a) cumulative distribution function and b) density function.

a)

b)
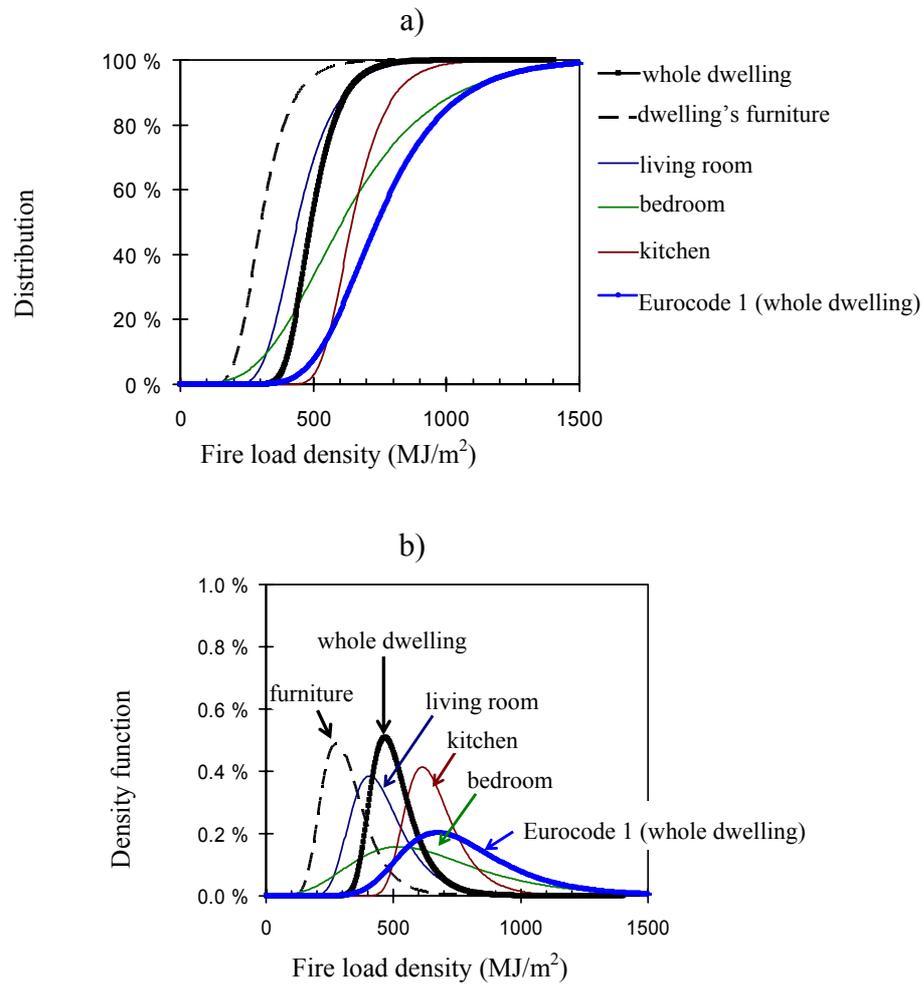
Figure 11. Results presented by Holm and Oksanen rounded up by 30 %.

Table 6. Estimation[2] of fire load in apartment buildings in Finland.

		Whole dwelling	**Dwelling's movables**	**Living room**	**Bedroom**	**Kitchen**
q'' (MJ/m^2)	Average value	509	321	460	656	665
	80 % fractile	575	390	548	871	747

[2] It should be pointed out that these values are formed like described in the text. There could be significant uncertainty with the presented values. Fire load in dwellings and other buildings should be updated with present real data.

35

5.2.2 Defining the rate of heat release

The fire load in dwellings comprises several materials that each has a specific rate of heat release. It is not possible to assess the heat release rate of the fire knowing only the fire load from the statistics. Rate of heat release can be evaluated using different fire test results and simulation. It must be recognised that the heat release rate evaluation is always case-specific.

In this study, two different approaches are used to transform the fire load entities to heat release rate:

- Trivial models can be used to evaluate the heat release rate using parameters that describe the essence of fire load [23, 24]. The uncertainties of the models are taken into account by stochastic processing.

- By using fire simulation in which all different substances are fire tested as follows: Substances are tested using the cone calorimeter, SBI or ignitability test method. Quantities describing the fire behaviour of the substances measured in fire tests and calculated in fire simulations are compared. Material parameters obtained from the tests are fixed so that the simulation reproduces the test results as accurately as possible. Those parameters are then used in the real scale to calculate the heat release [25].

The heat release rates of the materials and items forming the fire load in dwellings can be estimated by expert opinion. Approximations are usually based on values presented in literature and on experience obtained in fire tests. Only essential pieces of furniture and equipment are taken into consideration. Only materials constituting the majority of the fire load are taken into account. Typically, the fire load in a living room consists of sofas, armchairs, shelves, carpets and entertainment electronics.

Mass and calorific value are evaluated for each object. Energy content for each item is evaluated by multiplying its typical mass and calorific value (ranges of mass and calorific value rather than exact values). The fire load density can be calculated by dividing the fire load by room area. An estimate of fire load density is also available based on statistics as explained before. The number of movables in a living room can be adjusted so that the fire load density matches the statistical value.

When the number and the quality of the furniture in the room are determined, the simplified models can be applied to evaluate heat release rates of different pieces of furniture.

The rate of heat release of a room can be evaluated by adding up the rates of heat release of different movables. A partially closed space (walls and ceiling) tends to increase the fire development compared to fires that burn in open air. The effects of an enclosure can be calculated quantitatively from fire tests where same materials are burned both in open air and in a partially closed space [26].

Another possible way to determine the heat release rate is to use FDS 5 [7] fire simulation program. The fire load is calculated as before, but the heat release against time is solved directly using simulation. The FDS program has been validated by comparing calculations and fire test results. Validation studies have been performed at VTT [25, 27, 28, 29], in NIST [30, 31, 32, 33, 34, 35], and in many other research institutes [36, 37, 38, 39, 40, 41, 42]. As several references prove, the FDS simulation program is thoroughly validated, and it fulfils the National Building Code of Finland part E1 requirements for a simulation program [1].

The two approaches described above have been used to evaluate the heat release rate in a room fire. A comparison between these two methods is presented in Figure 12a). The heat release rate results of both methods look similar.
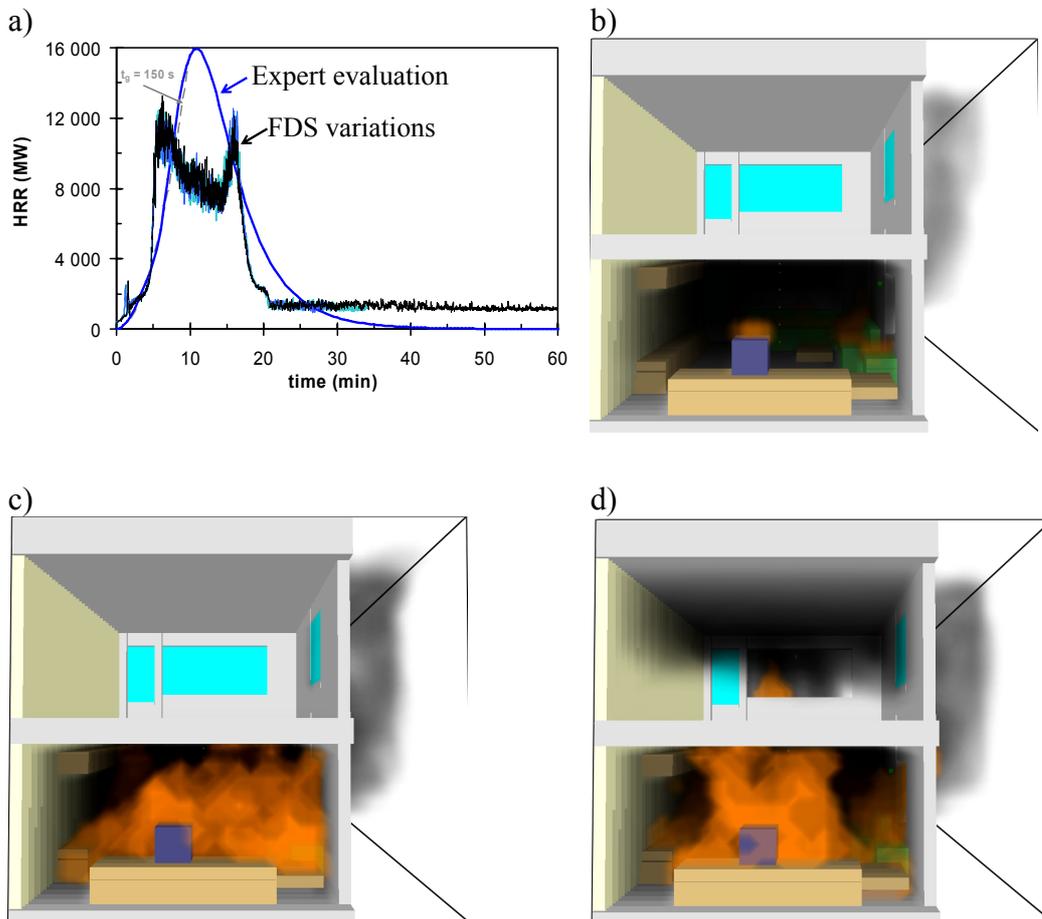

Figure 12. a) Comparison of two different approaches for determining heat release rate. An example of fire development in an apartment is shown in b)–d).

5.2.2.1 Heat release rate calculation using simplified models

Babrauskas [23, 24] has presented a model which predicts maximum heat release $\dot{Q}$ of upholstered furniture. This model is valid only when the fire can develop freely. The model predicts the heat release based on the mass of the combustibles and certain characteristic factors:

$$\frac{\dot{Q}}{\mathrm{kW}} = 210 \cdot FF \cdot PF \cdot SF \cdot FC \cdot \frac{m}{\mathrm{kg}}, \tag{5-1}$$

where the factors FF, PF, SF and FC depend on the fabric, padding, framework and shape of the upholstered furniture. Babrauskas gives the following numerical values for the parameters:

Factors	Description	Values for specific materials
FF	Fabric factor	1.00 for thermoplastic fabrics (e.g., polyolefin) 0.40 for cellulosic fabrics (e.g, cotton) 0.25 for PVC or polyurethane film-type coverings
PF	Padding factor	1.00 for polyurethane foam, latex foam or mixed materials 0.40 for cotton batting or neoprene foam
CM	Combustion mass (kg)	User's input
SF	Style factor	1.5 for ornate convoluted shapes 1.25 for intermediate shapes
		1.0 for plain, primarily rectilinear construction
FC	Frame combustibility factor	1.66 for non-combustible frames 0.58 for melting plastic 0.30 for wood 0.18 for charring plastic

The values above can be stochastically applied as in the following example:

Each parameter was randomly selected from its probability distribution. In practice, for the parameter FF, a value of 1.0 was given in 10 % of the cases, 0.4 in 70 % of the cases, and 0.25 in 20 % of the cases. In Finland, the fabric is seldom thermoplastic. Cotton and neoprene foam are evidently rarer than polyurethane foams. Therefore, the parameter PF was always set to 1.0. Furniture used in Finland is usually relatively simply shaped. So the parameter SF got a value of 1.25 in 50 % of the cases, and 1.0 in 50 % of the cases. The frame was assumed to be wood based; so the parameter FC was 0.3.

Excluding the mass, all the parameters in equation (5-1) include some uncertainty. The uncertainty was assumed to be normally distributed and described by a function with an average value of 1 and a standard deviation of 0.1.

The floor was supposed to participate to the fire. The floor thickness varied in the range of 5–20 mm. Calorific values typical for PVC plastics, 10–20 MJ/kg, where taken for floor thicknesses under 10 mm. For floor thicknesses over 10 mm, calorific values typical for wood based materials, 12–18 MJ/kg, were used. The burning intensity was

estimated using heat release rates per unit area limited by the values of typical wood and PVC (120–240 kW/m^2).

The quantities of different pieces of furniture included in the fire model were adjusted so that the energy content of the movables equalled the value of the fire load density distribution normalized to the room size. Statistical distributions on furniture's mass and calorific value are presented in Table 7. Distributions are mainly based on reference [22] and careful expert judgement. It is noteworthy that the model does not try to reproduce an exact copy of the furniture layout in a room. It rather tries to describe the factors which have a major effect on the burning. Furniture energy contents calculated from Table 7 are presented in Figure 12.

The results of fire intensity in a living room are given in Figure 14. An example of this case would be: average maximum heat release in a room with an area of 20 m^2 is about 13 000 kW (20 m^2 × 640 kW/m^2), and 80 % fractile is about 15 500 kW (20 m^2 × 770 kW/m^2).

5. Design fires for different occupancies
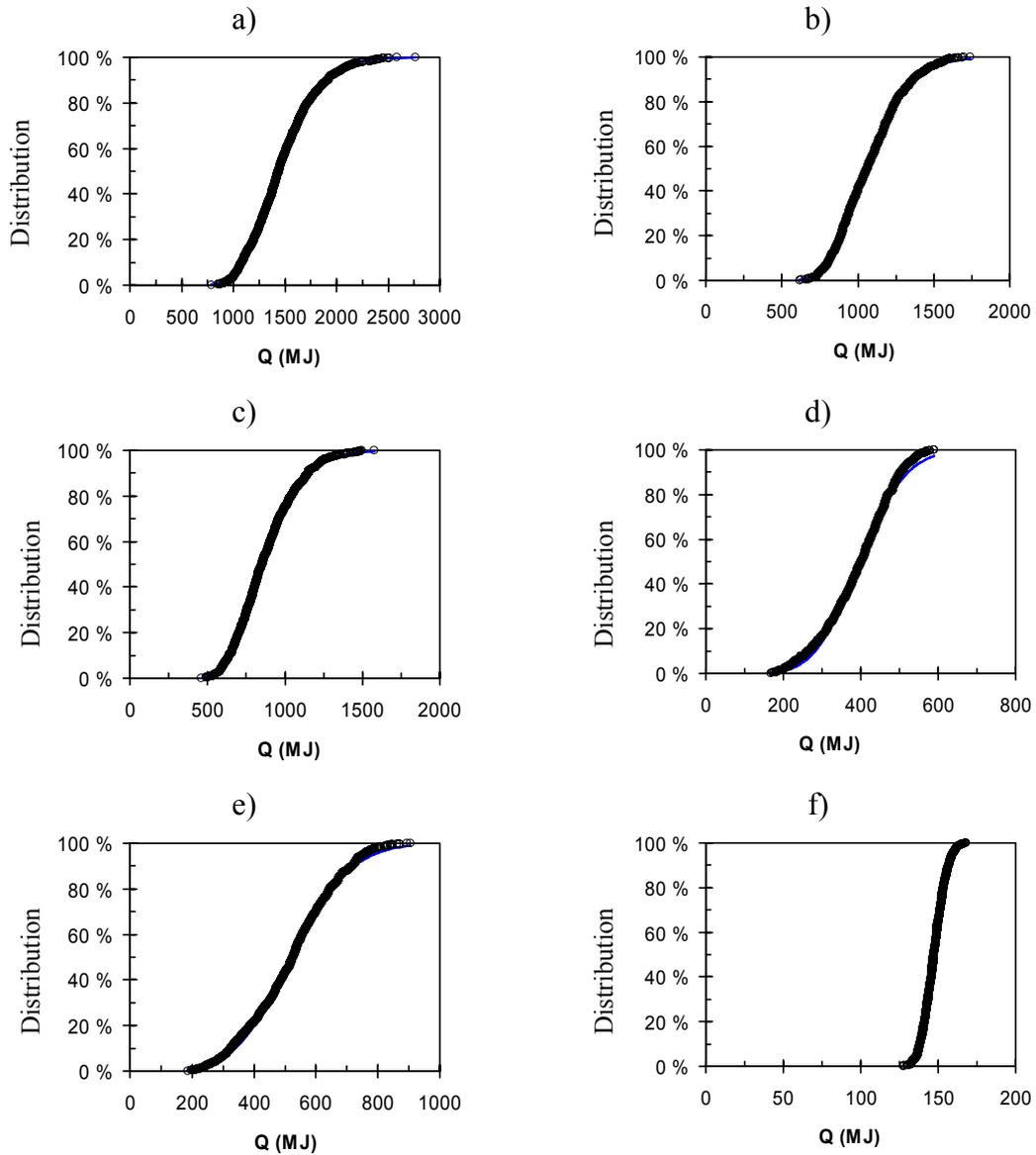
Figure 12. Energy content distributions of movables calculated from the values presented in Table 7: a) three-person sofa, b) two-person sofa, c) armchair, d) coffee table, e) book shelve and f) TV.

The maximum heat release rate value is not all needed for the fire simulation. The development of heat release from the ignition to the decay phase is also needed. The following model was used (see Figure 15):

- Heat release rate increases by the power of two, so that 1 000 kW is reached in 150 seconds.

- Maximum heat release is reached and the decay phase starts as in Figure 15. The decay phase is adjusted so that the heat release rate curve integrated with regard to time equals with the energy content released in the fire.

Table 7. Some movable-related attributes for fire engineering model.

Piece of furniture	Statistical distribution of mass	Statistical distribution of calorific value
three-person sofa	triangular distribution: min = 46 kg max = 91 kg mode = 65 kg	triangular distribution: min = 15 MJ/kg max = 33 MJ/kg mode = 18 MJ/kg
two-person sofa	triangular distribution: min = 38 kg max = 60 kg mode = 48 kg	triangular distribution: min = 15 MJ/kg max = 33 MJ/kg mode = 18 MJ/kg
armchair	triangular distribution: min = 27 kg max = 53 kg mode = 41 kg	triangular distribution: min = 15 MJ/kg max = 33 MJ/kg mode = 18 MJ/kg
coffee table	triangular distribution: min = 9 kg max = 32 kg mode = 24 kg	triangular distribution: min = 16 MJ/kg max = 18 MJ/kg mode = 20 MJ/kg
bookshelf	triangular distribution: min = 10 kg max = 48 kg mode = 30 kg	triangular distribution: min = 16 MJ/kg max = 18 MJ/kg mode = 20 MJ/kg
TV	triangular distribution: min = 4,5 kg max = 5,5 kg mode = 5,0 kg	triangular distribution: min = 27,5 MJ/kg max = 31,5 MJ/kg mode = 29,5 MJ/kg

5. Design fires for different occupancies
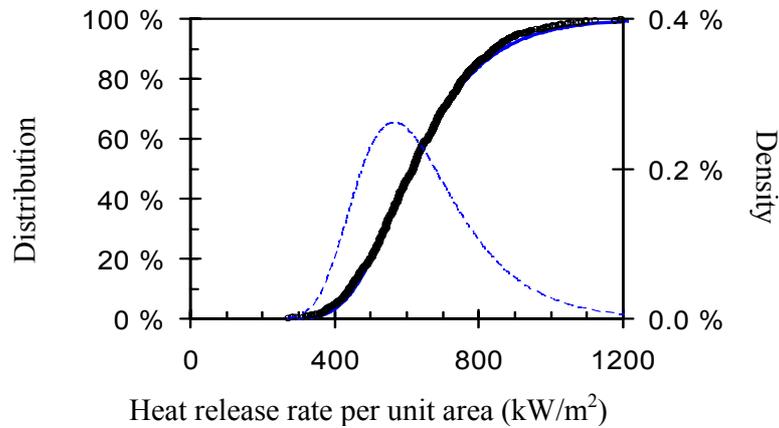
Figure 14. Intensity of fire in a living room. The distribution shows how much heat is released per floor area (average 640 kW/m^2, 80 % fractile 770 kW/m^2).
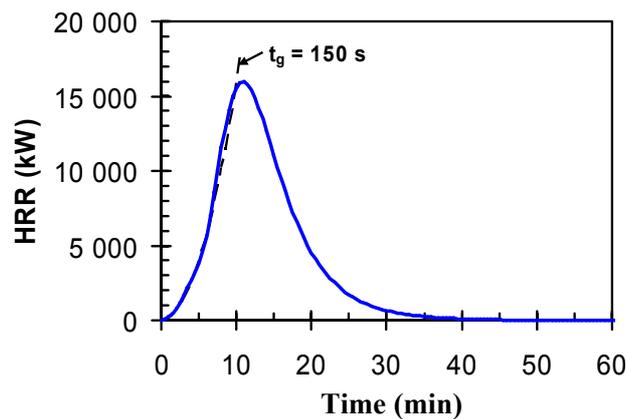
Figure 15. An example of heat release rate development.

5.2.2.2 Validation of the model

In this section, the presented model is validated by comparing calculated and tested heat release rates. Experimental data is available from three similar fire tests with a furnished room of 16m^2 performed by Blomqvist et al. [43].

The room and furnishing used in the fire experiments are shown in Figure 16a. The measured heat release rates are shown in Figure 16b. The heat release rate from the model (open space fire and oxygen restricted fire) is presented in Figure 17. The measured and modelled heat release curves are compared in Figure 18, showing good consistency.

a)

(All measurements in cm)

b)
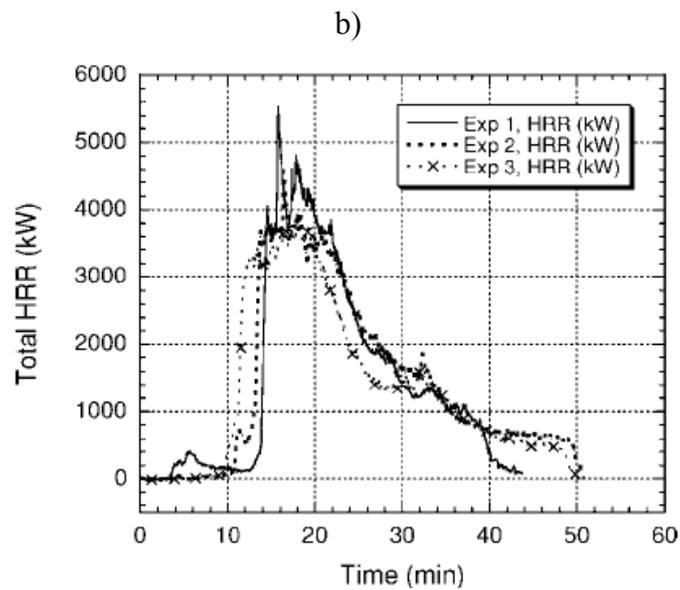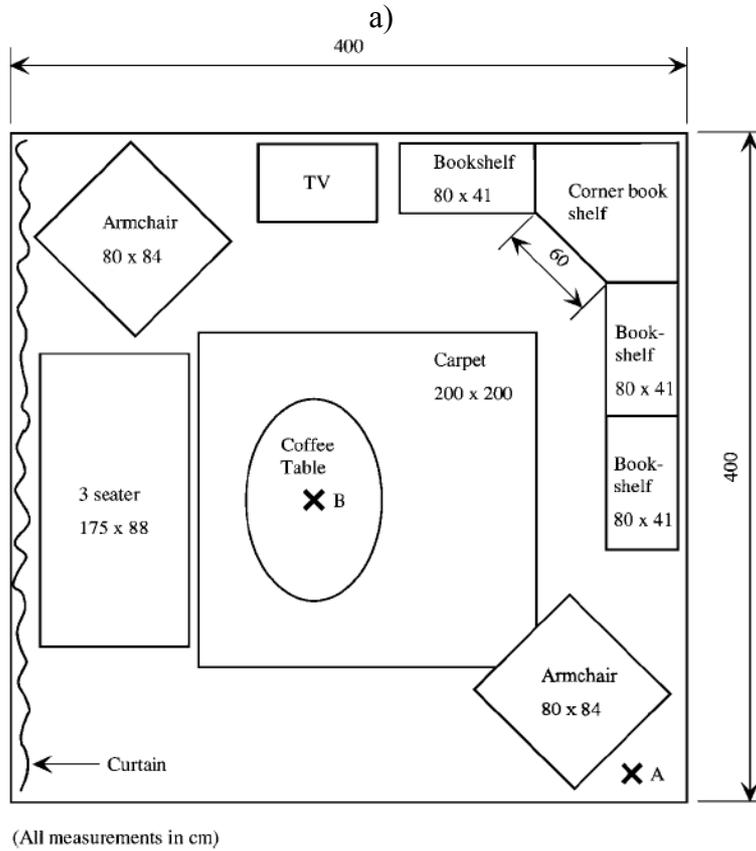
Figure 16. a) Furniture setting in the room fire experiment series performed by Blomqvist et al. [43], and b) the measured heat release rates.
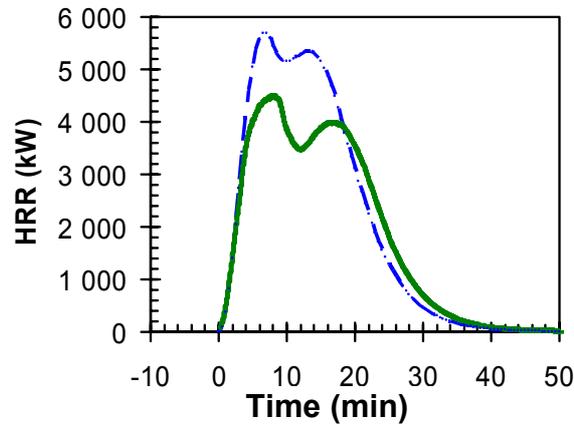
Figure 17. Modelled curves based on the results of room fire experiments by Blomqvist et al. [43]: the heat release rate curve using methodology explained above for open space fire (dashed line) and for oxygen restricted fire (solid line).
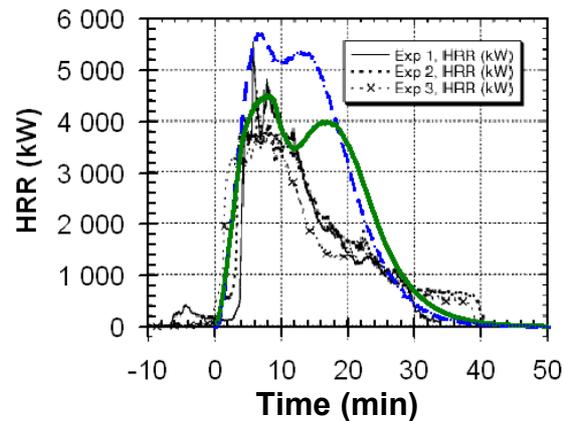
Figure 18. Comparison of heat release rates measured in the room fire tests (Blomqvist et al. [43]) and calculated using the presented model.

5.2.3 Summarising results

Table 8 summarises the analysis results for the fire load density and the rate of heat release per unit area. Distributions are formed using Gumbel distribution which fits well to the measured fire load density [17]. Gumbel distribution density function *f(x)* and cumulative function *F(x)* are

$$f(x) = \frac{\exp[-(x-a)/b - \exp[-(x-a)/b]]}{b}$$ (5-2)

$$F(x) = \exp\left[-\exp\left(-\frac{x-a}{b}\right)\right]$$ (5-3)

Gumbel distribution parameters a and b are presented in Table 8.

Table 8. Summary of results for fire load density and heat release rate per unit area.

Room	Fire load density	Heat release per unit area [a]
Living room	a = 405 MJ/m^2 b = 95.6 MJ/m^2 average = 460 MJ/m^2 80 % fractile =548 MJ/m^2	a = 565 kW/m^2 b = 134 kW /m^2 average = 642 kW/m^2 80 % fractile = 766 kW/m^2
Bedroom	a = 522 MJ/m^2 b = 233 MJ/m^2 average = 656 MJ/m^2 80 % fractile = 871 MJ/m^2	a = 805 kW/m^2 b = 191 kW /m^2 average = 916 kW/m^2 80 % fractile = 1 092 kW/m^2
Kitchen	a = 613 MJ/m^2 b = 88.9 MJ/m^2 average = 665MJ/m^2 80 % fractile = 747MJ/m^2	a = 816 kW/m^2 b = 194 kW /m^2 average = 928 kW/m^2 80 % fractile = 1 107 kW/m^2
Whole apartment	a = 467 MJ/m^2 b = 72.4 MJ/m^2 average = 509 MJ/m^2 80 % fractile = 575 MJ/m^2	a = 624 kW/m^2 b = 148 kW /m^2 average = 710 kW/m^2 80 % fractile = 847 kW/m^2

a) Heat release rate per unit area $\dot{Q}''$ distribution in the living room is calculated as explained in this chapter. Heat release rates per unit area in other rooms are defined using the living room $\dot{Q}''$-distribution and the fire load distribution for that particular room as follows: Adjusting parameters a and b for each room so that the $\dot{Q}''$ -distribution's 80 % fractile value and average value match to values defined using scaled fire load density distributions (average value and ratio between 80 % fractile and average values were used as fitting parameters).

5.3 Warehouses

5.3.1 Burning of stored goods

Direct assessment of the heat release rate of the combustibles in warehouses on the basis of experimental data involves some difficulties:

- The fires can be very large, of the order of tens of megawatts, and the amount of experimental data with so high HRR values is limited (but fortunately not entirely non-existent).

- The combustibles are not very well defined because
  - the stored items vary
  - the lay-out and storing height vary.

To overcome these problems, the methodology described in detail in section 6, enabled by the FDS fire simulation program, can be used to get *an estimate the heat release rate*. The results show that – given the inherent uncertainties involved in our knowledge of the stored goods and their configuration – the accuracy of the HRR predictions obtained by using the methodology is sufficient for FSE usage.

5.3.2 Heavy-goods vehicle fires

Relatively frequently it is possible to enter a warehouse by lorries or trailer trucks. In this section, these vehicles will be referred as heavy-goods vehicles, HGV's.

Data on HGV fires have been obtained from experiments which in most cases have addressed fire hazards in tunnels [44, 45, 46, 47]. Tunnels make up a confined geometry in which fires would most likely die out due to lack of oxygen. Hence, in most HGV-tunnel fire experiments, additional ventilation has been provided. It is important to take these issues in account when interpreting the heat release rate data of HGV-tunnel fire experiments for design fire usage in warehouses:

- The enhanced radiative feedback in the enclosed geometry of a tunnel increases the measured HRR as well as the fire growth rate (i.e., reduces the growth time factor t_g).

- The forced ventilation applied in the experiments increases the measured HRR and the fire growth rate.

The geometrical HRR enhancement factor Ψ_G has been studied by Carvel et al. [48] who propose the following expression for Ψ_G:

$$\psi_G = 24 \cdot \left(\frac{w_{fire}}{w_{tunnel}} \right)^3 + 1 \qquad (5\text{-}4)$$

where w_{fire} is the width of the fire and w_{tunnel} is the width of the tunnel. For example, if $w_{fire}/w_{tunnel} = 0.5$, the enhancement factor is $\Psi_G = 4$ and for $w_{fire}/w_{tunnel} = 0.75$, the enhancement factor is $\Psi_G = 11$.

The Runehamar experiments carried out by Ingason and Lönnermark [46] constitute the most recent set of data on really large HGV fires with the estimated peak HRR exceeding 200 MW. The HRR data recorded in these experiments are shown in Figure 19a. The theoretical combustible energy (fire load) of the burned items varied from ca. 60 GJ (60 000 MJ) to ca. 250 GJ and there appears to be a correlation between the fire load and the maximum HRR value that varied between ca. 70–210 MW, see Figure 19b. The cross section at the site of the fire in the Runehamar experiments is shown in Figure 20. The corresponding geometrical HRR enhancement factor is

$$\psi_{G,Runehamar} = 24 \cdot \left(\frac{2.9}{7.1} \right)^3 + 1 = 2.6 \qquad (5\text{-}5)$$

a)

b)
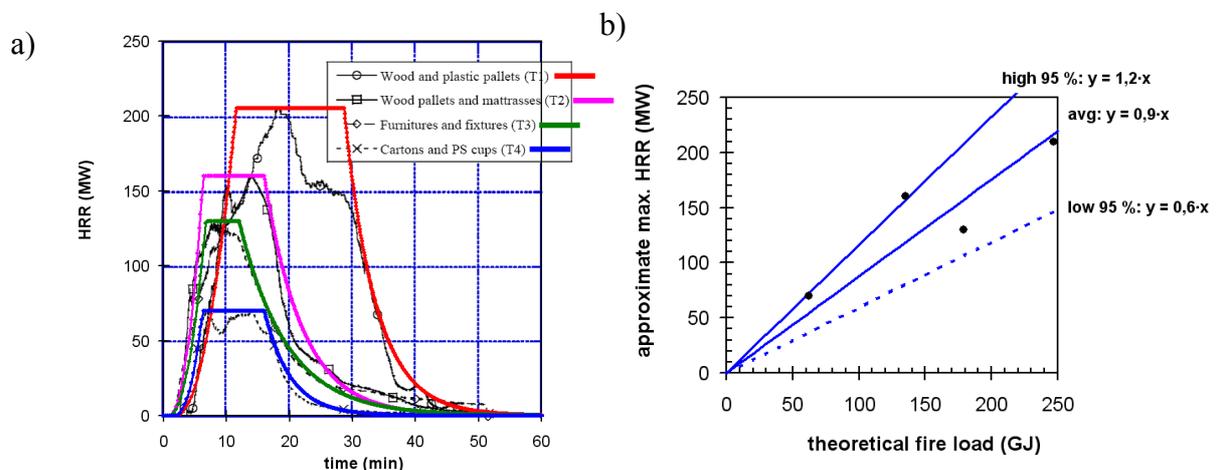
Figure 19. HRR results of Runehamar experiments [46]. The coloured curves represent t^2-models that reproduce the growth and decay phases as well as the peak HRR with reasonable accuracy (adjustment of the curves to fit the data is done only visually by the author of this document). b) Display of the apparent correlation ($R^2 = 0.97$) between the fire load of the burned item and the maximum HRR.

Figure 20. Cross section at the site of the fire in the Runehamar experiments [46] and the corresponding estimate to the geometrical HRR enhancement factor Ψ_G.

With respect to the enhancement of HRR by forced ventilation, factor Ψ_V, results of Carvel et al. [48, 49] are given in probabilistic terms. For example, the results indicate that the HRR of a HGV could increase by much more than a factor of four for a longitudinal flow rate of 3 m/s, but the most likely HRR enhancement is about a factor of four at 3 m/s and a factor of ten at 10 m/s. It was also established that the fire growth rate could increase by a factor of five for 3 m/s and by a factor of ten for 10 m/s [50]. A more rigorous quantitative analysis of the results presented by Carvel et al. in [48] is shown in Figure 21.

An application of the results of Figure 21 to estimate the ventilation induced enhancement of HRR in the Runehamar experiments where the flow speed was 2.4–2.5 m/s [45] is shown in Figure 22.

An estimate for the total HRR enhancement can be obtained by combining the ventilation and geometrical enhancement factors. For the Runehamar case, we obtain

$$\widetilde{\psi}_{total,Runehamar} = \psi_{v,Runehamar} \cdot \widetilde{\psi}_{G,Runehamar} = 2.6 \cdot \widetilde{\psi}_{v,Runehamar}, \tag{5-6}$$

where the tilde above the total and ventilation enhancement factors denotes that they are stochastic quantities. Factor $\psi_{total,Runehamar}$ is shown in Figure 23. The estimate for the non-enhanced maximum HRR is evaluated by Monte Carlo analysis. Its distribution is shown in Figure 24 and the characteristic values of the distribution are

– median value = 16 MW
– 80 % fractile = 30 MW
– 95 % fractile = 50 MW.

The International Fire Engineering Guidelines [8] suggest that for fire load a reasonable design value would be a relatively high fractile, 95 %. Following this suggestion, we propose that the design value for an HGV maximum heat release rate is the 95 % fractile, 50 MW. The resulting HRR curve and a simplified description for the FDS program are shown in Figure 25.
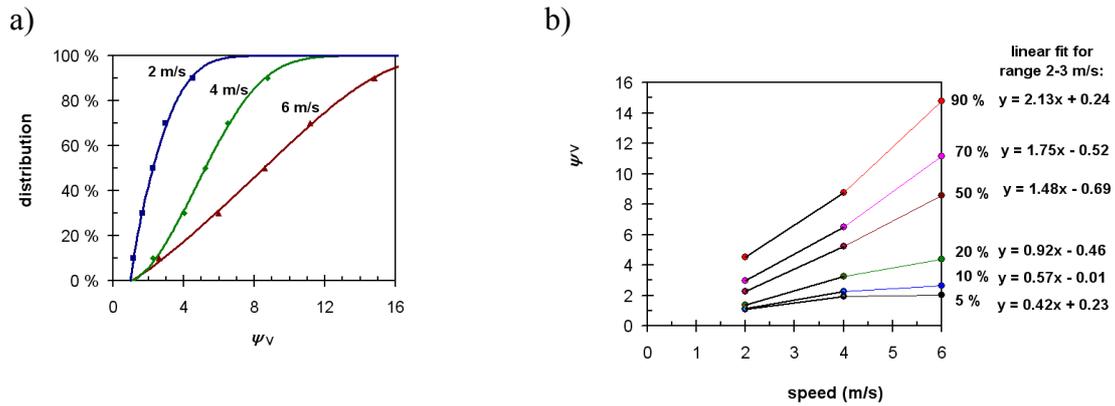
Figure 21. a) Estimated distributions of ψ_v for flow speeds based on the fractiles presented by Carvel et al. [49] and b) 5–90 % fractiles of ψ_v vs. the flow speed.
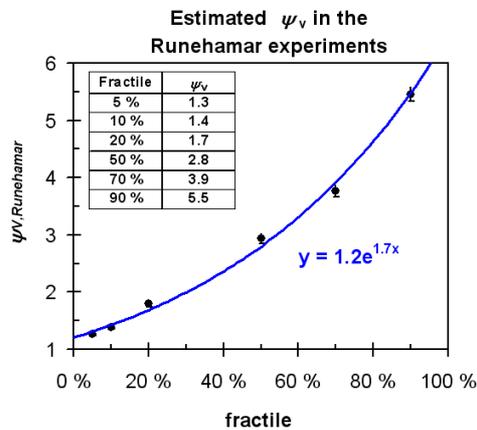
Figure 22. Estimated fractiles of the ventilation enhancement factor ψ_v in the Runehamar experiments.

49

5. Design fires for different occupancies
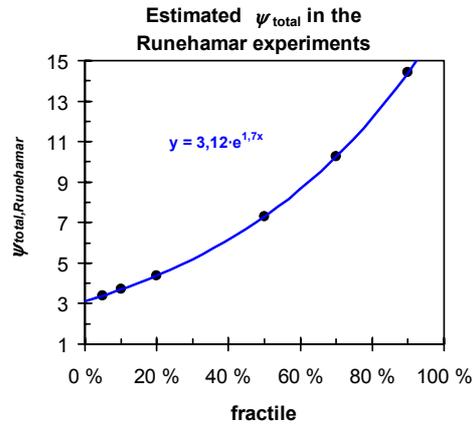
Figure 23. Estimated fractiles of the total enhancement factor ψ_{total} in the Runehamar experiments.
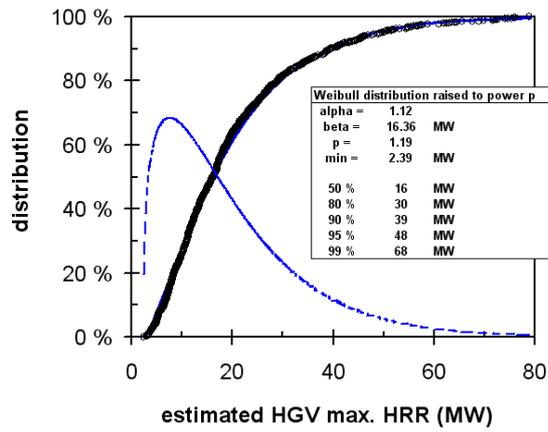
Figure 24. Estimate for the distribution of the HGV maximum heat release rate.

a)
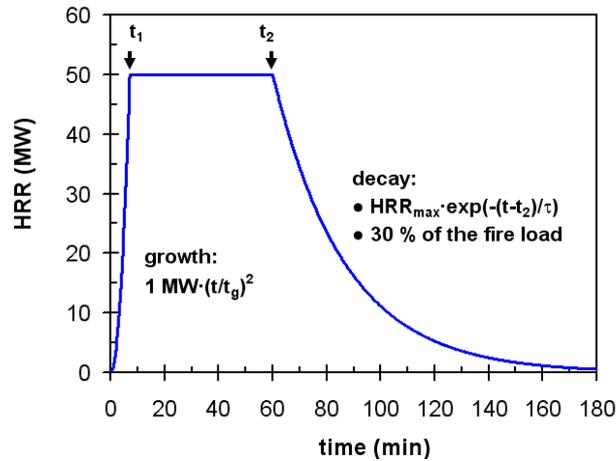
b)
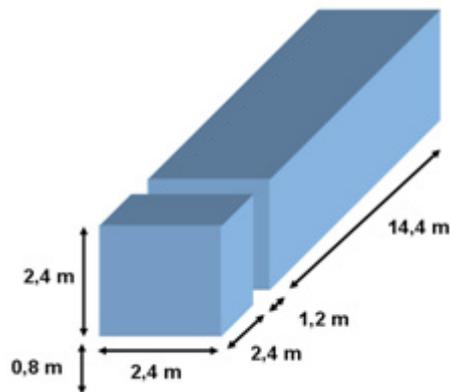
Figure 25. Estimate for HGV fire HRR corresponding to 95 % fractiles of the maximum HRR (50 MW) and fire load (245 GJ). The parameter values are: t_g = 60 s, t_1 = 424 s, t_2 = 3 600 s, τ = 1 600 s. b) Simplified description of a burning HGV for the FDS fire simulation program (dimensions selected to fit e.g. a 20 cm or 40 cm computation mesh).

5.4 Shops and other commercial occupancies

5.4.1 Heat release rates

The shop type that is common in a warehouse type of a shop includes a wide range of goods with the idea getting basically all the goods needed in household from one shop or from several shops adjacent to each other. The goods sold include

- groceries ranging from dry items such as flour and bread to moister items such as meat and beverages

- textiles including clothing, furnishing fabrics and even some pieces of furniture such as plastic/wooden chairs and tables for balconies and verandas

51

- toys, shoes, etc.

- cosmetics and cleaning products

- magazines, books and other basically cellulosic items

- entertainment electronics and their equipment

- hardware items such as tools and domestic appliance.

In the 1990's, Bennetts et al. [51] carried out a series of large-scale fire experiments to characterise fire hazards of shopping centres. The HRR data obtained in non-sprinklered experiments is presented below. The fires were very big, reaching up to 40–50 MW:

- heat release rate of a flashover fire in a shoe storage room (Figure 26)
- heat release rate of a flashover fire in a specialty shop (Figure 27).

- shape: t^p p = 3
- t_g = 150 s
- $\dot{Q}_{max}$ = 40 000 kW
- t_1 = 513 s
- t_2 = 570 s
- τ = 540 s
- Q_{tot} = 28 200 MJ
- D_{eff} = 4.5 m (estimate)
- A_b = 16 m^2 (estimate)
- $\dot{Q}''_{max}$ = 2 500 kW/m^2
- q'' = 1 760 MJ/m^2

Figure 26. Heat release rate of a flashover fire in a shoe storage room [51].

- shape: t^p, linear decay
- p = 2
- t_g = 71 s,
- $\dot{Q}_{max}$ = 47 000 kW
- t_1 = 487 s
- t_2 = 595 s
- t_3 = 2 055 s
- Q_{tot} = 47 000 MJ
- D_{eff} = 4,5 m (estimate)
- A_b = 16 m^2 (estimate)
- $\dot{Q}''_{max}$ = 2 900 kW/m^2
- q'' = 2 900 MJ/m^2
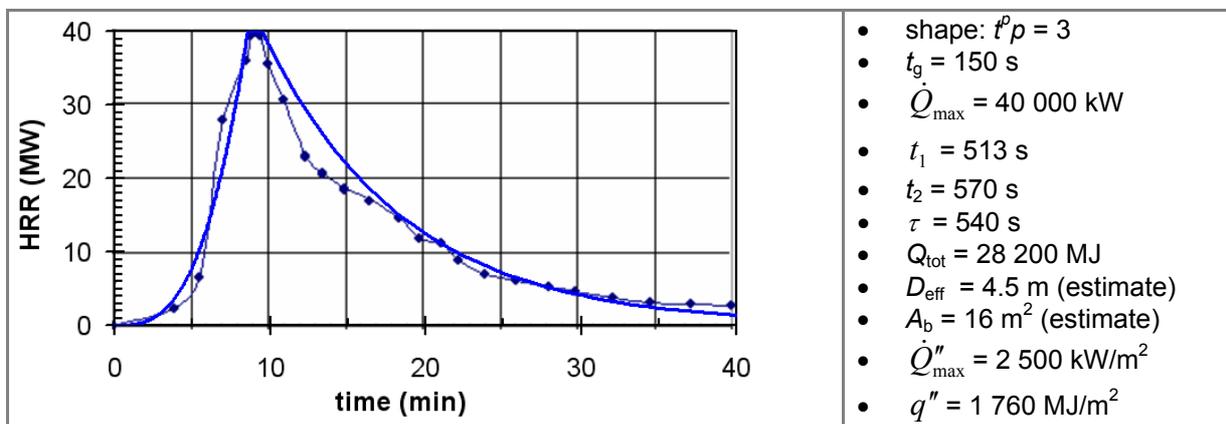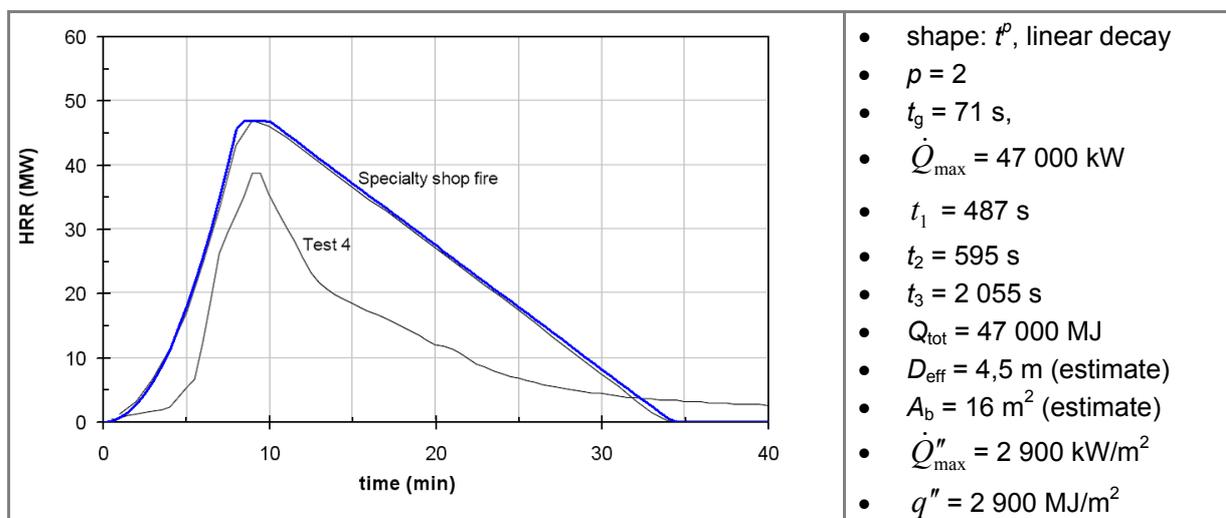
Figure 27. Heat release rate of a flashover fire in a specialty shop [51].

5.4.2 Example of influence of fire load on HRR development

In this example, the shelves system shown in Figure 28a is considered. The basic fire load characteristics are:

- Heat release rate per unit area (HRRPUA):

  – 150 kW/m^2 which corresponds typically to cellulosic materials such as wood and paper products.

  – 300 kW/m^2 which corresponds typically to fire load that may have cellulosic materials and some plastics that are fire retarded or otherwise not very highly combustible such as PET, POM, etc. Furniture fire load may fall to this or the next category.

  – 500 kW/m^2 which corresponds to such fire loads as mixtures of cellulosic materials (major ingredient) and highly combustible plastics such as ABS, PE, PP and PS, or fire load with such plastics as PET, POM, PMMA as the principal ingredient. Furniture fire load may fall also to this category.

  – 1 000 kW/m^2 which corresponds typically to fire load that contains notable amounts of non-fire retarded highly combustible plastics materials such ABS, PE, PP and PS. The other ingredients may be, e.g., cardboard boxes, etc.

  – 2 000 kW/m^2 which corresponds to fire load that has a very high percentage of non-fire retarded highly combustible plastics materials such ABS, PE, PP and PS.

- Effective heat of combustion is EHC = 20 MJ/kg

- Ignition temperature 320 °C

- Density 500 kg/m^3

- Specific heat 1 500 JK^{-1}kg^{-1}

- Thermal conductivity 0.2 WK^{-1}m^{-1}

- Ignition delay is taken as zero (instant ignition as the fuel surface temperature rises to the ignition temperature).

Other characteristics are summarised in Figure 28b. Illustration of the influence of the fuel HRRPUA on the strength of the fire is given in Figure 29 and evolution of the shelf system HRR for different fire load HRRPUA values is demonstrated in Figure 30.

5. Design fires for different occupancies

a)

Fire load entity
Fire load unit:
EHC = 20 MJ/kg
HRRPUA = 150-2000 kW/m^2

Initial fire:
area = 1 m × 0,1 m
height 0,1 m
HRRPUA 5000 kW/m^2
HRR = 500 kW

lowest shelf at
level 0,1 m
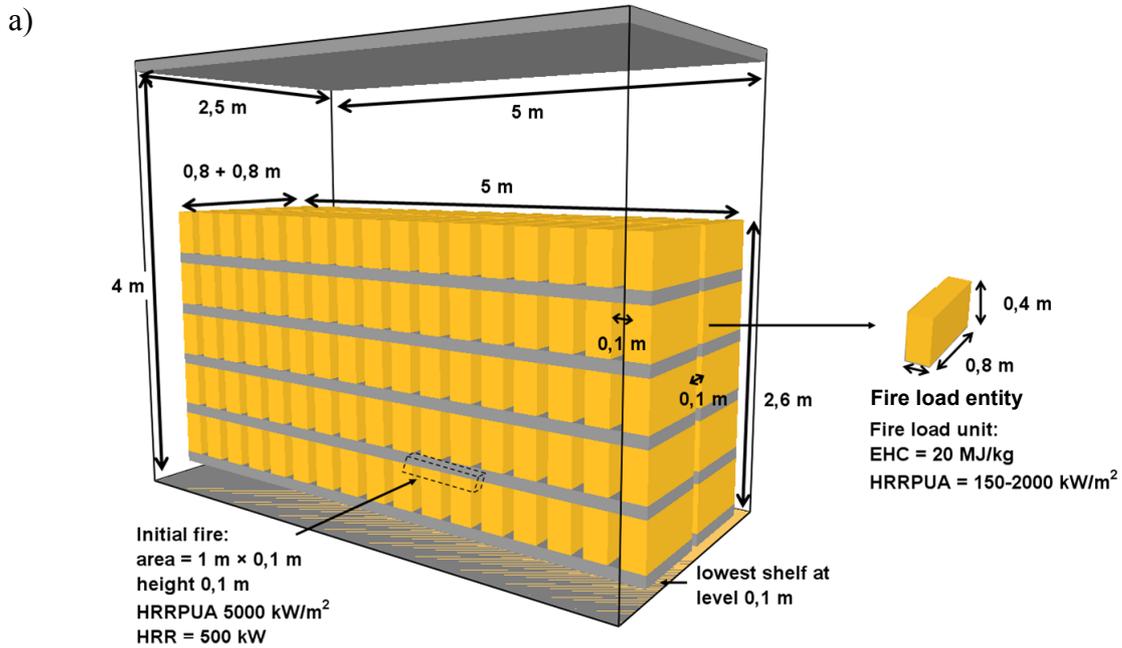
b)

Fuel envelope volume V_{FE}	22.1 m^3
Fuel envelope area A_{FE}	51.84 m^3
Floor area	8.5 m^2
No. packages	136
Fuel volume V_F	8.704 m^3
Single package exposed area:	
upper level	0.96 m^2
others	0.8 m^2
Fuel exposed area A_F	111.52 m^2
Filling ratio = V_F / V_{FE} =	39 %
Burning area ratio = A_F / A_{FE} =	215 %
Fuel density ρ_F	500 kg/m^3
Fuel mass M_F	4352 kg
Fuel heat of comb. ΔH_F	20 MJ/kg
Fire load $Q_F = \Delta H_F \times M_F$	87040 MJ
Aisles around	1 m
=> total floor area A_f	25.9 m^2
=> fire load density q"	3361 MJ/m^2

Figure 28. Model for the shop shelve fire load entity: a) schematic presentation and b) some calculated characteristics.

a)
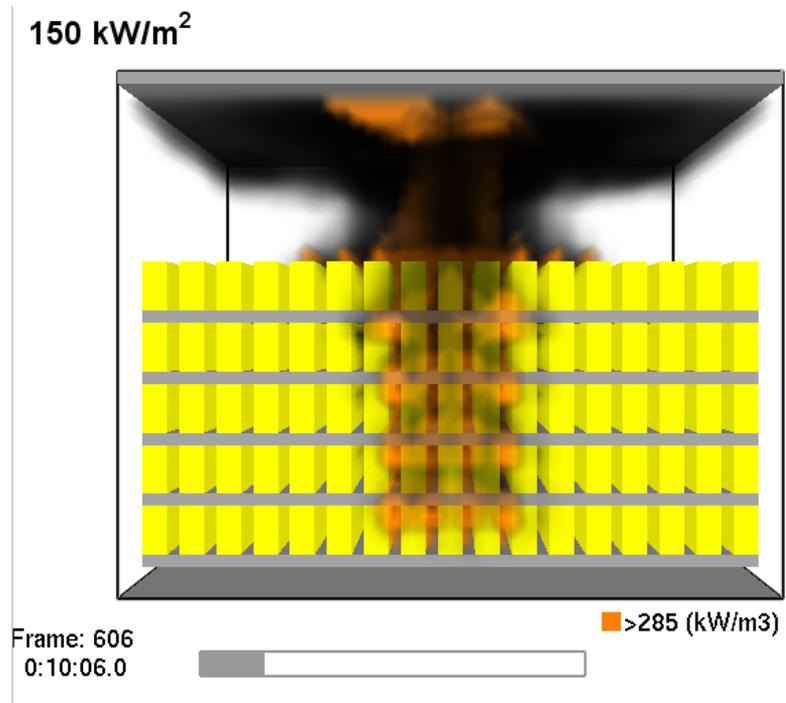
b)
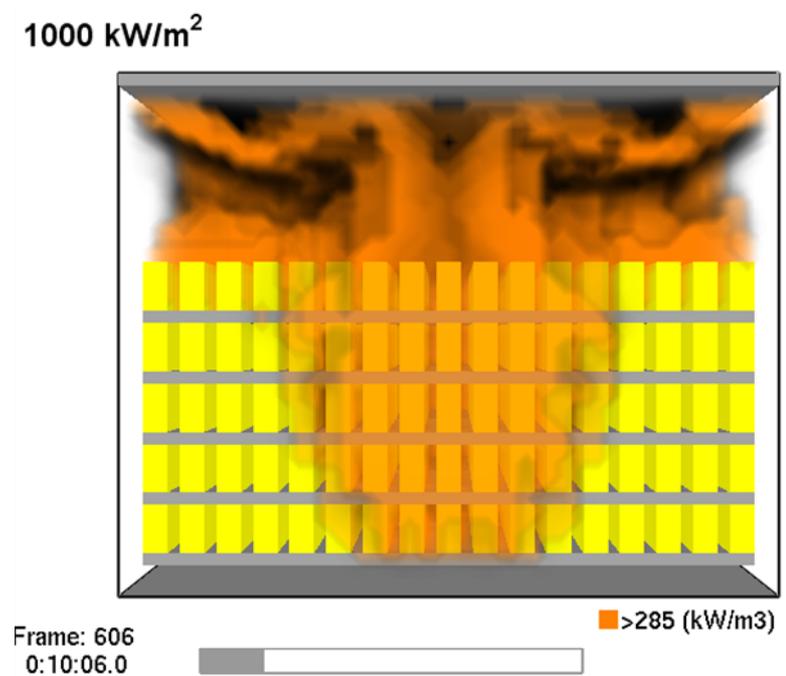
Figure 29. Illustration of the influence of the fuel HRRPUA on the strength of the fire: a) fuel HRRPUA = 150 kW/m^2 corresponding to cellulosic materials such as wood and paper products and b) fuel HRRPUA = 1 000 kW/m^2 corresponding to fire load that contains notable amounts of non-fire retarded plastics materials such ABS, PE, PP and PS.

5. Design fires for different occupancies
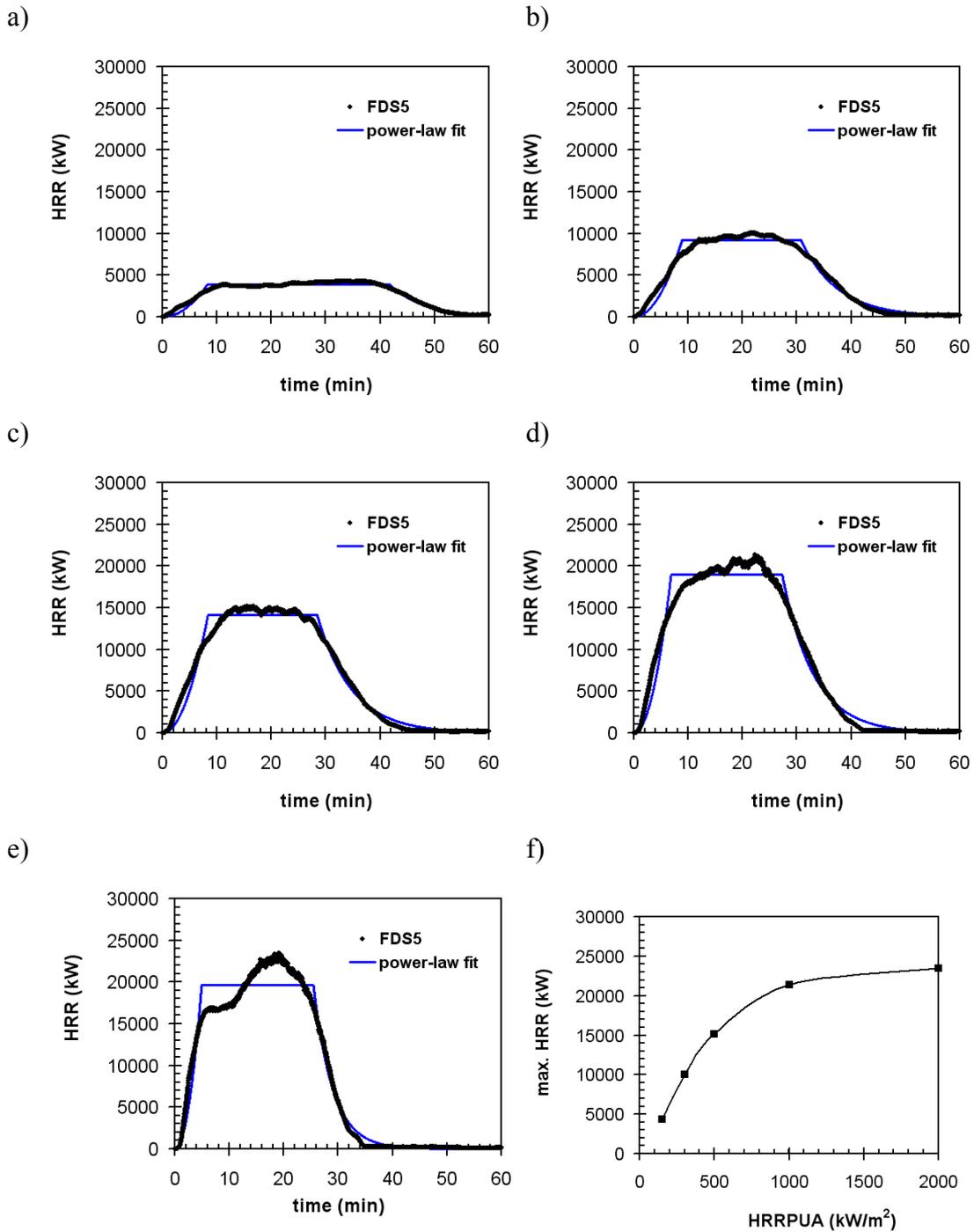
Figure 30. Evolution of the shelf system HRR for different fire load HRRPUA values: a) 150 kW/m^2, b) 300 kW/m^2, c) 500 kW/m^2, d) 1 000 kW/m^2, e) 2 000 kW/m^2 and f) maximum HRR vs. HRRPUA. The blue curves in a-e show t^2-shaped fits to FDS results.

6. Predicting heat release rate and data used

6.1 Overview of the prediction methodology

The fire simulation program FDS5 includes possibilities for calculating the pyrolysis and burning rates on the basis of the reaction kinetics of the material. This approach can already produce very good results regarding modelling of small-scale fire experiment data (typically the cone calorimeter data), see e.g. Figure 31. As there is extensive research going on related to this topic, e.g. [52, 53, 54], also large-scale heat release rate (HRR) predictions will evidently be possible in the forthcoming years. Yet, meanwhile, cruder phenomenological solutions are presented.

a)   b)
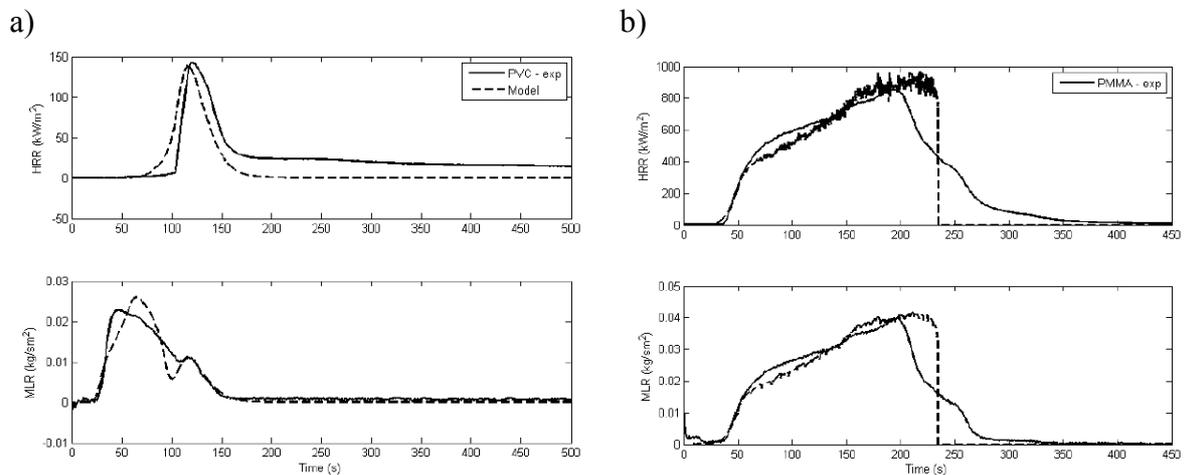
Figure 31. Examples of FDS5 predictions of small-scale fire experiment data (the cone calorimeter) on the basis of the material reaction kinetics: a) PVC and b) PMMA [55].

The methodology described in this report utilises the basic, simply measurable, combustion characteristics, i.e.

- the Heat Release Rate Per Unit Area (HRRPUA [kW/m^2]) that can be measured by the cone calorimeter and hence, due to the simplicity of the measurement, has been measured for most combustibles in our living environment.

- the Effective Heat of Combustion (EHC [MJ/kg]) that that can be measured by the cone calorimeter or some other calorimetric technique such as the bomb calorimeter.

The other parameters that have to be specified have been defined in section 4.1.2.

6.1.1 Heat release rate per unit area

The fire load in practical applications comprises several materials/products that each have a specific heat release rate per unit area, abbreviated as HRRPUA, and addressed below with the symbol $\dot{Q}''$, where Q refers to heat, the superscript-dot is the notation of temporal change and the superscript-double-prime refers to area-specific quantity. It is a quantity that is dependent on the material and the heat exposure to the material.

The dependence of HRRPUA on the heat exposure, i.e., the heat flux impinging the surface of the material/product is a more challenging problem as the actual surface heat flux varies considerably during the fire development. The most commonly used heat exposure in cone calorimeter experiments is 50 kW/m^2, chosen as a representative of a typical fire exposure. Guided by this selection, HRRPUA values corresponding to the 50 kW/m^2 heat exposure are considered as the advisable values to be used in the methodology.

To reduce the work needed in finding the appropriate HRRPUA values and to make the methodology simpler, it is convenient to categorise the combustible materials. One obvious division is that of solids and liquids. Within solids, a working classification is division to

- cellulosic materials and
- other materials (in a simple approach this means plastics).

Naturally, if the combustibles are definitely known in the building design phase, there is no reason to stick to this categorisation but use the data relevant to the particular materials: such a case may be, e.g., a chemical warehouse intended for storage of some defined chemical or a limited range of chemicals.

6.1.1.1 HRRPUA of cellulosic materials

Examples of the Heat Release Rate Per Unit Area (HRRPUA) for cellulosic materials are shown in Figure 32 [56] and Figure 33 [57].

a)

b)

c)

d)
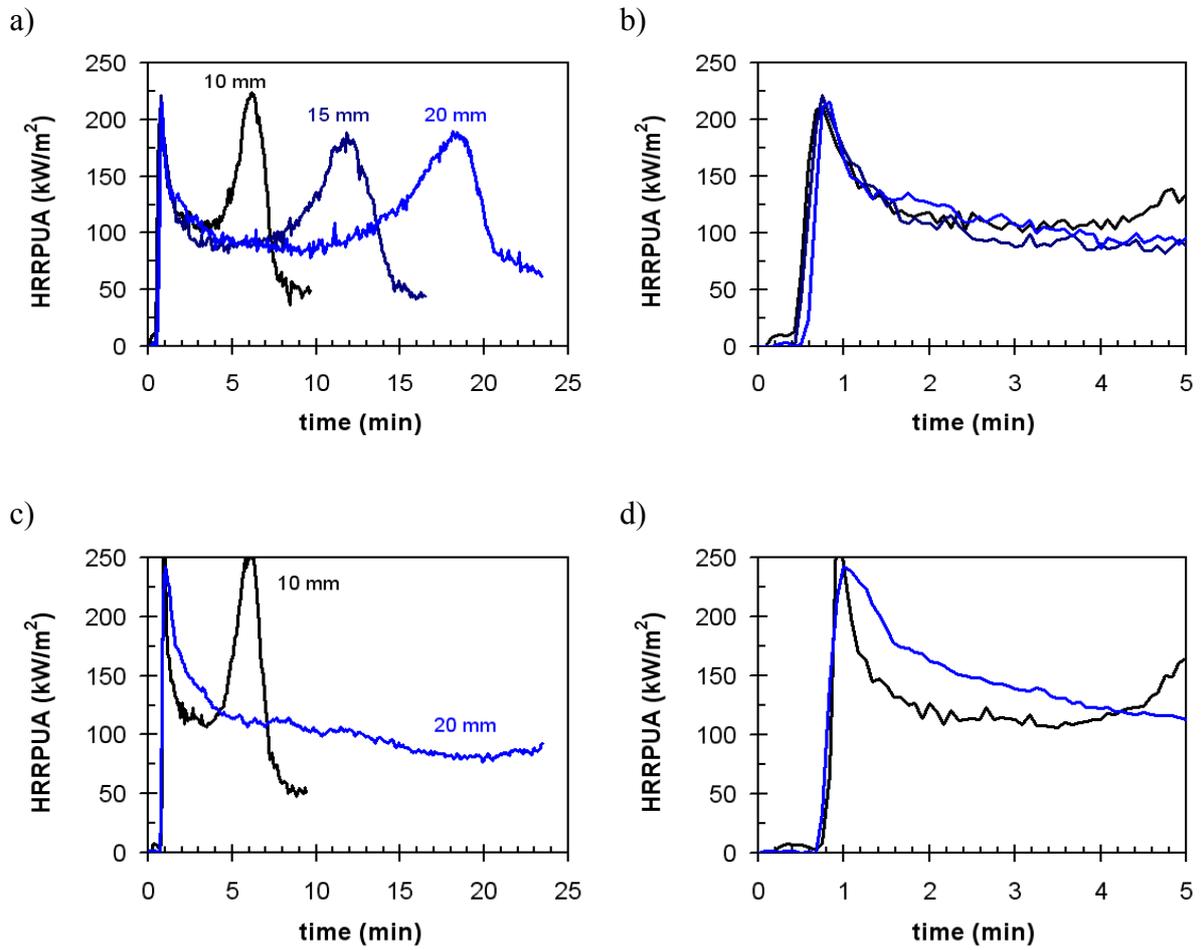
Figure 32. Examples of cone calorimeter data on wooden samples at heat exposure of 50 kW/m^2: a) and b) Finnish pine with three thicknesses (b shows the first 5 minutes of the experiment), and c) and d) Finnish spruce with two thicknesses (d shows the first 5 minutes of the experiment) [56].

a)

b)
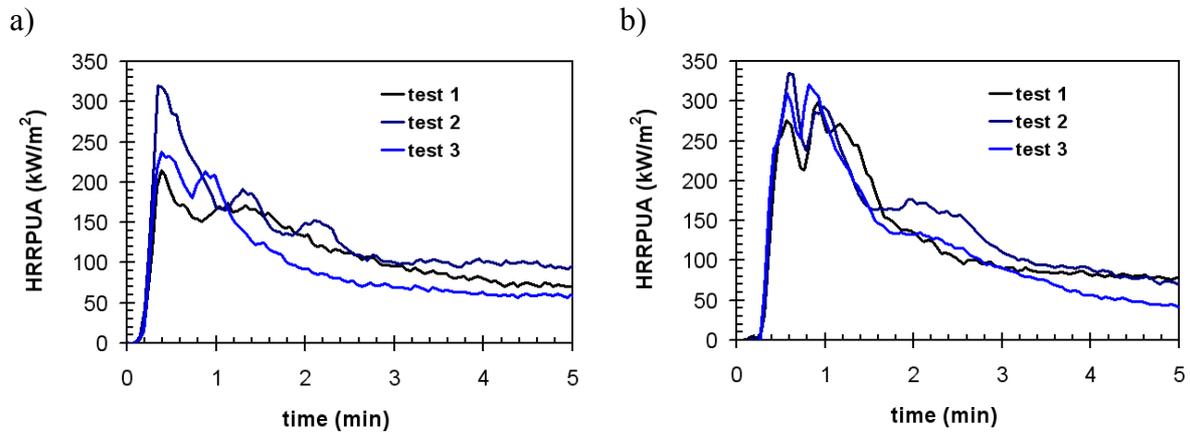
Figure 33. Examples of cone calorimeter data on paper/cardboard samples at heat exposure of 35 kW/m^2: a) about 400 g of paper stacked dwelling and b) paper stacked dwelling covered with cardboard. Data from [57].

6.1.1.2 HRRPUA of plastic materials

The class "plastics" is obviously too wide and shall be subdivided. This subdivision is based on the heat of combustion of the material. It is commonly known that some materials burn more intensively than others. Typically (but not always), the following can be observed: faster burning corresponds to higher heat of combustion. The categorisation proposed for plastics is the following:

- EHC < 10 MJ/kg: e.g. PFTE (teflon), heavily halogenated plastics

- 10 MJ/kg ≤ EHC < 20 MJ/kg: e.g., different PVCs, fire retarded plastics

- 20 MJ/kg ≤ EHC < 30 MJ/kg: e.g., PMMA (plexiglass), polycarbonate, PU, EPDM (rubber)

- 30 MJ/kg ≤ EHC < 40 MJ/kg: e.g., nylon, ABS

- EHC ≥ 40 MJ/kg: e.g., PE, PP.

The correspondence between the EHC classified according to the above scheme and the peak HRRPUA, measured using the cone calorimeter with heat exposures of 40 kW/m2 and 70 kW/m^2, is exemplified in Figure 34. A clear representation of the combustibility ranking of plastics is provided in a presentation by Lyon & Walters [58] where they plot 1) the heat release rate in a micro-scale test, i.e., the TGA/DTA test, and 2) the average

flaming HRRPUA as a function of the "heat-release capacity[3]". These results are shown in Figure 35.

a)

b)
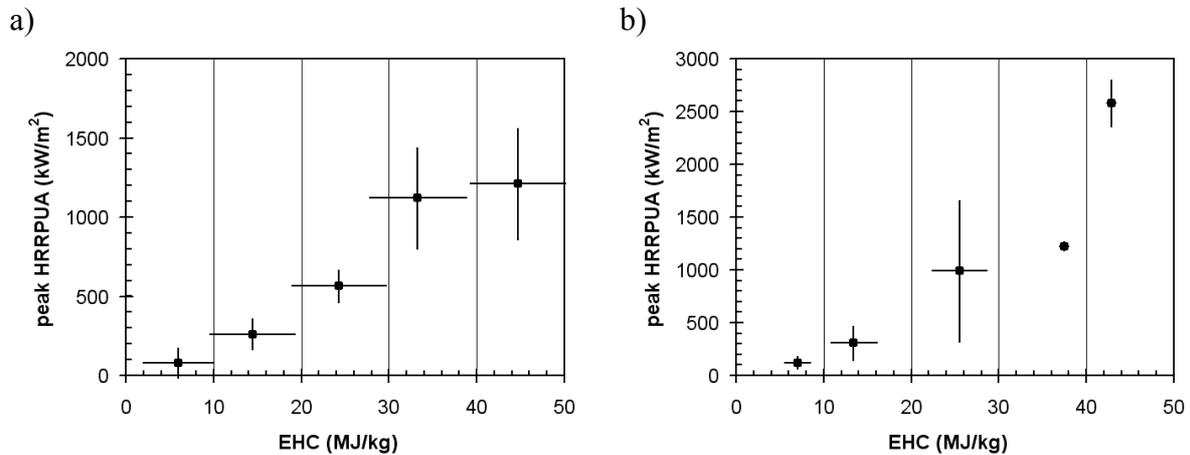
Figure 34. Examples of cone calorimeter fire experiment data on plastics at heat exposure of a) 40 kW/m^2 and b) 70 kW/m^2. Data taken from [59] and averaged over five EHC classes: EHC < 10 MJ/kg, 10 MJ/kg ≤ EHC < 20 MJ/kg, 20 MJ/kg ≤ EHC < 30 MJ/kg, 30 MJ/kg ≤ EHC < 40 MJ/kg and EHC ≥ 40 MJ/kg.

Examples of cone calorimeter HRRPUA curves for plastics are shown in Figure 36. Figure 37 shows examples on the effect of the cone calorimeter heat exposure level on the HRRPUA curves.

a)

b)
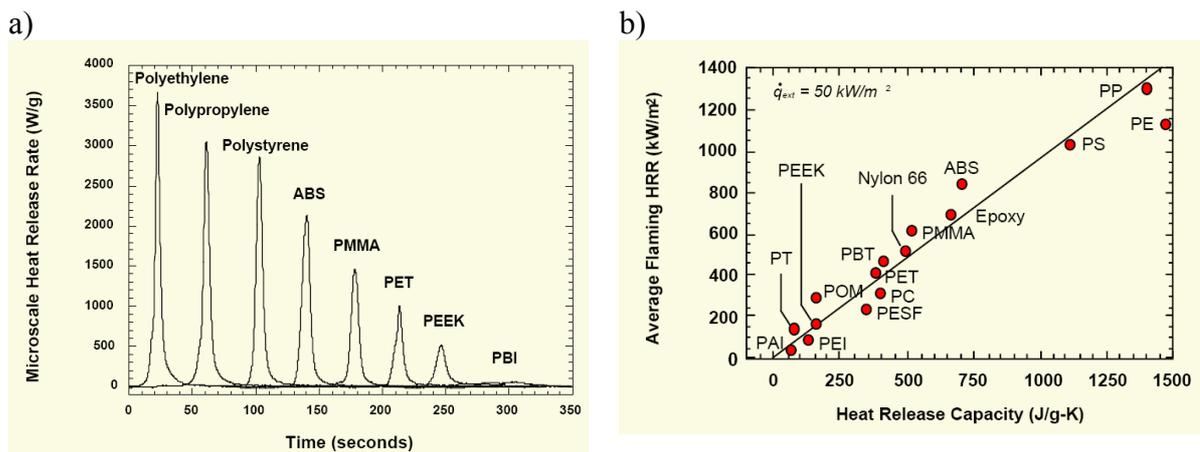
Figure 35. Examples of combustibility ranking of plastics given by Lyon & Walters [58]: a) TGA/DTA data and b) HRRPUA vs. the heat release capacity of the material.

---

[3] A quantity that depends, among other factors, on the heat of combustion of the material.

6. Predicting heat release rate and data used

a)

b)

c)

d)

e)
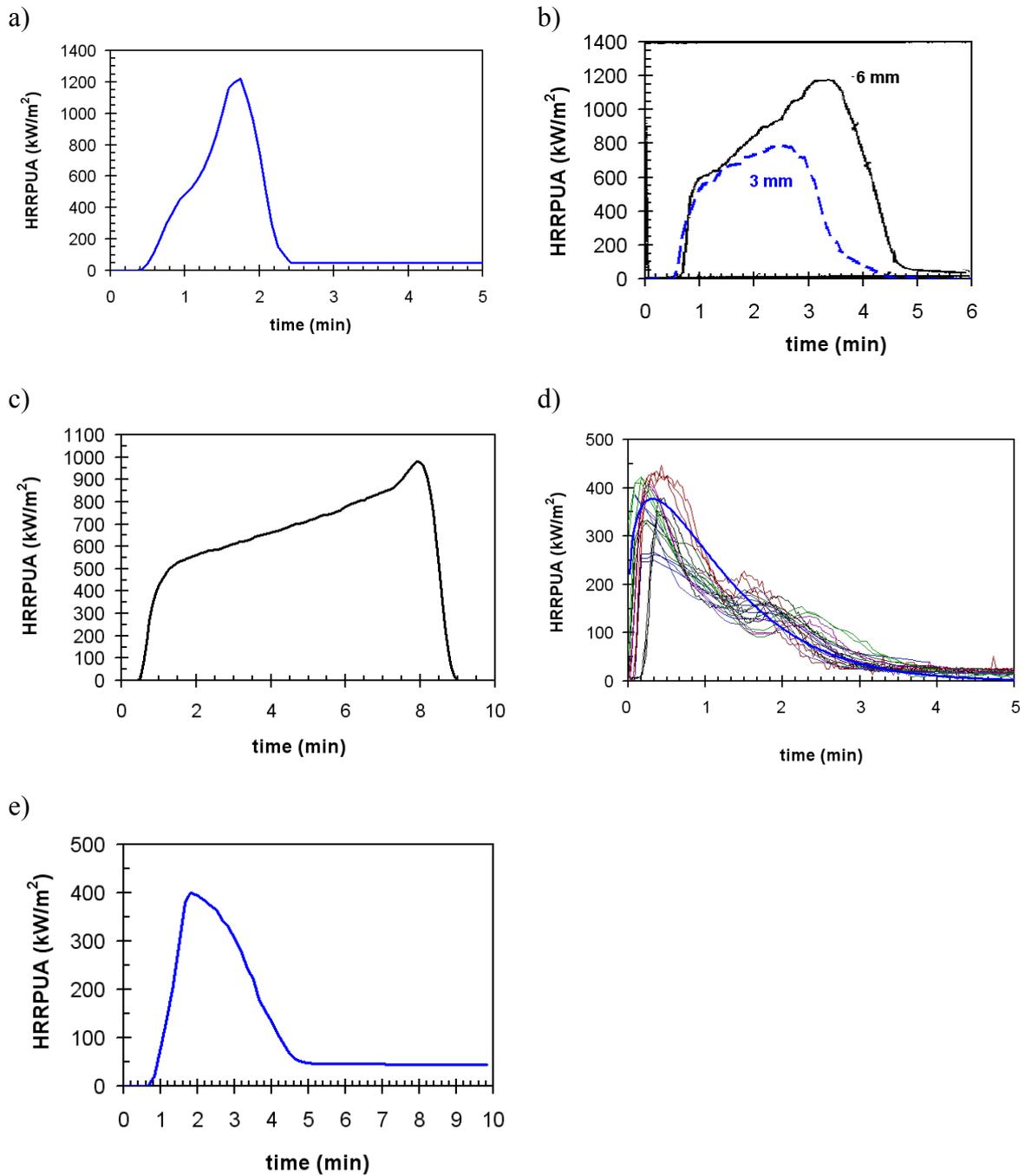
Figure 36. Examples of cone calorimeter data on paper/cardboard samples at heat exposure of 50 kW/m^2: a) 3 mm thick PP, b) ABS: the dotted curve is a 33-g or about 3-mm plastic sample from a washing machine [60] and the solid curve data from [61], c) black PMMA (plexiglass), 12 mm [62], d) flexible PU foam studied in the SAFIR project Round Robin exercise [63] and e) PET [64].

a)

b)
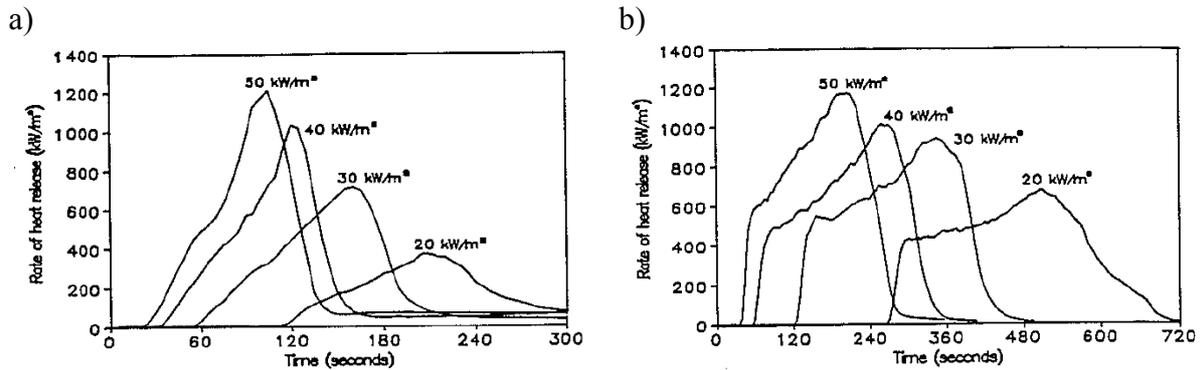
Figure 37. Examples of the influence of the cone calorimeter heat flux on the measured HRRPUA: a) PP and b) ABS. Data from [61].

6.1.2 Heat of combustion

The heat of combustion, ΔH_c, is the amount of heat energy that can be released when a unit mass of the combustible is consumed in burning. The effective value of the heat of combustion, EHC or symbolically, $\Delta H_{c,eff}$, is the heat of combustion that actually realises in fire where combustion efficiency χ is typically less than unity. Formally, we may write that

$\Delta H_{c,eff} = \chi \cdot \Delta H_c$, which is actually just one way to define what the combustion efficiency means.

Compared to HRRPUA, the heat of combustion is a much better-defined quantity. The effective heat of combustion is less well-defined because of the uncertainties involved in the combustion efficiency χ which depends e.g. on the time-varying ventilation and heat exposure conditions in the fire. The formulae developed by Hshieh et al. [65] on the basis of a study of 75 polymers (see Table 9 and Figure 38) are convenient. Expressed as molar values they read as follows:

For pure organic polymers

$$\Delta H_{c,mol} \text{ [MJ/mol]} = 0.41654 \cdot (C) + 0.10486 \cdot (H) - 0.10631 \cdot (O) + 0.02033 \cdot (N) + 0.42069 \cdot (S) - 0.02366 \cdot (Cl) - 0.04502 \cdot (F), \tag{6-1}$$

and for pure silicone polymers:

$$\Delta H_{c,mol} \text{ [MJ/mol]} = 0.41924 \cdot (C) + 0.12189 \cdot (H) - 0.12635 \cdot (O) + 0.03982 \cdot (N) + 0.79905 \cdot (Si) - 0.08852 \cdot (Br) + 0.01492 \cdot (I) - 0.25599 \cdot (S), \tag{6-2}$$

where C, H, etc. denote the number of C, H, etc. atoms in the monomer. The value in MJ/kg can be obtained by dividing the molar value by the monomer molecular MW:

$$\Delta H_c \text{ [MJ/mol]} = \Delta H_{c,mol} \text{ [MJ/mol]/MW [kg/mol]}. \tag{6-3}$$

63

For example, the polyethyleneterephthalate (PET) monomer is $C_{10}H_8O_4$ and its molar weight is MW = 0.194 kg/mol. Thus the molar heat of combustion is $\Delta H_{c,mol}$ [MJ/mol] = 0.41654·10 + 0.10486·8 - 0.10631·4 + 0 = 4.58 MJ/mol, and the heat of combustion is ΔH_c = 4.58 MJ/mol / 0.194 kg/mol = 23.6 MJ/kg.

Table 9. Data on the heat-of-combustion prediction studied by Hshieh et al. [65].

#	Polymer	Monomer	MW (g/mole)	$-H^\circ_{c,g,p}$ (kJ/mole)	$-H^\circ_{c,g,p}$ (MJ/kg)
1	Poly(oxymethylene) (POM)	CH_2O	30	519.95	17.33
2	Polyvinylalcohol (PVOH)	C_2H_4O	44	1146.20	26.05
3	Polyethylene (PE)	C_2H_4	28	1252.51	44.73
4	Polypropylene (PP)	C_3H_6	42	1878.77	44.73
5	Poly(methylmethacrylate) (PMMA)	$C_5H_8O_2$	100	2708.94	27.09
6	Poly(1,4-phenylenesulfide) (PPS)	C_6H_4S	108	3339.35	30.92
7	Poly(2,6-dimethyl-1,4-phenylene-oxide) (PPO)	C_8H_8O	120	4064.86	33.87
8	Polystyrene (PS)	C_8H_8	104	4171.17	40.11
9	Polyethyleneterephthalate (PET)	$C_{10}H_8O_4$	192	4579.01	23.85
10	Epoxy Novolac	$C_{10}H_{11}O$	147	5212.51	35.46
11	Poly(1,4-phenyleneethersulfone) (PES)	$C_{12}H_8O_3S$	232	5939.08	25.60
12	Poly(1,4-butanediolterephthalate) (PBT)	$C_{12}H_{12}O_4$	220	5831.52	26.51
13	Poly(hexamethyleneadipamide) (Nylon 66)	$C_{12}H_{22}O_2N_2$	226	7133.40	31.56
14	Poly(etherketone) (PEK)	$C_{13}H_8O_2$	196	6041.23	30.82
15	Poly(benzoxyl-1,4-phenylene)	$C_{13}H_8O$	180	6147.54	34.15
16	Poly(p-phenylenebenzobisoxazole) (PBO)	$C_{14}H_6O_2N_2$	234	6288.72	26.87
17	Poly(m-phenylene isophthalamide)	$C_{14}H_{10}O_2N_2$	238	6708.16	28.19
18	Aramid-arylester copolymer	$C_{14}H_{10}O_2N_2$	238	6708.16	28.19
19	Poly(p-phenylene terephthalamide)	$C_{14}H_{10}O_2N_2$	238	6708.16	28.19
20	Polyamideimide (PAI)	$C_{15}H_8O_3N_2$	264	6808.67	25.79
21	Poly(acrylonitrilebutadienestyrene) (ABS)	$C_{15}H_{17}N$	211	8050.99	38.16
22	Bisphenol-E Cyanate Ester	$C_{16}H_{12}O_2N_2$	264	7750.95	29.36
23	Polycabonate of bisphenol-A (PC)	$C_{16}H_{14}O_3$	254	7813.70	30.76
24	Bisphenol-A Cyanate Ester	$C_{17}H_{14}O_2N_2$	278	8377.21	30.13
25	Bisphenol-A Epoxy	$C_{21}H_{24}O_4$	340	10838.74	31.88
26	Poly(etheretherketone) (PEEK)	$C_{19}H_{12}O_3$	288	8853.58	30.74
27	Tetramethylbisphenol F Cyanate Ester	$C_{19}H_{18}O_2N_2$	306	9629.72	31.47
28	Polybenzimidazole (PBI)	$C_{20}H_{12}N_4$	308	9670.38	31.40
29	Polyimide (PI)	$C_{22}H_{10}O_5N_2$	382	9721.53	25.45
30	Novolac Cyanate Ester	$C_{23}H_{15}O_3N_3$	381	10895.31	28.60
31	Bisphenol-M Cyanate Ester	$C_{26}H_{24}O_2N_2$	396	13174.63	33.27
32	Polysulfone of bisphenol-A (PSF)	$C_{27}H_{22}O_4S$	442	13548.85	30.65
33	Polybenzoxazine of bisphenol-A/anilin- (b-a benzoxazine)	$C_{31}H_{30}O_2N_2$	462	15886.47	34.39
34	Polyetherimide (PEI)	$C_{37}H_{24}O_8N_2$	592	17331.30	29.28
35	Polyester of hydroxybenzoic and hydroxynapthoic acids	$C_{39}H_{22}O_{10}$	650	17488.76	26.91
36	Polyethylenenaphthlate (PEN)	$C_{14}H_{10}O_4$	242	6454.88	26.67
37	Dicyclopentadienyl bisphenol	$C_{17}H_{17}ON$	251	8777.76	34.97
38	Bisphenol A epoxy	$C_{11.85}H_{20.37}O_{2.83}N_{0.3}$	212	6777.20	31.97
39	Butadiene/styrene, 8.58% copolymer	$C_{4.18}H_{6.09}$	56	2379.72	42.50
40	Butadiene/styrene, 25.5% copolymer	$C_{4.60}H_{6.29}$	61	2575.63	42.22
41	Cellulose acetate (triacetate)	$C_{12}H_{16}O_8$	288	5825.73	20.23
42	Cellulose acetate (butyrate)	$C_{12}H_{18}O_7$	274	6141.76	22.42
43	Epoxy, unhardened	$C_{31}H_{36}O_{5.5}$	496	16102.88	32.47
44	Epoxy, hardened	$C_{39}H_{40}O_{3.5}$	644	19535.69	30.33
45	Melamine formaldehyde	$C_6H_6N_6$	162	3250.38	20.06
46	Nylon 11	$C_{12}H_{21}NO$	183	6697.98	36.60
47	Polyacenaphthalene	$C_{12}H_8$	152	5837.81	38.41
48	Polyacrylonitrile	C_3H_3N	53	1625.19	30.66
49	Poly-1,4-butadiene	C_4H_6	54	2295.30	42.51
50	Polycarbonate	$C_{16}H_{14}O_3$	202	7713.18	38.18
51	Poly-1-hexene sulfone	$C_6H_{12}SO_2$	148	4386.30	29.64
52	Polyisoprene	C_5H_8	68	2921.56	42.96
53	Poly-3-methyl-1-butene	C_5H_{10}	70	3131.28	44.73
54	Poly-4-methyl-1-pentene	C_6H_{12}	84	3757.53	44.73
55	Poly-α-methylstyrene	C_9H_{10}	118	4797.42	40.66
56	Polynitroethylene	$C_2H_3O_2N$	73	955.37	13.09
57	Polyoxytrimethylene	C_3H_6O	58	1772.46	30.56
58	Poly-1-pentene	C_5H_{10}	70	3131.28	44.73
59	Polypropene sulfone	$C_3H_6SO_2$	106	2086.84	19.69
60	Poly-β-propiolactone	$C_3H_4O_2$	72	1456.43	20.23
61	Polypropylene oxide	C_3H_6O	58	1772.46	30.56
62	Polytetrahydrofuran	C_4H_8O	72	2398.72	33.32
63	Polyurea	$C_{15}H_{18}O_4N_4$	318	7791.63	24.50
64	Polyurethane	$C_{6.3}H_{7.1}NO_{2.1}$	130	3165.77	24.35
65	Polyvinyl acetate	$C_4H_6O_2$	86	2082.69	24.22
66	Polyvinyl butyral	$C_6H_{14}O_2$	142	4587.71	32.31
67	Urea formaldehyde	$C_3H_6O_2N_2$	102	1706.82	16.73
68	Polyisoprene (natural rubber)	C_5H_8	68	2921.56	42.96
69	Hexafluorobisphenol-A Cyanate	$C_{17}H_8O_2N_2F_6$	386	7477.98	19.37
70	Polyvinylfluoride	C_2H_3F	46	1102.64	23.97
71	Polytetrafluoroethylene	C_2F_4	100	653.00	6.53
72	Polyvinylidene fluoride	$C_2H_2F_2$	64	952.76	14.89
73	Polyether, chlorinated	$C_5H_9OCl_2$	155	2767.95	17.86
74	Polyvinyl chloride	C_2H_3Cl	62	1124.00	18.13
75	Polyvinylidene chloride	$C_2H_2Cl_2$	97	995.48	10.26
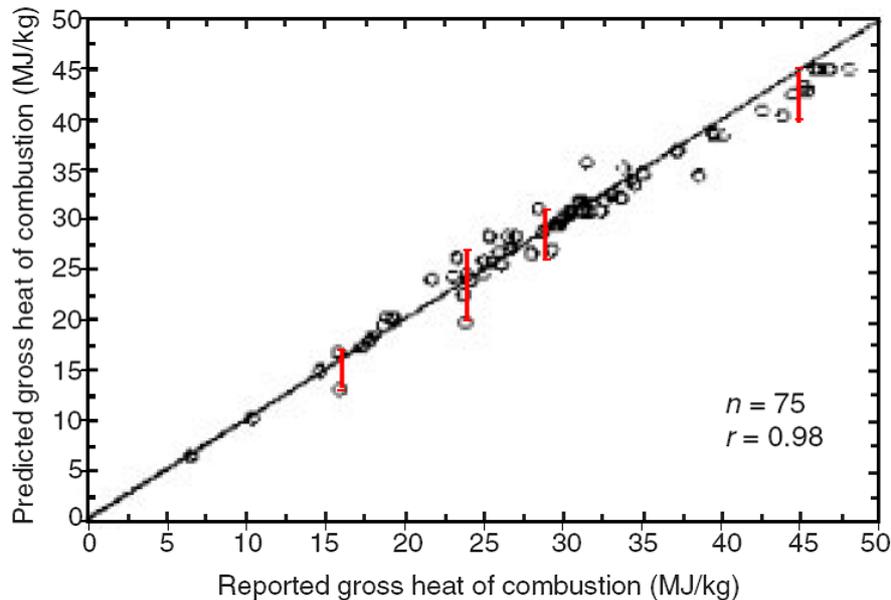
Figure 38. Example of the heat-of-combustion prediction developed by Hshieh et al. [65] for pure organic polymers.

6.1.3 Density, specific heat and thermal conductivity

6.1.3.1 Cellulosic materials

The density of some cellulosic products are summarised in the Forest Products Laboratory Wood Handbook [66] as

- solid wood, typically: 400– 800 kg/m^3 (there are also lighter species such as balsa and heavier such as oak)

- plywood: 400–800 kg/m^3

- particle and MDF boards: 600–800 kg/m^3

- paper: 500–1 100 kg/m^3.

Mikkola [67] quotes the following densities for some wood products:

- pine: 510 kg/m^3,
- spruce: 440 kg/m^3,
- laminated veneer lumber (LVL): 470 kg/m^3,
- plywood: 600 kg/m^3,
- particle board: 620 kg/m^3 (surface: 900 kg/m^3),
- light-weight fibre board: 280 kg/m^3.

The specific heat of dry wood depends on temperature T according to the Forest Products Laboratory Wood Handbook [66] as follows:

$$\frac{c(w=0)}{\text{JK}^{-1}\text{kg}^{-1}} = 103 + 3.867 \cdot \frac{T}{\text{K}} . \tag{6-4}$$

For example, at $T = 20\ °C = 293\ K$, $c(w = 0) = 1\ 240\ \text{JK}^{-1}\text{kg}^{-1}$.

For moist wood with moisture w, the specific heat increases with w as

$$\frac{c(w, T < 100\ °\text{C})}{\text{JK}^{-1}\text{kg}^{-1}} = \frac{c(w) + 4180 \cdot w}{1 + w} , \tag{6-5}$$

which is valid for $T < 100\ °C$.

According to Eurocode EN 1995-1-2, the specific heat of wood at moisture content of 12 % depends on temperature as presented in Table 10. Specific heat value estimates for wood at moisture contents of 0 %, 8 % and 10 % are given in Table 11.

Table 10. Temperature dependence of the specific heat of wood at 12 % moisture content according to EN 1995-1-2.

T (C)	c(*w* = 12 %, *T*) (J/K/kg)
20	1 530
99	1 770
99	13 600
120	13 500
120	2 120
200	2 000
250	1 620
300	710
350	850
400	1 000
600	1 400
800	1 650
1 200	1 650

Table 11. Temperature dependence of the specific heat of wood at moisture contents of 0 %, 8 % and 10 %.

T (C)	c(w, T) (J/K/kg)		
	w = 0 %	w = 8 %	w = 10 %
20	1 240	1 450	1 500
99	1 430	1 680	1 740
99	1 430	9 550	11 580
120	2 120	9 450	11 480
120	2 120	2 120	2 120
200	2 000	2 000	2 000
250	1 620	1 620	1 620
300	710	710	710
350	850	850	850
400	1 000	1 000	1 000
600	1 400	1 400	1 400
800	1 650	1 650	1 650
1 200	1 650	1 650	1 650

Thermal conductivity of wood at room temperature depends on its density ρ and moisture content w. According to the FPL Wood Handbook [66], the dependence is

$$\frac{\lambda_c(20\,^\circ\text{C})}{\text{WK}^{-1}\text{m}^{-1}} = 10^{-3} \cdot \frac{\rho}{\text{kgm}^{-3}} \cdot \left(0.1941 + 0.004046 \cdot \frac{w}{\%}\right) + 0.01864. \tag{6-6}$$

and according to McLean [68] and Mikkola [69]

$$\frac{\lambda_c(20\,^\circ\text{C})}{\text{WK}^{-1}\text{m}^{-1}} = 10^{-4} \cdot \left[a + \frac{2\rho}{\text{kgm}^{-3}}\left(1 + \frac{2w}{\%}\right)\right] \tag{6-7}$$

$a = 237$ (McLean)

$a = 200,...,400$ (Mikkola)

These relations are illustrated in Figure 39. According to EN 1995-1-2, the generic thermal conductivity of wood at room temperature is 0.12 $\text{WK}^{-1}\text{m}^{-1}$.

6. Predicting heat release rate and data used
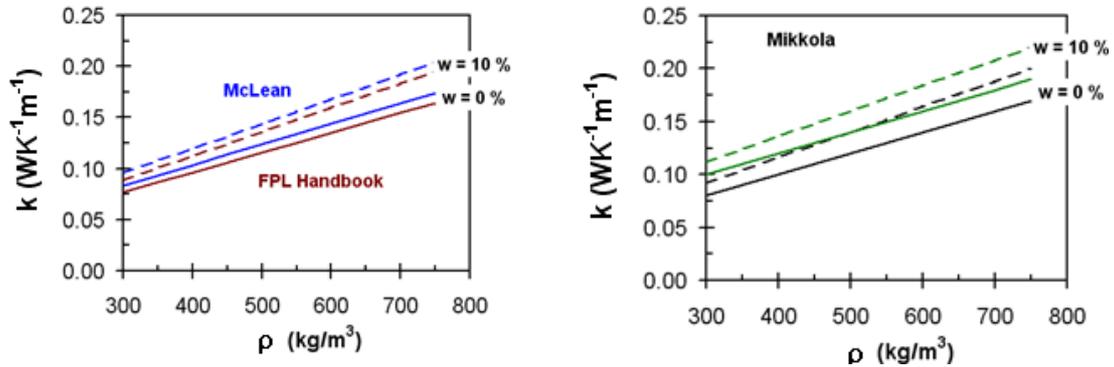
Figure 39. Dependence of the thermal conductivity of wood on its density at room temperature at moisture contents of 0 % and 10 %.

Thermal conductivities of some wood products and their dependence on temperature as given by Mikkola [67] are listed in Table 12. A generic temperature dependence of the thermal conductivity of wood given in the Eurocode EN1995-1-2 is shown in Table 13 and Figure 40.

Table 12. Temperature dependence of thermal conductivity of some wood products [67].

	ρ (kg/m^3)	k (W/mK)	
		T = 20 $^\circ$C	T = 20 $\rightarrow$ 360 $^\circ$C
Pine	510	0,142	0,185
Spruce	440	0,125	0,163
Glulam	470	0,134	0,174
Plywood	600	0,162	0,210
Particle board (surface)	620 900	0,166 0,23	0,216 0,30
Fibre board	280	0,091	0,118

Table 13. Temperature dependence of thermal conductivity of wood according to EN 1995-1-2.

Temperature T [°C]	Thermal conductivity $k(T)$ [WK^{-1}m^{-1}]
20	0.12
200	0.15
350	0.07
500	0.09
800	0.35
1 200	1.50

68
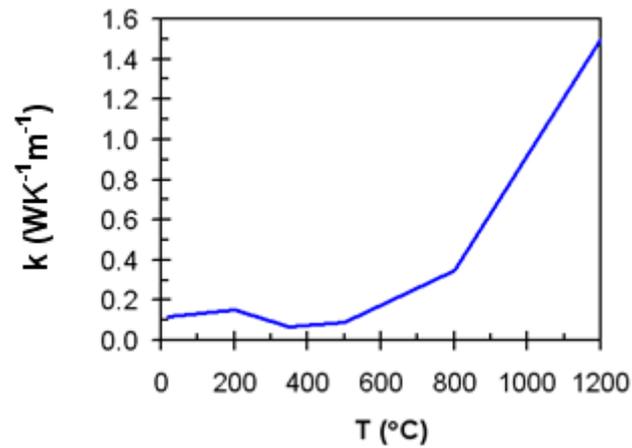
Figure 40. Temperature dependence of thermal conductivity of wood according to EN 1995-1-2.

6.1.3.2   Plastics

Densities, specific heats and thermal conductivities of some polymers are shown in Tables 14–17 [70, 71]. It can be seen that the data differ to some extent especially for the specific heat. For the coarse methodology presented here, the data of Tewarson [71] can be summarised as given in Table 18.

6. Predicting heat release rate and data used

Table 14. Temperature dependence of density of several polymers [70].

Material	Ref.	$\rho(T)$ [kg/m^3]							
Rubber (natural)	[141]	T 0	20						
		ρ 921	909						
Nylon 6	[141]	T 240	260	280	300				
		ρ 1176	1165	1154	1143				
Nylon 6,6	[141]	T 260	280	300					
		ρ 1100	1086	1071					
PC	[141]	T 40	80	120	160	200	240	280	340
		ρ 1192	1180	1167	1150	1123	1095	1067	1025
PE (branched)	[141]	T 120	140	160	180	200	220		
		ρ 801	790	780	769	759	749		
PE (linear)	[141]	T 140	160	180	200				
		ρ 785	774	762	751				
PET	[141]	T 140	160	180	200				
		ρ 1172	1156	1140	1125				
PMMA	[141]	T 40	80	120	160	200	220	240	260
		ρ 1181	1171	1153	1126	1097	1082	1067	1052
POM	[141]	T 100	120	140	160	180	200	220	
		ρ 1063	1048	1033	1018	1004	990	976	
PP (atactic)	[141]	T 80	100	120					
		ρ 827	816	802					
PP (isotactic)	[141]	T 180	200	220	240	260	280	300	
		ρ 764	754	744	734	724	714	705	
Polystyrene	[141]	T 40	80	120	160	200	240	280	320
		ρ 1040	1026	1005	984	961	939	916	893
PTFE	[141]	T 360	380						
		ρ 1548	1504						
PVC	[141]	T 100	120	140					
		ρ 1352	1338	1322					

Table 15. Temperature dependence of specific heat of several polymers. [70].

Material	Ref.					$c(T)$ [J/kg–K]				
PE (c)	[142]	T	17	47	77	107	137	157	177	187
		c	1515	1639	1804	2151	2585	2889	3213	3382
PE (a)	[142]	T	17	27	77	127	177	227	277	327
		c	2176	2206	2361	2516	2670	2824	2979	3134
PP (c)	[144]	T	17	47	77	107	127	147	167	187
		c	1563	1756	1970	2197	2354	2514	2679	2850
PP (a)	[144]	T	17	27	77	127	177	227	277	327
		c	2067	2103	2284	2464	2643	2824	3005	3183
PMMA	[152]	T	17	47	77	97	107	167	227	277
		c	1434	1564	1694	1781	2180	2333	2486	2613
PS	[145]	T	17	47	77	127	177	227	277	327
		c	1179	1317	1460	1935	2063	2190	2317	2445
PTFE	[147]	T	7	37	107	187	247	327	367	447
		c	976.4	1023	1109	1236	1357	1328	1379	1475
PVC	[147]	T	17	37	57	77	81	87	97	107
		c	922.2	978.2	1038	1102	1424	1457	1513	1569
Nylon 6,6	[148]	T	17	47	50	127	177	227	277	327
		c	1416	1566	2223	2383	2486	2590	2693	2797
Nylon 6	[148]	T	17	37	40	87	147	207	267	327
		c	1451	1559	2404	2468	2549	2630	2711	2792
PET	[148]	T	17	67	69	107	147	197	257	317
		c	1136	1322	1736	1792	1851	1924	2013	2101
POM	[143]	T	−3	17	27	47	67	87	107	117
		c	1152	1237	1284	1387	1500	1619	1740	1800
PC	[149]	T	17	57	107	145	147	187	237	287
		c	1168	1328	1534	1695	1891	1982	2096	2210

Table 16. Temperature dependence of thermal conductivity of several polymers. [70].

Material	Ref.					$k(T)$ [W/m–K]				
PC	[150]	T	28	83	119	146	169	204	225	248
		k	0.24	0.25	0.26	0.26	0.26	0.25	0.23	0.23
PE	[150]	T	17	45	107	118	129	139	160	214
		k	0.34	0.31	0.23	0.22	0.22	0.22	0.22	0.21
PP	[150]	T	71	105	116	138	146	156	222	234
		k	0.25	0.24	0.23	0.2	0.19	0.13	0.13	0.13
PS	[150]	T	35	44	89	108	115	163	216	238
		k	0.16	0.16	0.17	0.17	0.16	0.16	0.16	0.16
PMMA	[152]	T	0	105	275					
		k	0.2	0.2	0.16					

6. Predicting heat release rate and data used

Table 17. Density, thermal conductivity and specific heat for some polymers [71].

material	ρ kg/m³ at 20 C	k WK⁻¹m⁻¹ at 20 C	cp JK⁻¹kg⁻¹ at T(°C): -40	-20	0	20	40	60	80	100	200	cp JK⁻¹kg⁻¹ avg 20-200 °C	$\alpha \times 10^7$ m²/s	$\rho kc/10^6$ J²m⁻²K⁻²s⁻¹
ABS	1070	0.21	892	946	999	1057	1122	1182	1239	1303	1733	1273	1.54	2.9
ABS	890	0.10	1058	1154	1261	1362	1462	1560	1665	1750	1938	1623	0.69	1.4
ABS	1430	0.13	1288	1346	1419	1482	1558	1663	1771	1931	2415	1803	0.50	3.4
EPDM	1210	0.45	886	1005	1077	1109	1159	1147	1198	1250	1484	1225	3.04	6.7
EPDM	1150	0.30	1229	1327	1353	1382	1402	1449	1497	1541	1745	1503	1.74	5.2
EPDM	1160	0.36	821	927	988	1026	1030	1075	1124	1173	1394	1137	2.73	4.7
EPDM	440	0.07	1543	1601	1626	1690	1768	1852	1923	1990	2304	1921	0.83	0.6
EPDM	410	0.21	973	1051	1097	1137	1189	1203	1251	1300	1507	1265	4.05	1.1
Nylon	1480	0.41	844	896	964	1036	1138	1255	1360	1440	1912	1357	2.04	8.2
Nylon12	1040	0.18	867	973	1106	1211	1310	1410	1498	1595	1787	1469	1.18	2.7
Nylon6	1200	0.11	951	1071	1149	1222	1306	1392	1474	1578	2192	1527	0.60	2.0
Nylon6	1090	0.12	1303	1383	1496	1600	1727	1860	1963	2080	3049	2047	0.54	2.7
Nylon6	1270	0.11	979	1031	1101	1185	1267	1344	1408	1500	2133	1473	0.59	2.1
Nylon66	1500	0.58	813	867	923	990	1096	1196	1286	1314	1691	1262	3.06	11.0
Nylon66	1440	0.35	902	963	1038	1121	1255	1376	1483	1551	2718	1584	1.53	8.0
Nylon66	1400	0.31	996	1056	1133	1212	1351	1488	1585	1686	2141	1577	1.40	6.8
PC	1120	0.18	776	827	890	953	1018	1082	1144	1217	1679	1182	1.36	2.4
PC	1180	0.27	814	871	934	999	1074	1142	1194	1247	1510	1194	1.92	3.8
PC	1190	0.20	1076	1142	1210	1282	1357	1434	1559	1658	2061	1559	1.08	3.7
PC	1200	0.22	1301	1362	1427	1499	1566	1623	1698	1774	2177	1723	1.06	4.5
PC	1180	0.19	959	1015	1080	1156	1228	1297	1373	1445	1095	1266	1.27	2.8
PC	1180	0.34	1430	1568	1751	1885	2120	2481	2891	5303	2404	2847	1.01	11.4
PE	950	0.31	959	1044	1162	1274	1397	1553	1795	2200	2025	1707	1.91	5.0
PE	950	0.37	1044	1121	1216	1330	1473	1649	1882	2368	2122	1804	2.16	6.3
PE	940	0.30	1083	1152	1223	1353	1473	1631	1817	2217	2147	1773	1.80	5.0
PE	800	0.23	1325	1412	1527	1664	1827	2053	2379	3027	2463	2236	1.29	4.1
PE	1200	0.35	1270	1380	1497	1578	1734	2066	2481	4016	2048	2321	1.26	9.7
PE	990	0.29	1535	1747	1951	2098	2434	3031	4046	7921	2665	3699	0.79	10.6
PE/PP	910	0.17	963	1040	1142	1245	1346	1461	1581	1759	1983	1563	1.20	2.4
PE/PP	880	0.21	1019	1100	1202	1308	1425	1552	1712	1913	2147	1676	1.42	3.1
PET	690	0.04	866	932	1024	1101	1194	1271	1511	2287	1558	1487	0.39	0.4
PET	690	0.04	844	906	973	1043	1118	1184	1230	1291	1664	1255	0.46	0.3
PET	660	0.09	595	642	695	749	808	875	926	986	1319	944	1.44	0.6
PET	1170	0.31	1036	1109	1165	1216	1257	1336	1412	1498	1965	1447	1.83	5.2
Phenolic	160	0.28	1060	1087	1127	1164	1206	1247	1238	1311	1420	1264	13.84	0.6
POM	1410	0.27	1118	1167	1224	1285	1349	1425	1528	1659	1918	1527	1.25	5.8
PP	1060	0.23	958	1026	1130	1233	1347	1462	1577	1744	2082	1574	1.38	3.8
PP	1040	0.23	958	1023	1104	1183	1274	1379	1504	1652	1934	1488	1.49	3.6
PP	900	0.19	1068	1152	1264	1382	1501	1629	1773	2033	2247	1761	1.20	3.0
PP	900	0.21	1261	1337	1445	1562	1687	1829	1974	2174	2476	1950	1.20	3.7
PP	930	0.23	1164	1242	1310	1392	1492	1613	1743	1925	2200	1728	1.43	3.7
PP	1190	0.39	1053	1114	1182	1263	1352	1456	1537	1650	1895	1526	2.15	7.1
PP	1210	0.39	910	969	1039	1112	1199	1285	1377	1490	1760	1371	2.35	6.5
PP	1110	0.34	1149	1203	1291	1373	1456	1553	1672	1815	1947	1636	1.87	6.2
PP	1200	0.33	1167	1223	1301	1386	1474	1581	1686	1817	2015	1660	1.66	6.6
PP	1040	0.19	1454	1539	1650	1757	1867	2030	2198	2388	2614	2142	0.85	4.2
PP	1050	0.19	312	353	432	512	593	705	843	1024	1164	807	2.24	1.6
PP	1140	0.33	869	923	1003	1078	1150	1231	1315	1402	1663	1307	2.22	4.9
PP	1230	0.35	1175	1257	1360	1445	1544	1654	1786	1886	2219	1756	1.62	7.6
PP	1200	0.33	1091	1158	1263	1365	1446	1552	1667	1805	1999	1639	1.68	6.5
PP	1170	0.29	1042	1108	1196	1278	1364	1468	1582	1705	1954	1559	1.59	5.3
PP/PE	880	0.33	1559	1660	1777	1870	2013	2216	2439	2795	2693	2338	1.60	6.8
PP/PE	890	0.24	1563	1660	1780	1880	2020	2250	2450	2750	2820	2362	1.14	5.0
PP/PE	880	0.24	1434	1545	1654	1756	1893	2072	2266	2528	2703	2203	1.24	4.7
PP/PE	1110	0.28	1363	1426	1502	1583	1683	1782	1893	2028	2177	1858	1.36	5.8
PP/PE	950	0.20	1504	1594	1705	1796	1919	2062	2223	2426	2539	2161	0.97	4.1
PS	900	0.17	1063	1118	1173	1234	1300	1378	1434	1487	1700	1422	1.33	2.2
PS	1300	0.10	984	1043	1098	1159	1231	1310	1362	1412	1624	1350	0.57	1.8
PS	960	0.26	890	942	1009	1066	1128	1197	1264	1329	1706	1282	2.11	3.2
PS/phenolic	1360	0.12	1122	1191	1271	1329	1392	1471	1551	1646	2054	1574	0.56	2.6
PU	110	0.04	986	1040	1117	1182	1252	1314	1383	1471	1768	1395	2.61	0.1
PU	90	0.06	1066	1113	1156	1197	1235	1272	1312	1349	1556	1320	5.05	0.1
PU	20	0.02	1131	1189	1244	1292	1341	1383	1426	1471	1653	1428	7.00	0.0
PU	1040	0.14	1295	1371	1442	1513	1576	1642	1749	1991	219	1448	0.93	2.1
PU	180	0.12	1176	1261	1339	1416	1468	1519	1564	1590	1782	1557	4.28	0.3
PU	210	0.12	1344	1414	1474	1533	1607	1659	1721	1772	1882	1696	3.37	0.4
PU	1230	0.29	930	980	1050	1150	1200	1310	1410	1530	1690	1382	1.71	4.9
PU	90	0.17	1148	1263	1304	1362	1413	1446	1497	1541	1638	1483	12.74	0.2
PU	1220	0.39	1028	1089	1178	1254	1337	1434	1540	1665	1857	1515	2.11	7.2
PU	110	0.19	1212	1259	1340	1424	1477	1478	1513	1557	1712	1527	11.31	0.3
PU	1710	0.17	1296	1342	1403	1467	1541	1612	1740	1798	2021	1697	0.59	4.9
PVC	1200	0.14	836	877	933	976	1022	1068	1119	1182	1374	1124	1.04	1.9
PVC	1950	0.25	718	777	824	861	898	942	987	1032	1141	977	1.31	4.8
PVC	1000	0.23	651	690	724	753	785	821	855	888	1052	859	2.68	2.0
PVCHyd	1600	0.10	795	851	896	932	973	1016	1058	1098	1239	1053	0.59	1.7
Rubber	1260	0.24	827	940	986	1029	1084	1144	1166	1204	1391	1170	1.63	3.5
SA	1110	0.09	1076	1131	1199	1255	1319	1393	1481	1619	2014	1514	0.54	1.5
SMC	1640	0.37	620	653	689	726	767	813	858	906	1140	868	2.60	5.3
TPO	930	0.09	1190	1294	1344	1385	1446	1526	1609	1705	1961	1605	0.60	1.3
TPO	970	0.13	1246	1334	1358	1408	1457	1520	1592	1658	1865	1583	0.85	2.0
TPO	980	0.05	1265	1369	1398	1441	1478	1541	1614	1690	1933	1616	0.32	0.8
TPO	970	0.33	1092	1185	1224	1260	1328	1413	1497	1599	1872	1495	2.28	4.8

Table 18. Thermal properties of some plastics deduced from the data of Tewarson [71]. Standard deviation related to the last digits is shown in the parenthesis.

Material	Density ρ [kg/m^3]	Thermal conductivity k [WK^{-1}m^{-1}]	Specific heat c [JK^{-1}kg^{-1}]	Thermal diffusivity $k/(\rho c)$ [m^2/s]	Thermal inertia $k\rho c$ [J^{2}m^{-2}K^{-2}s^{-1}]
PE	1 000 (100)	0,30 (5)	2 250 (750)	1,5 (5)	6,8 (2,7)
PP	1 100 (100)	0,3 (1)	1 600 (300)	1,7 (4)	4,9 (1,7)
PE/PP	1 000 (100)	0.28 (7)	1 850 (550)	1,5 (4)	5,3 (2,0)
ABS & PS	1 100 (200)	0,16 (6)	1 450 (200)	1,1 (6)	2,5 (0,8)
nylon	1 300 (200)	0,27 (17)	1 550 (250)	1,4 (0,9)	5,4 (3,5)
PET	800 (250)	0,12 (13)	1 300 (300)	1,0 (7)	1,6 (2,4)
PC	1 180 (30)	0,23 (6)	1 650 (650)	1,3 (3)	4,8 (3,3)
EPDM (heavy)	1 170 (30)	0,4 (1)	1 300 (200)	2,5 (7)	5,5 (1,0)
EPDM (light)	420 (20)	0,1 (1)	1 600 (450)	2,4 (2,3)	0,8 (4)
PU (light)	120 (60)	0.10 (6)	1 500 (150)	6,6 (4,0)	0,2 (2)
PVC	1 400 (400)	0,18 (7)	1 000 (100)	1,4 (9)	2,6 (1,5)

6.1.4 Ignition temperature

The ignition temperature T_{ig} of solids is basically not a very well-defined parameter, but we can define fairly good estimates on it. The thermal response parameter TRP [(kW·s$^{1/2}$/m^2)] is defined in terms of the thermal inertia $k\rho c$ and the temperature rise of the solid above the ambient temperature T_∞ as follows [72]:

$$TRP = (T_{ig} - T_\infty) \cdot \sqrt{\frac{\pi}{4} \cdot k\rho c} \qquad (6\text{-}8)$$

which suggests that

$$T_{ig} = T_\infty + \frac{TRP}{\sqrt{\frac{\pi}{4} \cdot k\rho c}} . \qquad (6\text{-}9)$$

The problem with using the TRP parameter is the large uncertainty associated with the predicted ignition temperature: the data for TRP reported by Tewarson [71] varies ca. between 10–40 %. Yet, the above equation for the ignition temperature T_{ig} expressed in terms of the TRP parameter can be used for comparison purposes.

6.1.4.1 Cellulosic materials

Results of some ignition temperature measurements of wood-based materials using the cone calorimeter at heat exposure of 50 kW/m^2 are summarised in

Table 19. It can be seen that the temperature range 300–350 °C is characteristic for (piloted) ignition of cellulosic fuels.

Table 19. Results of some ignition temperature measurements of cellulosic materials using the cone calorimeter. ρ is the material density and w its moisture content.

Material characterisation	T_{ig} (°C)	Reference
Radiata pine, $w = 0$ % Radiata pine, $w = 15$ %	305 343	[73]
-	300–364	[74]
-	296–330	[75]
Particle board, 700 kg/m^3	303	[72]
Corrugated cardboard, double-wall, 6 mm	343	[72]

6.1.4.2 Plastics

Ignition temperatures of some plastics given by Babrauskas [72] are summarised in Table 20. It can be seen that the temperature range 280–360 °C is characteristics for (piloted) ignition of plastic fuels.

Table 20. Results of some ignition temperature measurements of plastic materials using the cone calorimeter [73].

Material	Density (kg/m^3)	T_{ig} (°C)
PE	920	363
PMMA	1 180	311
POM[a)]	1 420	281
PP	905	334
PS	1 040	366

[a)] Polyoxymethylene

6.1.5 Time to sustained ignition and time to peak HRR

Time to sustained ignition t_{ig} depends e.g. on the material chemical composition, its thermal parameters (k, ρ and c), type of heat exposure (radiant, oven heating, etc.,) and

heat exposure level $\dot{q}''$, as well as the moisture content w of the material. Experimental findings that can be used as guiding values for the selection of t_{ig} for simulations are summarised in this section. Guidance on how different parameters affect the time to ignition can be obtained from the equations below [67, 72].

$$t_{ig} \propto \left(\frac{TRP}{\dot{q}''-CHF}\right)^2 = \left(\frac{(T_{ig}-T_\infty)\cdot\sqrt{k\rho c}}{\dot{q}''-CHF}\right)^2 \tag{6-10}$$

$$t_{ig} \propto (1+4w)^2$$

where CHF is an empirical constant of the order of 10–20 kW/m^2 (it characterises the heat exposure at which the time to ignition becomes very long = practically no ignition).

6.1.5.1 Cellulosic materials

Results of some ignition time measurements of wood-based materials using the cone calorimeter at heat exposure of 50 kW/m^2 are summarised in Table 21. If there is moisture – as there usually is – the time to ignition, t_{ig}, varies between ca. 20–40 s. The peak HRR is typically reached relative rapidly after the ignition; we can estimate that the delay to reach the peak HRR, Δt_p, is of the order of magnitude of t_{ig}, and hence $t_p = t_{ig} + \Delta t_p \approx 40$–80 s [56].

Table 21. Results of some ignition time measurements wood-based materials using the cone calorimeter at heat exposure of 50 kW/m^2. ρ is the material density, w its moisture content and d its thickness.

Material characterisation	t_{ig} (s)	Reference
Spruce, $\rho = 440$ kg/m^3, $w = 0$ %, $d = 37$ mm	16 ± 3	[67]
Spruce, $\rho = 500$ kg/m^3, $w = 10$ %, $d = 6$ mm	14 ± 4	[67]
Spruce, $\rho = 500$ kg/m^3, $w = 10$ %, $d = 2$ mm	16 ± 3	[67]
Pine, $\rho = 550$ kg/m^3, $w = 0$ %, $d = 36$ mm	22 ± 3	[67]
Pine, $\rho = 500$ kg/m^3, $w = 0$ %, $d = 36$ mm	13	[76]
Particle board, $\rho = 620$ kg/m^3, $w = 0$ %, $d = 18$ mm	37 ± 3	[67]
Plywood	24	[77]

6.1.5.2 Plastics

Results of cone calorimeter experiments (heat exposure of 50 kW/m^2) of some plastics for the time to ignition, t_{ig}, and the time to reach the peak HRR, t_p, are reported in [71], see Table 22. The mean values for EPDM, nylon, PC, PE or PP and PVC are (in round numbers)

- EPDM: $t_{ig} = 14$ s, $t_p = 68$ s, $\Delta t_p = 54$ s
- Nylon: $t_{ig} = 40$ (5) s, $t_p = 120$ (30) s, $\Delta t_p = 80$ (30) s
- PC: $t_{ig} = 50$ (25) s, $t_p = 180$ (20) s, $\Delta t_p = 130$ (4) s
- PE or PP: $t_{ig} = 20$ (10) s, $t_p = 85$ (40) s, $\Delta t_p = 70$ (30) s
- PVC: $t_{ig} = 23$ s, $t_p = 80$ s, $\Delta t_p = 57$ s
- PET: $t_{ig} = 40$ s, $t_p = 100$ s, $\Delta t_p = 70$ s, (from ref. [64]).

The number shown in the parentheses is the standard deviation related to the last digits deduced from the data.

Table 22. Results of cone calorimeter experiments at 50 kW/m^2 heat exposure of some plastics: time to ignition, t_{ig}, and time to reach peak HRR, t_p, [71].

Material	t_{ig} (s)	t_p (s)	$\Delta t_p = t_p - t_{ig}$ (s)
EPDM Rubber	14	68	54
Fiberglass/polyester/styren	45	83	38
Nylon 6	34	85	51
Nylon 66	36	138	102
Nylon 66	44	135	91
PC	32	165	133
PC	66	193	127
PE/PP	16	85	69
PET	4	20	16
PP	8	43	35
PP	19	125	106
PP	24	108	84
PP	36	128	92
PP/PE	16	95	79
PP/PE	18	78	60
PVC	23	80	57

6.1.6 Amount of the combustible material and its characteristic thickness

To ensure that a proper amount of combustible material will be included in the model, one must also know – or estimate – the fire load density q'' [MJ/m^2] of the building: the sum of the energy of the fire load entities Q_i that can be released in the fire divided by the floor area A_{floor} should correspond to a characteristic value of the fire load density.

$$q''_c = \frac{\sum_i Q_i}{A_{floor}}$$

(6-11)

A value suggested in the International Fire Engineering Guidelines, 2005 Edition [8], for the characteristic value of the fire load density is 95 % fractile.

The characteristic thickness d_c is an FDS input parameter that can be symbolically expressed as

$$d_c = avg\left(\frac{V_n}{A_n}\right)$$

(6-12)

where V_n and A_n are the volumes and surface areas of the different constituents of the fire load entity.

6.1.7 Geometrical characteristics

The geometrical characteristics of the fire load entity may be evident by the application: for example, in modelling of warehouses or shops with storage/selling units of certain size and spacing, the fire load entities should reflect this geometry. When modelling targets with more complex or uncertain geometries, it is in the spirit of the methodology to keep the assumptions as simple as possible, and such target may be modelled by using, e.g., boxes or rectangles with size corresponding to the FDS spatial mesh division. Examples of the approaches to the description of the geometrical aspects of the model are given in next section.

6.1.8 Constructing a fire load entity

In reality, there may be numerous different combustibles in the fire load but it is advisable to reduce this number to N principal combustibles by combining materials and products with reasonably similar combustibility properties. As explained above, taking into account the uncertainties, one should aim at two types of combustibles: cellulosic and plastic materials. Typically one can make an estimate on the mass fractions μ_n of the different combustibles to be used in the process.

Next, the size and spacing of the units (cubes/rectangles) used to describe the fire load geometry of the combustibles are defined. There will be K cubes/rectangles and the decision on their geometry yields the volumes V_k and surface areas A_k of the $k = 1$, $2, \ldots, K$ fuel cubes/rectangles. This choice also defines the floor area A_f of the fire load entity and – as described above – combined with the characteristic fire load density q''_c it defines the fire load Q.

Next, the effective heat of combustion of the homogeneous K fuel cubes/rectangles is determined as a mass-weighted average of the different combustibles:

EHC
$$\Delta H_{c,eff} = \sum_{n=1}^{N} \mu_n \cdot \Delta H_{c,eff,n}$$
(6-13)

where $\Delta H_{c,eff,n}$ are the effective-heat-of-combustion values of the N combustibles.

The known total heat energy Q of the fire load entity defines the total mass of the K fuel cubes/rectangles:

total mass M
$$M = \frac{Q}{\Delta H_{c,eff}} .$$
(6-14)

On the other hand, this total mass is the sum of the masses m_k of the K fuel cubes/rectangles:

$$M = \sum_{k=1}^{K} m_k .$$
(6-15)

which can be used to define the mean density ρ of each fuel cube/rectangle as

DENSITY
$$\rho_k = \rho$$
(6-16)
$$M = \sum_{k=1}^{K} \rho_k \cdot V_k = \rho \cdot \sum_{k=1}^{K} V_k .$$
$$\Rightarrow \rho = \frac{M}{\sum_{k=1}^{K} V_k}$$

With this homogenous density characteristic defined, one can assign a specific area A_n for each combustible as follows: the mass fraction of each combustible reads

$$\mu_n = \frac{\rho_n \cdot V_n}{M} = \frac{\rho \cdot V_n}{M} \approx \frac{\rho \cdot A_n^{2/3}}{M}$$
(6-17)
$$\Rightarrow \cdot A_n = \left(\frac{M \cdot \mu_n}{\rho} \right)^{3/2}$$

where the conversion between the volume and area is made on purely dimensional basis. If some better knowledge is available, it should naturally be used.

With the specific area A_n of the combustibles calculated, the HRRPUA of the homogenous fuel is obtained as an area-weighted property as

HRRPUA

$$\dot{Q}'' = \frac{\sum_{n=1}^{N} A_n \cdot \Delta H_{c,eff,n}}{\sum_{n=1}^{N} A_n}$$

(6-18)

The thermal conductivity is obtained as a thickness-weighted property as

CONDUCTIVITY

$$k = \frac{d}{\sum_{n=1}^{N} d_n / k_n}$$

(6-19)

The ignition temperatures Tig, ignition times tig and time-to-peak-HRRPUA values tp are obtained as averages

IGNITION TEMPERATURE

$$T_{ig} = \frac{\sum_{n=1}^{N} T_{ig,n}}{N}$$

(6-20)

IGNITION TIME

$$t_{ig} = \frac{\sum_{n=1}^{N} t_{ig,n}}{N}$$

(6-21)

TIME-TO-PEAK-HRRPUA

$$t_p = \frac{\sum_{n=1}^{N} t_{p,n}}{N}$$

(6-22)

6.2 Examples of use and validity of the methodology

6.2.1 Wooden crib of mass of 920 kg

As the first example, the fire experiment W31 with large wooden cribs carried out in the EUREKA project [78] is presented. The wooden cribs consisted of 950 kg of wooden sticks stacked 3.2 m long by 0.8 m wide and 2.4 m high. The heat released during the first hour of the experiment was about 13 000 MJ. These pieces of data form all the information used in the FDS5 model for the geometry shown in Figure 41a. The model parameters are shown in Figure 41b. The agreement between the measured and the simulated HRR curves is very good as shown in Figure 42.

The key input values and their justification are as follows:

- HRRPUA = 200 kW/m^2 corresponding the average HRRPUA of wood burning during 30–60 s after the ignition

- EHC = 18 MJ/kg; selected to produce the approximate heat released in the experiment during 1 hour with the density given below and the geometrical arrangement shown in Figure 41a

- density ρ = 450 kg/m^3: a typical value for spruce/pine

- specific heat c_p = 1 500 JK^{-1}kg^{-1}: a typical value for wood

- thermal conductivity k = 0.1 WK^{-1}m^{-1}: a typical value for wood

- ignition temperature T_{ig} = 320 °C: a typical value for wood

- timing of the ignition and early HRR evolution: from 45–60 s in accordance with the data shown above

- amount of combustible material: 700 kg (not all of the 950 kg will burn; this value corresponds to the heat released during the first hour of the experiment)

- characteristic thickness 0.2 m = FDS Mesh size.

a)

b)
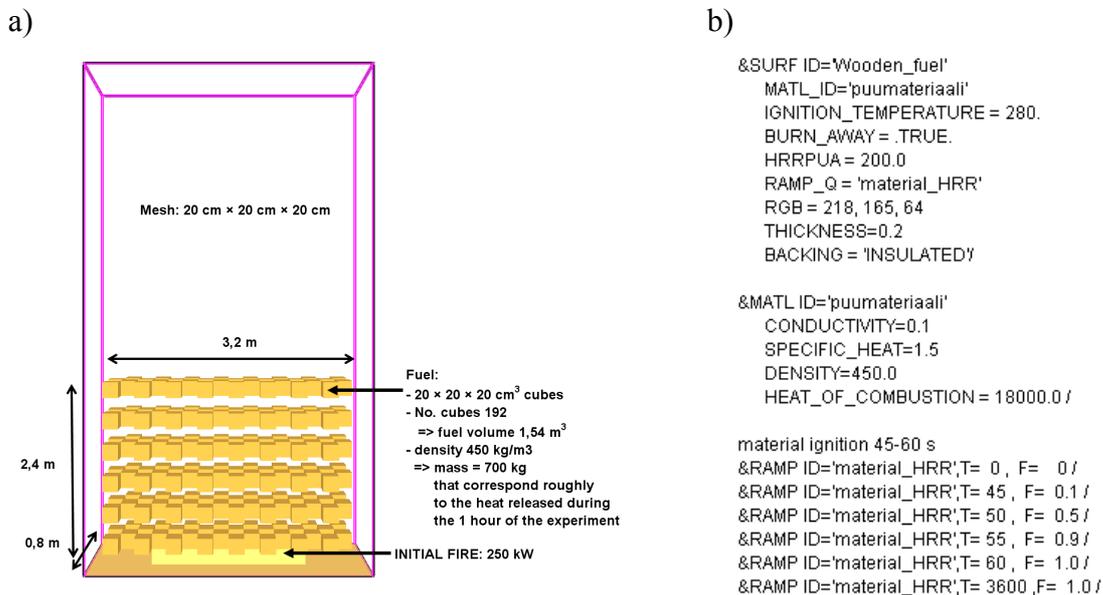
Figure 41. a) FDS5 model of the EUREKA fire experiment W31 and b) model parameters.

80
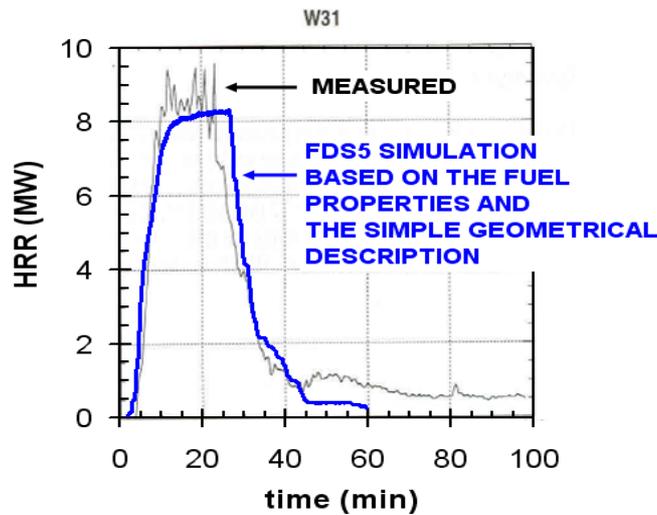
Figure 42. Comparison of the measured and simulated heat release rates of the EUREKA fire experiment W31 [78].

6.2.2 PET bottles stored in cardboard boxes

The next example is a fire experiment on plastic bottles made of PET in cardboard boxes. The detailed description of the experimental set-up is given by Babrauskas in the SFPE Handbook [79]. The measured HRR curve is shown in Figure 43. The heat released during the experiment was about 5 800 MJ.

The experiment was simulated on the basis of the cone calorimeter data on cardboard and PET. The quantities used in the FDS5 model construction are shown in Table 23. The FDS5 model is shown in Figure 44. The simulated and measured HRR curves are compared in Figure 45: the agreement of the calculated and measured results is reasonable.
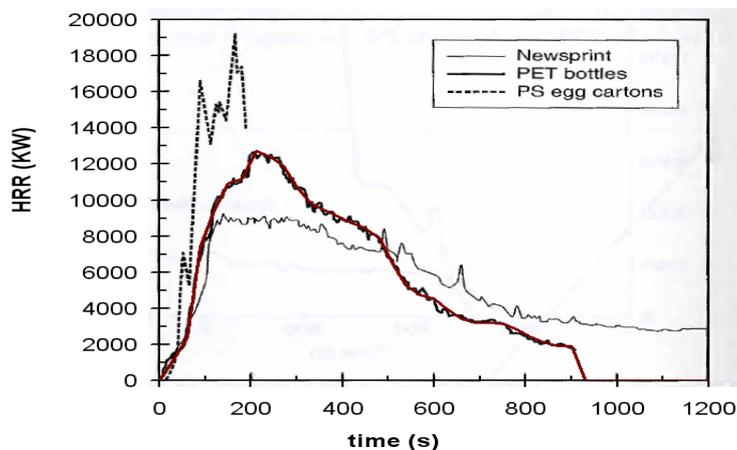
Figure 43. Heat release rate measured in the fire experiment with PET plastic bottles in cardboard boxes. Reproduced from [79].

6. Predicting heat release rate and data used

Table 23. Description of the fire experiment on PET plastic bottles in cardboard boxes for the FDS5 model.

Quantity	value	unit
Cartoon dimension	0.53	m
PET per cartoon	2.55	kg
Cardboard per cartoon	1.29	kg
Cartoon total mass	3.84	kg
No. cartoons	64	kg
PET mass	163.2	kg
Cardboard mass	82.56	kg
Total mass	245.76	kg
PET Q	3917	MJ
Cardboard Q	1238	MJ
Total Q	5155	MJ
PET density	900	kg/m3
Cardboard density	800	kg/m3
PET cp	1300	J/K/kg
Cardboard cp	1300	J/K/kg
PET k	0.12	W/K/m
Cardboard k	0.12	W/K/m
PET EHC	24	MJ/kg
Cardboard EHC	15	MJ/kg
PET HRRPUA	400	kW/m2
Cardboard HRRPUA	300	kW/m2
PET tig	40	s
Cardboard tig	20	s
PET tp	110	s
Cardboard tp	50	s
cartoon density	25.8	kg/m3
cartoon cp	1300	J/K/kg
cartoon k	0.12	W/K/m
cartoon EHC	21.0	MJ/kg
cartoon HRRUA	305	kW/m2
cartoon tig	30	s
cartoon tp	80	s
cartoon surface area	1.69	m2
cartoon effective thickness	0.0883	m2

a)

53 cm cubes: model 45 cm cubes with 15 cm spacings

b)

(-1,35 m;-1,35 m)   (-1,35 m;1,35 m)

y

(1,35 m;-1,35 m)

(1,35 m;1,35 m)

x

Mesh: 15 cm × 15 cm × 15 cm

INITIAL FIRE:
80 kW
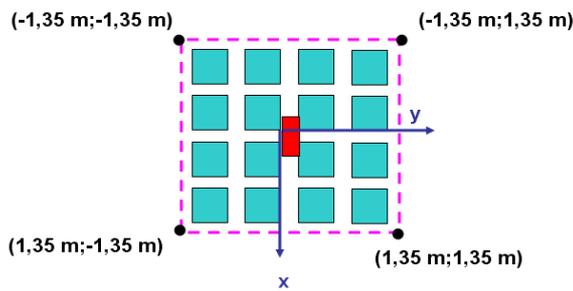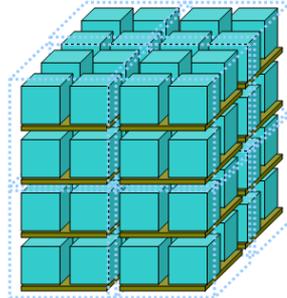
```
&SURF ID='PET_Cartoon'
    MATL_ID='PET_Cardboard'
    IGNITION_TEMPERATURE = 320.
    BURN_AWAY = .TRUE.
    HRRPUA = 305.0
    RAMP_Q = 'material_HRR'
    RGB = 218, 175, 84
    THICKNESS=0.15
    BACKING = 'INSULATED'/

&MATL ID='PET_Cardboard'
    CONDUCTIVITY=0.12
    SPECIFIC_HEAT=1.3
    DENSITY=26.0
    HEAT_OF_COMBUSTION = 21000.0 /
```
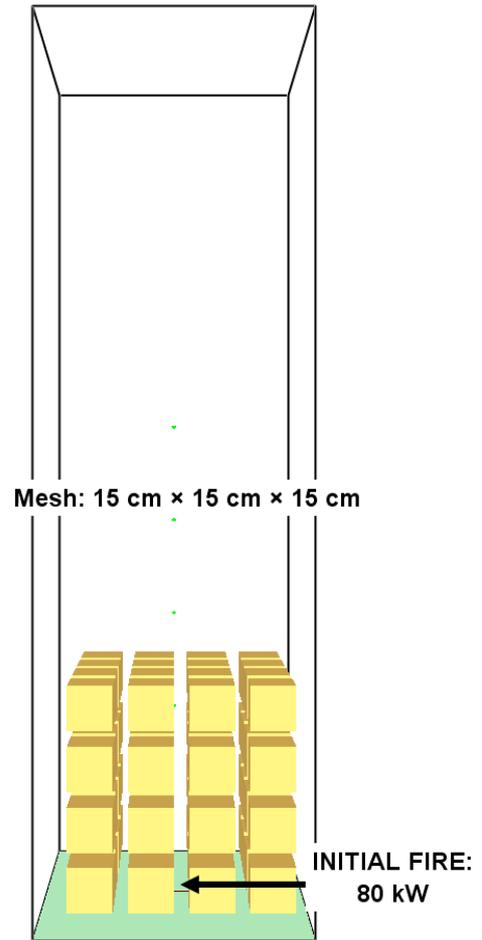
Figure 44. The FDS5 model of PET/cardboard fire experiment: a) schematic description and b) the actual model.
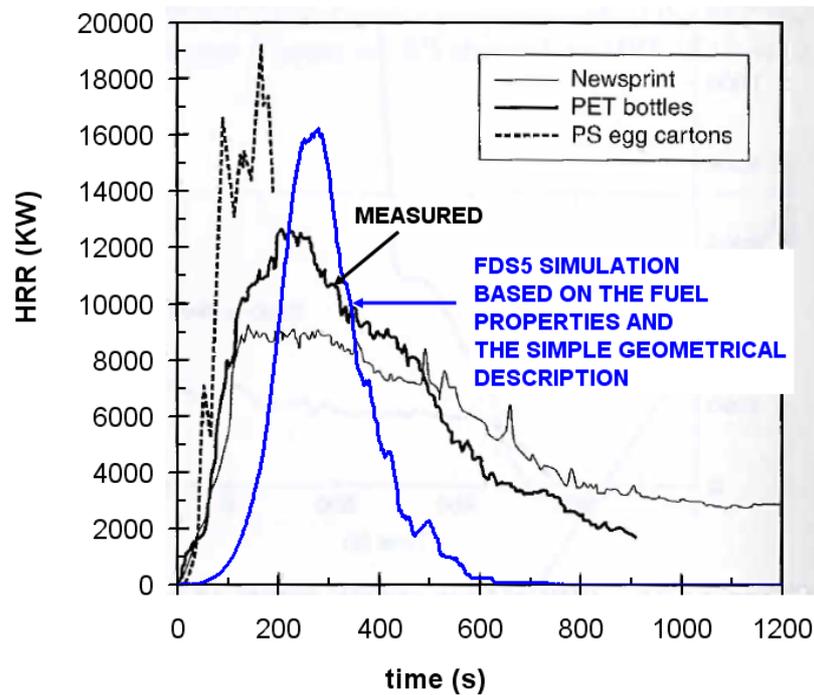
Figure 45. Comparison of the measured and simulated heat release rate of fire experiment on PET plastic bottles in cardboard boxes.

6.2.3 Office workstation fire

The third example is a fire experiment of an office workstation carried out and reported by Madrzykowski and Walton [57]. Such workstation consists of several different kinds of combustibles with more complex geometries than those addressed of the two examples described above. Thus its modelling is very challenging for the simple methodology considered here.

   The description of the combustibles of the fire experiment is given in detail in Table 24. The heat released during the experiment was about 1 600 MJ. The experiment was simulated on the basis of the cone calorimeter data reported in [57] using the FDS5 model described in Figure 46. The simulated and measured HRR curves are compared in Figure 47. It can be seen that taking into account the complexity of the modelled target, the agreement of the calculated and measured results is very good.
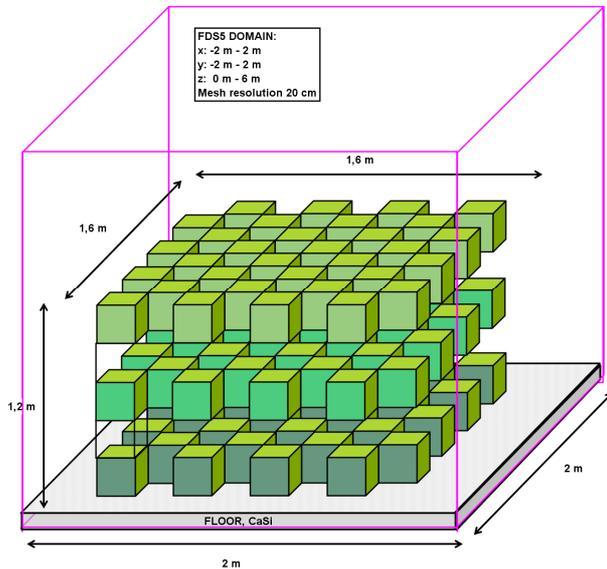
Table 24. Description of the combustibles of the office workstation fire experiment carried out by Madrzykowski and Walton. Reproduced from [57].

Item	kg
Carpet 2.13 m x 1.5 m (7 ft x 4.9 ft)	7.9
Workstation panels, connectors, trim and metal base plates	84
0.61 m x 1.07 m (2 ft x 3.5 ft) Work surface with metal drawer unit	57.2
0.76 m x 1.52 m (2.5 ft x 5 ft) Work surface	27.8
Keyboard shelf w/ metal bracing and support arm	12
Computer monitor	15.8
Keyboard	1.9
Computer	13.5
Office chair	20.5
Plastic letter trays (7)	1.1
#4 LDPE small recycle bin 0.28 m x 0.18 m x 0.305 m high (0.91 ft x 0.58 ft x 1 ft high)	0.5
#4 LDPE black wastebasket 0.36 m x 0.26 m x 0.38 m high (1.21 ft x 0.85 ft x 1.25 ft)	0.8
#4 LDPE large blue recycling bin 0.36 m x 0.26 m x 0.38 m (1.21 ft x 0.85 ft x 1.25 ft)	0.8
75 mm (3 in) Vinyl notebook 0.3 m x 0.29 m high (0.98 ft x 0.96 m with paper (2)	4
Files in hanging folders for file drawer	6
Reports on work surface	2
Reports placed in drawer above file drawer	1.2
Phonebook 0.27 m x 0.22 m x 0.045 (0.90 ft x 0.73 ft x 0.15 ft)	1.4
1 kg of paper 216 mm x 280 mm (8.5 in x 11 in) in small recycle bin	1
Trash (separate table)	0.2
1 kg of loose paper in large recycle bin	1
1 kg of newspaper in large recycle bin	1
Sled base chair	11.8
Desk blotter/calendar	0.4
Total (Individual weights have been rounded and may not sum to total weight)	273.2

6. Predicting heat release rate and data used

a)

b)

```
FDS5 DOMAIN:
x: -2 m - 2 m
y: -2 m - 2 m
z:  0 m - 6 m
Mesh resolution 20 cm
```

1,6 m

1,6 m

1,2 m

2 m

FLOOR, CaSi

2 m

Mesh: 20 cm × 20 cm × 20 cm

INITIAL FIRE:
50 kW, on 0-200 s

```
&SURF ID='Office_WS'
    MATL_ID='office_fuel'
    IGNITION_TEMPERATURE = 350.
    BURN_AWAY = .TRUE.
    HRRPUA = 290.0
    RAMP_Q = 'material_HRR'
    RGB = 218, 165, 64
    THICKNESS=0.2
    BACKING = 'INSULATED'/

&MATL ID='office_fuel'
    CONDUCTIVITY=0.1
    SPECIFIC_HEAT=2.0
    DENSITY=165.0
    HEAT_OF_COMBUSTION = 15000.0 /
```
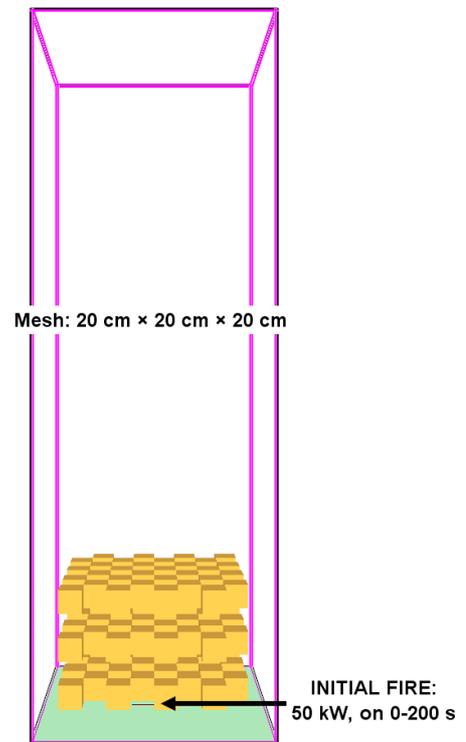
Figure 46. The FDS5 model of the office workstation fire experiment: a) schematic description and b) the actual model.
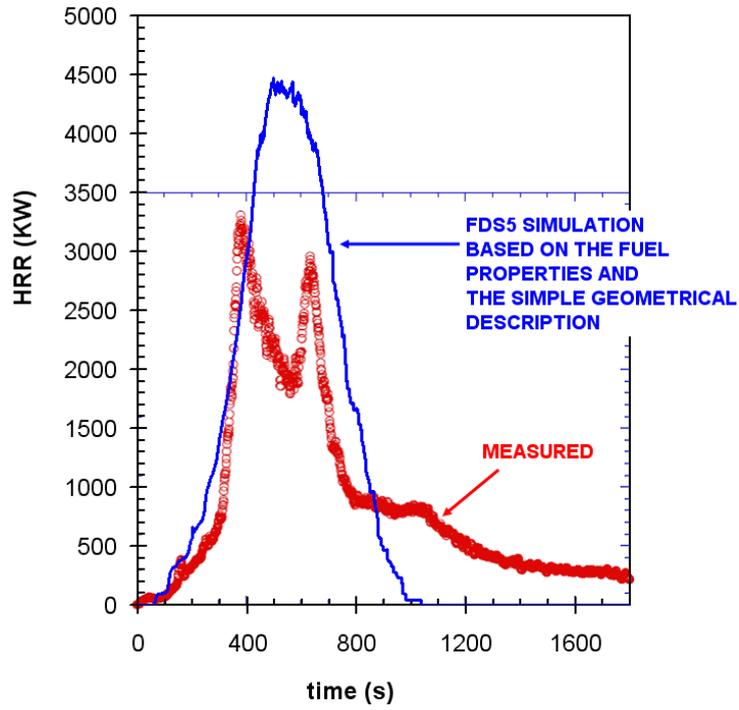
Figure 47. Comparison of the measured and simulated heat release rates of the office workstation fire experiment carried out by Madrzykowski and Walton [57].

7. Timber structures and design fires

7.1 Methods for analysing structural performance

A full analytical procedure for structural fire design would take into account the behaviour of the structural system at elevated temperatures, the potential heat exposure, and the beneficial effects of active fire protection systems, together with the uncertainties associated with these three features, and the importance of the structure (the consequences of a failure).

At the present time, it is possible to undertake a performance based procedure for determining adequate performance which incorporates some (if not all) parameters, and to demonstrate that the structure, or its components, will give adequate performance in a real building fire. Also in the procedure based on a nominal (standard) fire and the related classification system, which calls for specific periods of fire resistance, an overall structural performance with associated uncertainties is assumed to be taken into account (though not explicitly). Options for the application of Part 1–2 of EN 1995 [80] are illustrated in Figure 48.
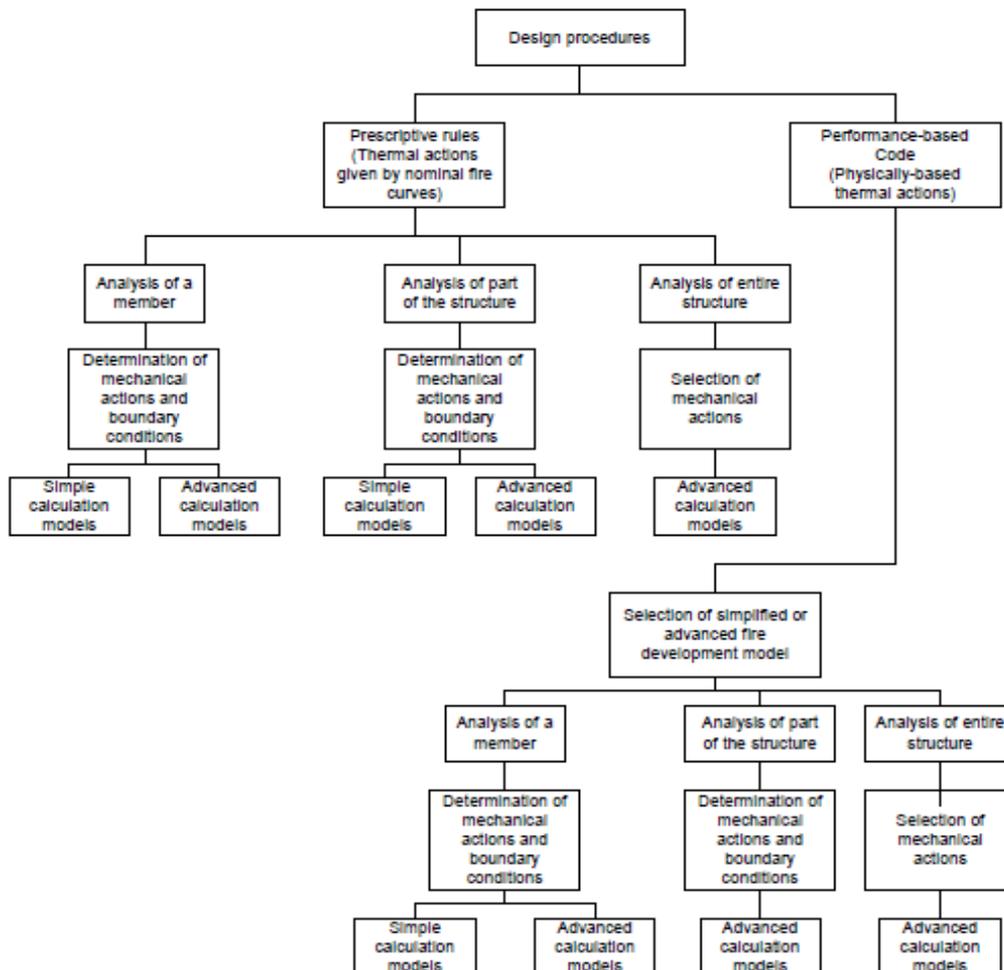
Figure 48. Design procedures according to EN 1995-1-2.

In this section, some methods and concepts for analysing non-standard fire exposure conditions are shortly summarised.

The informative Annex F of EN 1991-1-2 [17] defines *Equivalent time of fire exposure* concept. However, it is not applicable to timber structures because material specific data has not been available. In this method, the equivalent time of standard fire exposure is dependent on

- the design fire load density
- a conversion factor which is related to the thermal properties of the enclosure
- a ventilation factor taking into account vertical and horizontal openings
- a correction factor (function of the material composing structural cross-sections).

The principles of fire safety engineering approach for structural performance of timber elements are shown in Figure 49.
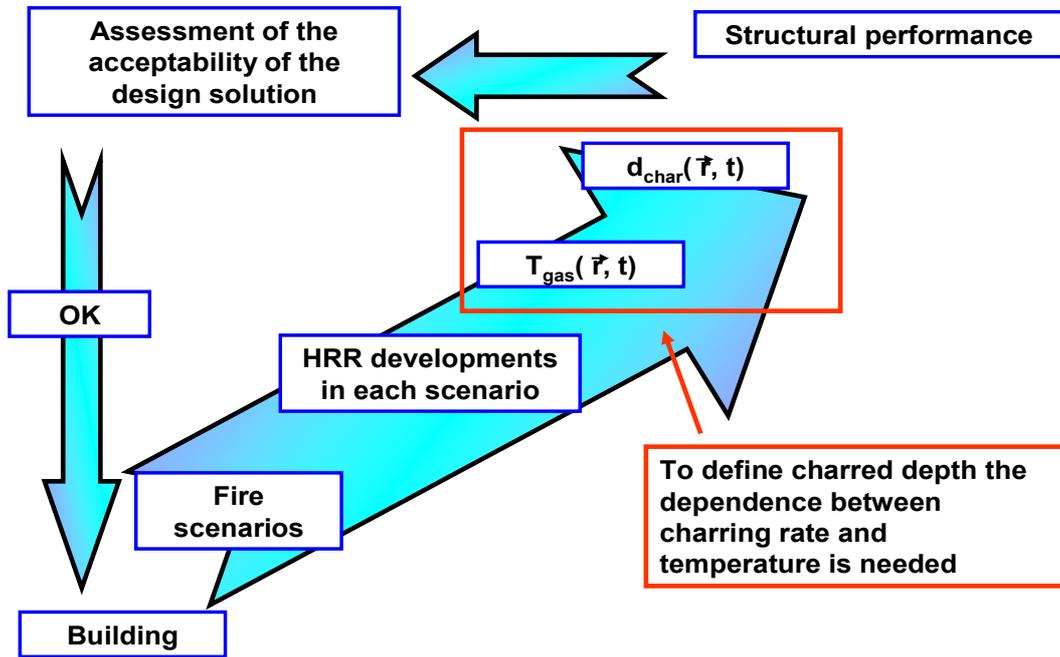
Figure 49. Design concept for structural performance of timber.

A cumulative radiation energy method [81] has been demonstrated in New Zealand to predict failure times of wooden doors under different fire exposures. The method assumes that the predominant mode of heat transfer in a fire compartment is by radiation rather than by convection. The radiant heat transfer is therefore a function of the absolute temperature T (K) raised to the fourth power. The severity of a fire can therefore be quantified by calculating the cumulative radiation energy over the exposure time.

7.2 Charring and design fires

The heat flux (to which the building element is exposed) can be calculated according to the following expression (including convection) for the standard fire curve

$$HF_{std} = \alpha_c \cdot (T_{std} - T_0) + \Phi \varepsilon \sigma \cdot \left((T_{std} + 273\ ^\circ C)^4 - (T_0 + 273\ ^\circ C)^4 \right)$$
$$T_{std} = 20\ ^\circ C + 345\ ^\circ C \cdot \log_{10}\left(8 \cdot \frac{t}{\min} + 1 \right)$$

(7-1)

where α_c is the convective heat transfer coefficient, Φ is the configuration factor, ε is the emissivity of the surface and σ is the Stefan-Boltzmann constant. For non-standard fire exposure, here named FSE curve,

$$HF_{FSE} = \alpha_c \cdot (T_{FSE} - T_0) + \Phi \varepsilon \sigma \cdot \left((T_{FSE} + 273\ ^\circ C)^4 - (T_0 + 273\ ^\circ C)^4 \right)$$

(7-2)

where T_{FSE} is a case-specific temperature representing the chosen design fire of the case of concern. The standard temperature-time fire curve and an example of a design fire curve (FSE) are shown in Figure 50. The corresponding heat flux curves are presented in Figure 51. Integration of these heat flux curves over time results in cumulative values of energy received by the building element as a function of time (see Figure 52).
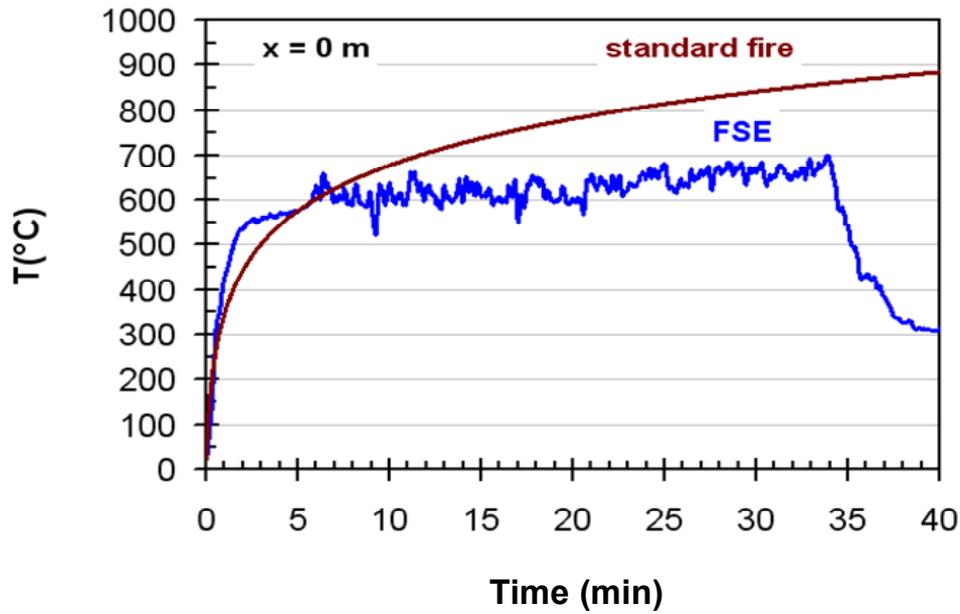

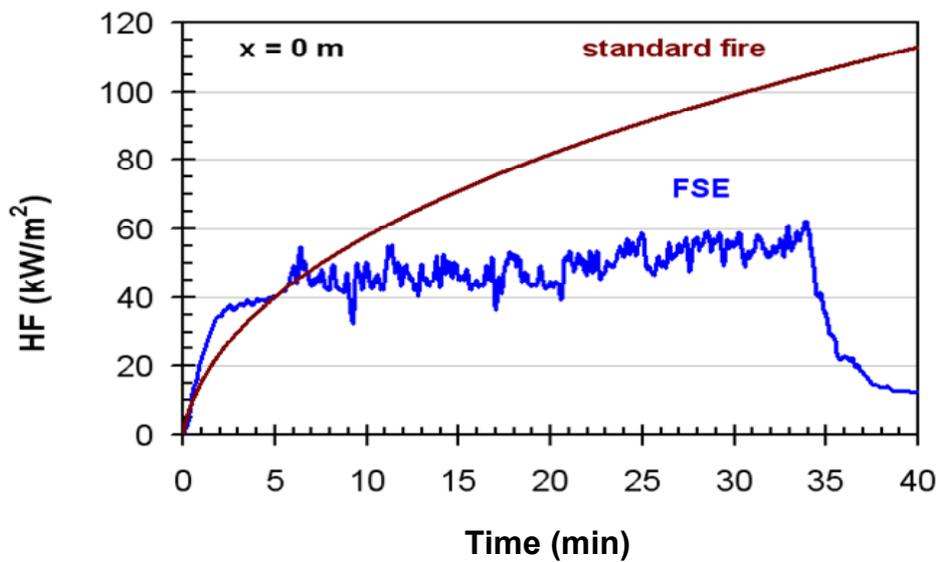Figure 50. Standard fire curve and an example of a design fire curve (FSE).

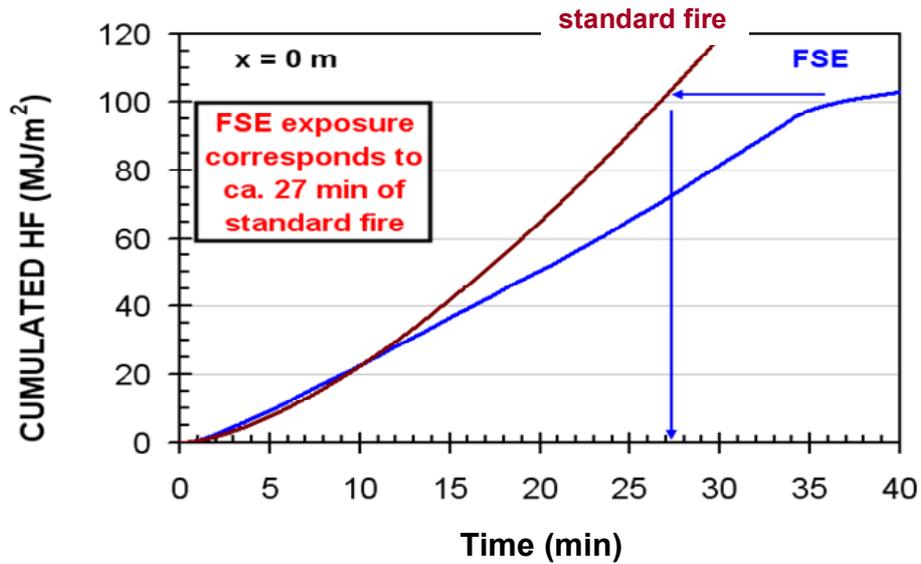Figure 51. Heat fluxes of standard fire curve and FSE curve of Figure 50.

Figure 52. Integrated heat fluxes of standard fire and FSE heat fluxes of Figure 51.

In the example case shown in Figure 52, the total energy received by the structural element is just above 100 MJ/m², which corresponds to the total energy in 30 minutes of the standard fire curve.

The mean value of charring rate for a given period of time is dependent on the total energy received during that time, which means that the resulting char depth during a defined period of time can be calculated if the charring rate is known. The following expression applies for standard fire exposure

$$d_{std}(t_{std}) = F\left(\int_0^{t_{std}} HF_{std}\, dt \right)$$ (7-3)

and for the FSE exposure

$$d_{FSE} = F\left(\int_0^{\infty} HF_{FSE}\, dt \right)$$ (7-4)

where F is a function describing the dependence between char depth of a specific timber product and the integrated heat flux for a given time (in the simplest case, F can be a constant).

For the standard fire exposure, charring rates are well known. In cases where the two curves do not essentially differ from each other, mean charring rate estimates for the FSE curves can be made based on the standard fire value. For other cases, experimental data close to the FSE curve of concern are needed.

The principles of the reduced cross-section method of EN 1995-1-2 [80] could be used for calculating the mechanical performance of timber structures. The char depth is

calculated as described above, and the material close to the char line is assumed to have zero strength and stiffness. The strength and stiffness properties of the remaining cross-section are assumed to be unchanged. However, use of the zero-strength layer (d_0) value of 7 mm used in EN 1995-1-2 [80] does lead to unsafe results in the parametric fire exposure cases of Annex A in EN 1995-1-2. Thus, more information is needed to take into account correctly thermal and mechanical properties in the non-charred timber to define d_0 and its time dependence.

In FSE analysis char depth and zero-strength layer calculations based on standard fire exposure charring rates and performance are safe side assumptions for cases when the FSE exposure curve is under or only shortly exceeding the standard fire curve.

8. Conclusions

For construction design fire safety is one of the key requirements. Fire loads, which define the possible fires that can occur, need to be known both in magnitude and quality. This report describes a simplified approach to fire characterisation that is based on the concept of fire load entities. Design fires appropriate for use in Fire Safety Engineering (FSE) design are generally valid and thus applicable also for building with wood. In the approach used the initial fires are quantified using heat release rates which are dependent on the usage of the building. Assessment of fire growth and spread is based on the capability of the FDS fire simulator to make *conservative estimations* how rapidly and to how large a fire may grow within a given space.

This report summarises the basics of performance criteria, fire safety engineering process and procedure for estimation of initial fires and fire development. Design fires for different occupancies are described in detail: sports and multipurpose halls, dwellings, warehouses and shops. The used prediction methodology for heat release in fires utilises the basic, measurable combustion characteristics, i.e. the heat release rate per unit area and the effective heat of combustion. Also examples of use and validity of the methodology are given.

At the end of the report key issues concerning timber structures under design fire exposures are described with the idea to provide visions for future development by utilising new possibilities in fire safe building with wood.

Acknowledgements

References

1. The National Building Code of Finland, Part E1: Fire safety of buildings. Regulations and guidelines 2002. Decree of the Ministry of the Environment on fire safety of buildings. Helsinki: 2002. 41 p.

2. EN 1990. Eurocode – Basis of Structural Design. CEN.

3. Ohlemiller, T. J., Mulholland, G. W., Maranghides, A. Filliben, J. J. & Gann, R. G. 2005. Fire Tests of Single Office Workstations. NIST NCSTAR 1-5C.

4. Madrzykovski, D. 1996. Office Workstation Heat Release Rate Study: Full Scale vs. Bench Scale. Proceedings: 7th International Interflam Conference1996. Pp. 47–55.

5. Madrzykovski, D. & Walton, W. D. 2003. County Cook Administration Building Fire 69 West Washington Chicago, Illinois, October 17, 2003: Heat Release Rate Experiments and FDS Simulation. NIST Special Publication SP-1021.

6. Kakegawa, S., Yashiro, Y., Satoh, H., Kurioka, H., Kasahara, I., Ikehata, Y., Saito, N. & Turuda, T. 2003. Design Fires for Means of Egress in Office Buildings Based on Full-Scale Fire Experiments. Fire Safety Science – Proceedings of the Seventh International Symposium. Pp. 975–986.

7. National Institute of Standards and Technology, Gaithersburg, Maryland, USA, and VTT Technical Research Centre of Finland, Espoo, Finland. Fire Dynamics Simulator, Technical Reference Guide, 5th edition, October 2007. NIST Special Publication 1018-5 (Four volume set). http://fire.nist.gov/fds/.

8. International Fire Engineering Guidelines. 2005 Edition. National Research Council of Canada (NRC), International Code Council (ICC), United States of America, Department of Building and Housing, New Zealand (DBH) & Australian Building Codes Board (ABCB). 415 p. ISBN 1741 614 562.

9. Babrauskas, V. Will the Second Item Ignite? Fire Safety Journal, 1981/1982, Vol. 4, No. 4, pp. 281–292.

10. Hietaniemi, J. & Rinne, T. 2007. Historiallisesti arvokkaan kohteen toiminnallinen palo-turvallisuus-suunnittelu. Esimerkkitapauksena Porvoon museo. Espoo: VTT. 136 p. + app. 44 p. VTT Working Papers 71. http://www.vtt.fi/inf/pdf/workingpapers/2007/W71.pdf. (In Finnish.)

11. Alpert, R. L. 1972. Calculation of response time of ceiling mounted fire detectors. Fire Technology, Vol. 8, pp. 181–195.

12. Vaari, J. 2004. Sammutustekniikan luonnontieteelliset perusteet. (Fundamentals of fire suppression technology.) Helsinki: Edita Publishing Oy. 215 p. ISBN 951-37-4077-3. (In Finnish.)

13. Paloilmoittimen suunnittelu- ja asennusohje, 2002 (Guide for Design and Installation of Fire detection System, in Finnish).

14. CEA 4001. Sprinkler Systems: Planning and Installation. CEA: the European insurance and reinsurance federation, 2009. 190 p.

15. Bush, S. E. & McDaniel, D. L. 1997. Systems Approaches to Property Classes – Library and Museum Collections. In: Cote, A. E. (ed.). Fire Protection Handbook. 18th Edition. Quincy, MA: National Fire Protection Association. Pp. 9-92–9-109.

16. Holm, C. & Oksanen, P. 1970. Palokuorman määrä kerrostalojen asuinhuoneistoissa. Palontorjuntatekniikka, No. 2, pp. 1–4. (In Finnish.)

17. EN 1991-1-2:2002. Eurocode 1: Actions on Structures – Part 1–2: General Actions – Actions on structures exposed to fire. Brussels: CEN 2002. 59 p.

18. Nilsson, L. 1970. Brandbelastning/Bostadslägenheter/Fire Loads in Flats, Statens Institut for Byggnadsforskning; Stockholm, Rapport R 34. Svensk Byggtjänst, Stockholm. National Swedish Building Research Summaries R 34.

19. Kersken-Bradley, M. (ed.). 1983. A Conceptual Approach Towards a Probability Based Desing Guide on Structural Fire safety. Fire Safety Journal, Vol. 6, pp. 1–79.

20. Bryl, S. 1975. Brandbelastung in Hochbau. Schweizerische Bauzeitung, special reprint from Jahrgang 93, Heft 17.

21. Cambell, J. A. 1981. Confinement of Fire in Buildings. Fire Protection Handbook. NFPA Handbook, USA.

22. Bwalya, A. C. 2004. An Extended Survey of Combustible Contents in Canadian Residential Living Rooms. Ottawa, Canada: National Research Council Canada. Research Report No. 176.

23. Babrauskas, V. 1986. Free burning fires. Fire Safety Journal, Vol. 11, pp. 33–51.

24. Babrauskas, V. & Walton, W. D. 1986. A Simplified Characterization of Upholstered Furniture Heat Release Rates. Fire Safety Journal, Vol. 11, pp.181–192.

25. Hietaniemi, J., Hostikka, S. & Vaari, J. 2004. FDS simulation of fire spread – comparison of model results with experimental data. Espoo: Technical Research Centre of Finland, 2004. 45 p. + App. 6 p. VTT Working Papers 4. ISBN 951-38-6556-8. http://www.vtt.fi/inf/pdf/workingpapers/2004/W4.pdf.

26. Denize, H. 2000. The Combustion Behaviour of Upholstered Furniture Materials in New Zealand. Christchurch, New Zealand: University of Canterbury. 107 p. + app. 28 p. (Master's Thesis).

27. Hietaniemi, J., Hakkarainen, T., Huhta, J., Korhonen, T., Siiskonen, J. & Vaari, J. 2002. Ontelotilojen paloturvallisuus. Ontelopalojen tutkimus kokeellisesti ja mallintamalla. Espoo: VTT. VTT Tiedotteita 2128. 125 p. + app. 63 p. ISBN 951-38-5953-3; 951-38-5954-1. http://www.vtt.fi/inf/pdf/tiedotteet/2002/T2128.pdf. (In Finnish.)

28. Hostikka, S. & Axelsson, J. Modelling of the radiative feedback from flames in cone calorimeter 2003. NORDTEST, Espoo. NORDTEST technical report 540. 41 p.

29. Korhonen, T. & Hietaniemi, J. 2004. Puujulkisivujen paloturvallisuus lähiökerrostaloissa. Espoo: VTT. 58 p. + app. 36 p. VTT Tiedotteita 2253. ISBN 951-38-6482-0; 951-38-6483-9. http://www.vtt.fi/inf/pdf/tiedotteet/2004/T2253.pdf. (In Finnish.)

30. Friday, P. & Mowrer, F. W. 2001. Comparison of FDS Model Predictions with FM/SNL Fire Test Data. NIST GCR 01-810, National Institute of Standards and Technology, Gaithersburg, Maryland.

31. Hamins, A., Maranghides, A., McGrattan, K. B., Johnsson, E., Ohlemiller, T. J., Donnelly, M., Yang, J., Mulholland, G., Prasad, K., Kukuck, S., Anleitner, R. & McAllister, T. 2004. Report on Experiments to Validate Fire Dynamic and Thermal-Structural Models for Use in the World Trade Center Investigation. NIST Special Publication in preparation, National Institute of Standards and Technology, Gaithersburg, Maryland.

32. Hamins, A., Maranghides, A., McGrattan, K.B., Ohlemiller, T.J. & Anletiner, R. 2004. Experiments to Validate Models of Fire Growth and Spread for use in the World Trade Center Investigation. NIST Special Publication in preparation, National Institute of Standards and Technology, Gaithersburg, Maryland.

33. Floyd, J. 2002. Comparison of CFAST and FDS for Fire Simulation with the HDR T51 and T52 Tests. NIST GCR 01-810, National Institute of Standards and Technology, Gaithersburg, Maryland.

34. Hamins, A. & McGrattan, K. B. 2003. Reduced-Scale Experiments on the Water Suppression of a Rack-Storage Commodity Fire for Calibration of a CFD Fire Model. In Fire Safety Science – Proceedings of the Seventh International Symposium. International Association for Fire Safety Science. Pp. 457–468.

35. McGrattan, K. B. & Hamins, A. 2003. Numerical Simulation of the Howard Street Tunnel Fire, Baltimore, Maryland, July 2001. NISTIR 6902, National Institute of Standards and Technology, Gaithersburg, Maryland. Joint Publication of NIST and the US Nuclear Regulatory Commission (NUREG/CR-6793).

36. Floyd, J. E., Wieczorek, C. & Vandsburger, U. 2001. Simulations of the Virginia Tech Fire Research Laboratory Using Large Eddy Simulation with Mixture Fraction Chemistry and Finite Volume Radiative Heat Transfer. In: Proceedings of the Ninth International Interflam Conference. Interscience Communications.

37. Piergiorgio, A., Giuseppe, D., Dino, F., Zappellini, G. & Ferrari, A. 2001. CFD Simulations of a Truck Fire in the Underground Gran Sasso National Laboratory. In: Proceedings of the 5th Italian Conference on Chemical and Process Engineering. Associazione Italiana Di Ingegneria Chimica (AIDIC).

38. D'Souza, V., Sutula, J. A., Olenick, S. M., Zhang, W. & Roby, R. J. 2001. Use of Fire Dynamics Simulator to Predict Smoke Detector Activation. In: Proceedings of the 2001 Fall Technical Meeting, Eastern States Section. Pittsburgh, Pennsylvania: Combustion Institute.

39. Xin, Y., Gore, J. P., McGrattan, K. B., Rehm, R. G.& Baum, H. R. 2002. Large Eddy Simulation of Buoyant Turbulent Pool Fires. In: Proceedings of the 2002 Spring Technical Meeting, Central States Section. Pittsburgh, Pennsylvania: Combustion Institute.

40. Kashef, A., Benichou, N., Lougheed, G. D. & McCartney, C. 2002. A Computational and Experimental Study of Fire Growth and Smoke Movement in Large Spaces. Technical Report NRCC-45201, National Research Council, Canada.

41. Cochard, S. 2003. Validation of Fire Dynamics Simulator (Version 2.0) Freeware. Tunnel Management International Journal, 6(4), December.

42. Zhang, W., Hamer, A., Klassen, M., Carpenter, D. & Roby, R. 2002. Turbulence Statistics in a Fire Room Model by Large Eddy Simulation. Fire Safety Journal.

43. Blomqvist, P., Rosell, L. & Simonson, M. 2004. Emissions from Fires Part II: Simulated Room Fires. Fire Technology, Vol. 40, pp. 59–73.

44. French, S. E. 1994. EUREKA 499 – HGV Fire Test (Nov. 1992) – Summary Report. In: Proceedings of the International Conference on Fires in Tunnels (E. Ivarson, Ed.), SP Swedish National Testing and Research Institute, Borås, Sweden. Pp. 63–85.

45. Fires in Transport Tunnels: Report on Full-Scale Tests. Edited by Studiensgesellschaft Stahlanwendung e. V., EUREKA-Project EU499:FIRETUN, Düsseldorf, Germany, 1995.

46. Ingason, H. & Lönnermark, A. 2005. Heat release rates from heavy goods vehicle trailer fires in tunnels. Fire Safety Journal 40 (2005), pp. 646–668.

47. Lemaire, T. & Kenyon, Y. 2006. Large Scale Fire Tests in the Second Benelux Tunnel. Fire Technology, Vol. 42, pp. 329–350.

48. Carvel, R., Beard, A., Jowitt, P. & Drysdale, D. 2004. The influence of tunnel geometry and ventilation on the heat release rate of a fire. Fire Technology, Vol. 40, pp. 5–26.

49. Carvel, R., Beard, A., Jowitt, P. & Drysdale, D. 2005. Fire Size and Fire Spread in Tunnels with Longitudinal Ventilation Systems. Journal of Fire Sciences, Vol. 23, No. 6, pp. 485–518.

50. Ingason, H. 2005. Model Scale Tunnel Fire Tests. Longitudinal ventilation. Borås: SP Fire Technology. SP Report 2005:49 (Brandforskprojekt 404-011). 80 p. ISBN 91-85303-82-8.

51. Bennetts, I. D., Poh, K. W., Poon, S. L., Thomas; I. R., Lee; A. C., Beever; P. F., Ramsay, G. C. & Timms, G. R. 1998. Fire Safety in Shopping Centres. Australia: Fire Code Reform Centre Limited. Final Research Report, Project 6. Fire Code Reform Research Program. 265 p.

52. Matala, Anna; Hostikka, Simo; Mangs, Johan. 2009. Estimation of pyrolysis model parameters for solid materials using thermogravimetric data. Fire Safety Science 9: 1213–1223. doi:10.3801/IAFSS.FSS.9-1213.

53. Lautenberger, C., Rein, G. & Fernandez-Pello, C. 2006. The application of a genetic algorithm to estimate material properties for fire modeling from bench-scale fire test data. Fire Safety Journal, 41, pp. 204–214.

54. Biteau, H., Steinhaus, T., Schemel, C., Simeoni, A., Marlair, G., Bal, N. & Torero, J.L. 2008. Calculation Methods for the Heat Release Rate of Materials of Unknown Composition. Fire Safety Science. Proc. 9th IAFFS Symposium. Karlsruhe, Germany. 2008. (Preprint).

55. Matala, A. 2008. Estimation of solid phase reaction parameters for fire simulation. Master's Thesis. Helsinki University of Technology.

56. Hietaniemi, J., Hakkarainen, T., Mikkola, E., Ahola, P., Nurmi, A., Salonvaara, M. & Vanhatalo, L. 2002. Palosuojatut puutuotteet. Tutkimus palo-, puu- ja kosteusteknisistä ominaisuuksista sekä ympäristövaikutuksista. VTT/RTE internal report. (In Finnish.)

57. Madrzykowski, D. & Walton, W. D. 2004. Cook County Administration Building Fire, 69 West Washington, Chicago, Illinois, October 17, 2003: Heat Release Rate Experiments and FDS Simulations. NIST Special Publication SP-1021.

58. Lyon, R. E & Walters, R. N. 2001. Heat Release Capacity. Fire & Materials Conference, San Francisco, CA, January, 2001.

59. Hirschler, M. 1992. Heat Release from Plastic Materials. In: Heat Release in Fires. Babrauskas & Grayson, Ed.

60. Data by VTT. Internal report.

61. Scudamore, M. J., Briggs, P. J. & Prager, F. H. 1991. Cone Calorimetry – A Review of Test Carried out on Plastics for Association of Plastics Manufacturers in Europe. Fire and Materials, Vol. 15, pp. 65–84.

62. Cone calorimeter data presented on the WPI web site: address http://www.wpi.edu/Academics/Depts/Fire/Lab/Cone/Data/.

63. Hietaniemi, J. 2008. Data analysis of CC data from "Hakkarainen, T. (ed.). Smoke gas analysis by Fourier transform infrared spectroscopy. The SAFIR project. 1999. VTT, Espoo. 81 p. VTT Tiedotteita - Meddelanden - Research Notes 1981.

64. Laoutid, F., Ferry, L., Lopez-Cuesta, J. M. & Crespy, A. 2005. Flame-retardant action of red phosphorus/magnesium oxide and red phosphorus/iron oxide compositions in recycled PET. Fire and Materials. 2006, Vol. 30, pp. 343–358.

65. Hshieh, F.-Y., Hirsch, D. B. & Beeson, H. D. 2003. Predicting heats of combustion of polymers using an empirical approach. Fire and Materials, Vol. 27, pp. 9–17.

66. Forest Products Laboratory. 2008. Wood Handbook. Chapter 10, Wood-Based Composites and Panel Products: Available at http://www.fpl.fs.fed.us/rwu4706/handbook.html. (Referred to 6th October 2008.)

67. Mikkola, E. 1989. Puupinnan syttyminen. VTT, Espoo. VTT Tiedotteita 1057. 48 p. (In Finnish.)

68. McLean, J. D. 1941. Thermal conductivity of wood. Heating, piping and air conditioning, Vol. 13, pp. 380–193.

69. Mikkola, E. 1990. Charring of wood. Espoo: VTT. VTT Tutkimuksia 689. 40 p. ISBN 951-38-3711-4.

70. Lautenberger. C. W. 2007. A Generalized Pyrolysis Model for Combustible Solids. A dissertation submitted in partial satisfaction of the requirements for the degree of Doctor of Philosophy in Engineering – Mechanical Engineering in the Graduate Division of the University of California, Berkeley. 370 p.

71. Tewarson, A. 2005. Thermophysical and Fire Properties of Automobile Plastic Parts and Engine Compartment Fluids. TECHNICAL REPORT #0003018009, VOLUME III. FM Global. (Project ID 0003018009-3.)

72. Babrauskas, V. 2003. Ignition Handbook. Issaquah, USA: Fire Science Publishers. 1116 p. ISBN 0-9728111-3-3.

73. Moghtaderi, B., Novozhilov, V., Fletcher, D. F. & Kent, J. H. 1997. A New Correlation for Bench-scale Piloted Ignition Data of Wood. Fire Safety J., 29, pp. 41–59.

74. Janssens, M. L. 1991. Fundamental Thermophysical Characteristics of Wood and Their Role in Enclosure Fire Growth (Ph. D. dissertation), University of Gent, Belgium.

75. Fangrat, J., Hasemi, Y., Yoshida, M., and Hirata, T. 1997. Surface Temperature at Ignition of Wooden Based Slabs, Fire Safety J. 27, pp. 249–259 (1996); 28, pp. 379–380.

76. Bluhme, D. A. 1987. ISO ignitability test and proposed criteria. Fire and Materials, Vol. 11, Issue 4, pp. 195–199.

77. Delichatsios, M. A. 2005. Piloted ignition times, critical heat fluxes and mass loss rates at reduced oxygen atmospheres. Fire Safety Journal 40 (2005), pp. 197–212.

78. Studiensgesellschaft Stahlanwendung e. V., editor. Fires in transport tunnels: report on full-scale tests. EUREKA-Project EU499: FIRETUN, Dusseldorf, Germany, 1995.

79. Babrauskas, V. 2002. Heat Release Rates. In: The SFPE Handbook of Fire Protection Engineering. 3rd Edition. Quincy, MA: National Fire Protection Association. Pp. 3-1–3-37. ISBN 087765-451-4.

80. EN 1995-1-2:2004. Eurocode 5: Design of timber structures – Part 1–2: General – Structural fire design. Brussels: CEN 2004.

81. Barnett, C.R. 2007. A new T-equivalent method for fire rated wall constructions using cumulative radiation energy. Journal of Fire Protection Engineering, Vol. 17, pp. 113–127.

VTT CREATES BUSINESS FROM TECHNOLOGY

Technology and market foresight • Strategic research • Product and service development • IPR and licensing • Assessments, testing, inspection, certification • Technology and innovation management • Technology partnership

VTT WORKING PAPERS 139   DESIGN FIRES FOR FIRE SAFETY ENGINEERING

VTT Working Papers

120 Veikko Kekkonen & Göran Koreneff. Euroopan yhdentyvät sähkömarkkinat ja markkinahinnan muodostuminen Suomen näkökulmasta. 2009. 80 s.

121 Rinat Abdurafıkov. Russian electricity market. Current state and perspectives. 2009. 77 p. + app. 10 p.

122 Bettina Lemström, Juha Kiviluoma, Hannele Holttinen & Lasse Peltonen. Impact of wind power on regional power balance and transfer. 2009. 43 p.

123 Juha Forsström. Euroopan kaasunhankinnan malli. 2009. 80 s.

124 Jyrki Tervo, Antti Manninen, Risto Ilola & Hannu Hänninen. State-of-the-art of Thermoelectric Materials Processing, Properties and Applications. 2009. 29 p.

125 Salla Lind, Björn Johansson, Johan Stahre, Cecilia Berlin, Åsa Fasth, Juhani Heilala, Kaj Helin, Sauli Kiviranta, Boris Krassi, Jari Montonen, Hannele Tonteri, Saija Vatanen & Juhani Viitaniemi. SIMTER. A Joint Simulation Tool for Production Development. 2009. 49 p.

126 Mikko Metso. NoTA L_INdown Layer Implementation in FGPA Design results. 2009. 20 p.

127 Marinka Lanne & Ville Ojanen. Teollisen palveluliiketoiminnan menestystekijät ja yhteistyösuhteen hallinta - Fleet asset management - hankkeen työraportti 1. 2009. 63 s. + liitt. 10 s.

128 Alternative fuels with heavy-duty engines and vehicles. VTT´s contribution. 2009. 109 p. + app. 8 p.

129 Stephen Fox. Generative production systems for sustainable product greation. 2009. 104 p.

130 Jukka Hemilä, Jyri Pötry & Kai Häkkinen. Tuotannonohjaus ja tietojärjestelmät: kokemuksia sekä kehittämisperiaatteita. 2009. 37 s.

131 Ilkka Hannula. Hydrogen production via thermal gasification of biomass in near-to-medium term. 2009. 41 p.

132 Hannele Holttinen & Anders Stenberg. Tuulivoiman tuotantotilastot. Vuosiraportti 2008. 2009. 47 s. + liitt. 8 s.

133 Elisa Rautioaho & Leena Korkiala-Tanttu. Bentomap: Survey of bentonite and tunnel backfill knowledge – State-of-the-art. 2009. 112 p. + app. 7 p.

134 Totti Könnölä, Javier Carrillo-Hermosilla, Torsti Loikkanen & Robert van der Have. Governance of Energy System Transition. Analytical Framework and Empirical Cases in Europe and Beyond. GoReNEST Project, Task 3. 2009. 49 p.

137 Eija Kupi, Jaana Keränen & Marinka Lanne. Riskienhallinta osana pk-yritysten strategista johtamista. 2009. 51 s. + liitt. 8 s.

139 Jukka Hietaniemi & Esko Mikkola. Design Fires for Fire Safety Engineering. 2010. 101 p.